# THE ROLE OF CYCLOPHILIN D IN MITOCHONDRIAL CALCIUM HOMEOSTASIS IN ADULT NEURONS

By

Anna G. Barsukova

A DISSERTATION

Presented to the Department of Physiology & Pharmacology
and the Oregon Health & Science University
School of Medicine
in partial fulfillment of
the requirements for the degree of
Doctor of Philosophy

June 2009

School of Medicine
Oregon Health & Science University

CERTIFICATE OF APPROVAL

This is certify that the Ph.D. dissertation of

Anna G. Barsukova

has been approved

Mentor/Advisor Dr. Michael Forte

Member Dr. Dennis Bourdette

Member Dr. Gary Banker

Member Dr. Charles Allen

Member Dr. John Williams

## TABLE OF CONTENTS


List of illustrations Page iv

List of abbreviations Page viii

Acknowledgements Page x

Abstract Page xii

**PART 1. INTRODUCTION** Page 1

1.1. Calcium roles and regulation in neurons and mitochondria Page 4

1.2. What is mitochondrial permeability transition? Page 10

1.3. Cyclophilin D is a regulator of the PTP Page 13

1.4. Mitochondrial $Ca^{2+}$ imaging in live cells Page 19

1.5. Alteration of $Ca^{2+}$ homeostasis in neurodegenerative diseases Page 22

1.6. CyPD and neuroprotection in a multiple sclerosis model Page 23

1.7. Adult mouse cortical culture model Page 25

1.8. Thesis Rationale Page 29

**PART 2. METHODS** Page 32

2.1. Animals Page 32

2.2. Pericam constructs Page 32

2.3. Mouse embryonic cell culture and transfection Page 33

2.4. Neuronal cell culture and transfection Page 33

2.5. Fura-FF and TMRM Page 35

2.6. Fluorescence imaging Page 36

2.7. Image analysis Page 37

2.8. Statistical analysis Page 38

**PART 3. RESULTS** Page 39

3.1. Mitochondrial $Ca^{2+}$ in mouse embryonic fibroblasts Page 39

3.2. Mitochondrial $Ca^{2+}$ in neurons in response to a single stimulus Page 42

3.3. Mitochondrial $Ca^{2+}$ in neurons in response to dual stimuli Page 53

3.4. Mitochondrial $Ca^{2+}$ in neurons pretreated with cyclosporine A in response to dual stimuli Page 59

3.5. Mitochondrial membrane potential in neurons in response to dual stimuli Page 62

3.6. Mitochondrial $Ca^{2+}$ in neurons in response to oxidative stress Page 66

3.7. Mitochondrial $Ca^{2+}$ in neurons pretreated Page 74

with CsA in response to oxidative stress

3.8. Mitochondrial membrane potential in neurons Page 76

in response to oxidative stress

**PART 4. DISCUSSION** Page 78

4.1. No PTP formed in neurons in response to a single stimulus Page 78

4.2. PTP opening was activated in neurons by dual stimuli Page 81

4.3. Role of CyPD inactivation in PTP opening in neurons Page 84

in response to dual stimuli

4.4. Role of CyPD inactivation in PTP opening in neurons Page 89

under oxidative stress

**PART 5. CONCLUSIONS** Page 94

**PART 6. REFERENSES** Page 98

## LIST OF ILLUSTRATIONS

**Figure 1**. Principal organelles that play role in cellular $Ca^{2+}$ Page 8

**Figure 2.** $Ca^{2+}$ influx and extrusion pathways in inner mitochondria membrane Page 12

**Figure 3.** $Ca^{2+}$ uptake in isolated brain mitochondria from WT and CyPD-KO mice Page 17

**Figure 4.** Image of cortical neurons in adult mouse cortical culture Page 27

**Figure 5.** Co-localization of mitochondrially-targeted $Ca^{2+}$ indicator inverse pericam and Mitotracker in a mouse embryonic fibroblast Page 40

**Figure 6.** Cytosolic and mitochondrial $Ca^{2+}$ in responses to ATP in WT and CyPD-null mouse embryonic fibroblasts Page 41

**Figure 7.** Image of a live adult cultured cortical neuron transfected with mitochondrially-targeted $Ca^{2+}$ indicator ratiometric pericam. Page 43

**Figure 8.** Cytosolic $Ca^{2+}$ responses to ATP in WT and CyPD-null cortical neurons Page 45

**Figure 9.** Mitochondrial $Ca^{2+}$ responses to ATP in WT and CyPD-null cortical neurons Page 47

**Figure 10.** Cytosolic $Ca^{2+}$ responses to DHPG in WT and CyPD-null cortical neurons Page 48

**Figure 11.** Mitochondrial $Ca^{2+}$ responses to DHPG in WT and CyPD-null cortical neurons Page 49

**Figure 12.** Cytosolic $Ca^{2+}$ responses to KCl in WT and CyPD-null cortical neurons Page 51

**Figure 13**. Mitochondrial $Ca^{2+}$ responses to KCl in WT and CyPD-null cortical neurons Page 52

**Figure 14.** Cytosolic $Ca^{2+}$ responses to $ATP^{+}KCl$ in WT and CyPD-null cortical neurons Page 54

**Figure 15**. Mitochondrial $Ca^{2+}$ responses to $ATP^{+}KCl$ in WT and CyPD-null cortical neurons Page 56

**Figure 16**. Mitochondrial $Ca^{2+}$ retention in response to $ATP^{+}KCl$ in WT and CyPD-null cortical neurons Page 57

**Figure 17**. Mitochondrial morphology in WT and CyPD-null cortical neurons before and after the stimulation with $ATP^{+}KCl$ Page 58

**Figure 18**. Mitochondrial $Ca^{2+}$ responses to $ATP^{+}KCl$ in WT and CyPD-null cortical neurons pretreated with cyclosporin A — Page 60

**Figure 19**. Mitochondrial $Ca^{2+}$ retention in response to $ATP^{+}KCl$ in WT and CyPD-null cortical neurons pretreated with cyclosporin A — Page 61

**Figure 20**. Mitochondrial membrane potential responses to $ATP^{+}KCl$ in WT and CyPD-null cortical neurons — Page 64

**Figure 21**. Mitochondrial membrane potential responses to ATP in WT and CyPD-null cortical neurons — Page 65

**Figure 22.** Viability of WT and CyPD-null neurons following hydrogen peroxide treatment — Page 67

**Figure 23.** Cytosolic $Ca^{2+}$ responses to 20 μM hydrogen peroxide in WT and CyPD-null cortical neurons — Page 69

**Figure 24.** Cytosolic $Ca^{2+}$ responses to 100 μM hydrogen peroxide in WT and CyPD-null cortical neurons — Page 70

**Figure 25.** Mitochondrial $Ca^{2+}$ responses to 20 μM hydrogen peroxide in WT and CyPD-null cortical neurons — Page 71

**Figure 26.** Mitochondrial $Ca^{2+}$ responses to 100 μM hydrogen peroxide in WT and CyPD-null cortical neurons Page 72

**Figure 27.** Mitochondrial $Ca^{2+}$ responses to 100 μM hydrogen peroxide in WT and CyPD-null cortical neurons pretreated with cyclosporin A Page 75

**Figure 28.** Mitochondrial membrane potential responses to 100 μM hydrogen peroxide in WT and CyPD-null cortical neurons Page 77

**Figure 29.** Mitochondrial $Ca^{2+}$ responses to ATP pulses in WT and CyPD-null neurons prepared from adult mice Page 80

**Figure 30.** Mitochondrial $Ca^{2+}$ responses to ATP in WT and CyPD-null cortical neurons (longer time course) Page 86

## LIST OF ABBREVIATIONS

AD, Alzheimer's disease

ALS, amyotrophic lateral sclerosis

ANT, adenine nucleotide translocator

ATP, adenosine triphosphate

CIRC, calcium-induced calcium release

CsA, cyclosporin A

CyPD, cyclophilin D

DHPG, (*S*)-3,5-dihydroxyphenylglycine

EAE, experimental autoimmune encephalomyelitis

ER, endoplasmic reticulum

GFP, green fluorescent protein

HD, Huntington disease

IMM, inner mitochondrial membrane

IP3R, inositol 1,4,5-trisphosphate receptor

mGluR, metabotropic glutamate receptor

MEF, mouse embryonic fibroblast

MitoIP, mitochondrially-targeted inverse pericam

MitoRP, mitochondrially-targeted ratiometric pericam

MS, Multiple sclerosis

NMDA, N-methyl-D-aspartic acid

OMM, outer mitochondrial membrane

PD, Parkinson's disease

PT, permeability transition

PTP, permeability transition pore

ROS, reactive oxygen species

RyR, ryanodine receptor

VDAC, voltage-dependent anion channel

## ACKNOWLEDGMENTS

I would like thank my mentor, Dr. Mike Forte, for his teaching, knowledge, patience, care and support which were invaluable to the completion of this project and to my graduate study.

I would like to thank my co-mentor Dr. Dennis Bourdette for his encouragement, support and creating an environment that allowed this challenging project to succeed.

I would like to thank members of my graduate committee, Dr. Gary Banker and Dr. Charles Allen, for their guidance and support which greatly aided the progress of this project.

I would like to thank Dr. Gyorgy Hajnoczky, Thomas Jefferson University, for his teaching and guidance in learning the essential techniques necessary for this project.

I would like to thank members of Dr. Mike Forte's laboratory for their assistance on this project.

I would like to thank the faculty and staff of the Neuroscience Graduate Program for their teaching and truly wonderful graduate years at OHSU.

I would like to thank my dear father and mother for introducing me to the beauty of science from a very young age and for supporting me on this path throughout my life.

I would like to thank my husband Steve for his love, support and kind admiration of my work.

I would like to thank my friend Dr. Irina Minko, OHSU, for her encouragement and advice throughout my study.

This thesis work was supported by grants from the National Institutes of Health, the National Multiple Sclerosis Society, the Laura Fund for Innovation in Multiple Sclerosis

Research, OHSU Brain Institute Fellowship, The St. Laurent Foundation and Eugene Group for Multiple Sclerosis.

## ABSTRACT

Numerous studies have shown that critical aspects of the pathology associated with a wide variety of neurodegenerative diseases may be based in mitochondrial dysfunction, in particular defects in mitochondrial $Ca^{2+}$ homeostasis. A key aspect of the mitochondrial $Ca^{2+}$ regulation is the permeability transition (PT), which depends on the opening of an inner membrane channel, the mitochondrial permeability transition pore (PTP). Inappropriate activation of the PTP depletes mitochondrial $Ca^{2+}$ stores, elevates cytosolic $Ca^{2+}$ and increases the generation of reactive oxygen species, ultimately leading to depletion of cellular ATP and cell death. A key regulator of the PTP is cyclophilin D (CyPD), a cyclophilin found exclusively in mitochondria. Initial studies in mice have demonstrated that inactivation of the nuclear gene encoding CyPD (CyPD-KO) results in neuroprotection following a number of pathologic challenges such as ischemia/reperfusion and experimental autoimmune encephalomyelitis, EAE, a mouse model of multiple sclerosis. Studies on isolated mitochondria prepared from a number of tissues demonstrate that many cell types from CyPD-KO animals are able to accumulate higher levels of $Ca^{2+}$ than WT mitochondria yet the cellular correlate of this *in vitro* response has not been carefully investigated. To address this question, the present study compared mitochondrial $Ca^{2+}$ dynamics in primary cortical neurons isolated from adult CyPD-KO and WT mice using a fluorescent, $Ca^{2+}$ indicator, ratiometric pericam, targeted to mitochondria. Mitochondria in CyPD-KO neurons were able to accumulate significantly higher levels of $Ca^{2+}$ than mitochondria in WT neurons in response to the combined actions of depolarization and receptor activation coupled to $Ca^{2+}$ release from endoplasmic reticulum (ER), while no difference was observed in response to either

stimulus alone. This suggest that CyPD inactivation leads to a delay in the PTP opening in CyPD-null neurons in response to elevated cytosolic $Ca^{2+}$ levels created by combined stimuli. Furthermore, the study shows that CyPD inactivation leads to a modulation of PTP opening and mitochondria $Ca^{2+}$ dynamics in response to the oxidative stress. The results also show that CyPD-null adult cortical neurons are significantly less susceptible to oxidative challenges. Therefore, this study demonstrates for the first time mitochondrial $Ca^{2+}$ dynamics in live adult cortical neurons and the modulation of mitochondrial $Ca^{2+}$ and PTP opening by CyPD inactivation under elevated cytosolic $Ca^{2+}$ levels and oxidative stress. Establishing the parameters for the prevention of PTP opening in neurons under elevated cytosolic $Ca^{2+}$ and oxidative stress is essential for the development of neuroprotective strategies. CyPD inactivation may become a key neuroprotective target in the development of therapies for neurodegenerative diseases.

# 1. INTRODUCTION

Mitochondria are the cellular organelles responsible for the cellular energy supply and therefore for sustaining cellular well-being. While this role for mitochondria in cell function has been well established, over the past decade abundant evidence has also demonstrated that mitochondria are key players in multiple cellular processes, including cell death. Investigation of pathologic mechanisms at play in a number of neurodegenerative conditions suggests that mitochondrial dysfunction could be a central event in apoptosis and necrosis in neurons. In particular, the focus of the thesis work presented here supports the idea that defects in mitochondrial $Ca^{2+}$ uptake and release are at the heart of the mitochondrial dysfunction associated with neurodegenerative diseases. Indeed, increasing evidence generated through animal models and detailed study of human subjects facing neurological challenges demonstrate perturbed mitochondrial $Ca^{2+}$ homeostasis in a variety of neurodegenerative diseases of different etiologies, such as stroke, multiple sclerosis, Alzheimer's disease and amyotrophic lateral sclerosis. In these neurodegenerative pathologies changes in glutamate homeostasis, exposure of neurons to hydrogen peroxide, superoxide, nitric oxide, hydroxyl radicals and other important players result in altered mitochondrial $Ca^{2+}$ homeostasis and the ensuing mitochondrial dysfunction, amplifying the $Ca^{+}$-driven mitochondrial dysfunction and ultimately, the release of pro-apoptotic proteins. While much about the molecular players involved in these pathologies is known, it is not known how such degeneration can be prevented.

This thesis describes studies that test the role of one pathway proposed to be involved in neuronal mitochondrial $Ca^{2+}$ homeostasis, the permeability transition (PT).

Permeability transition represents the major pathway for $Ca^{2+}$ release from mitochondria under normal conditions. Opening of the permeability transition pore (PTP) in response to elevated mitochondrial $Ca^{2+}$ regulates the PT, and inappropriate PTP activation in response to pathological triggers has dramatic consequences on mitochondrial function, leading to respiratory inhibition. Inappropriate regulation of the PTP has long been studied as a key mechanism underlying mitochondrial dysfunction and cell death in pathological events. A particular target for the prevention of the inappropriate PTP activation – cyclophilin D (CyPD), a protein found exclusively in the mitochondrial matrix – has been shown to play an important role in neuroprotection.

In the past decade, the role of CyPD inactivation in neuroprotection was firmly established in mouse models of stroke (Schinzel *et al.*, 2005), multiple sclerosis (Forte *et al.*, 2007), Alzheimer's disease (Du *et al.*, 2008) and amyotrophic lateral sclerosis (Martin et al., 2009). In all of these studies, the assumed target of CyPD inactivation is the mitochondrial PTP. While CyPD almost certainly participates in other mitochondrial protein complexes, its role in the regulation of the PTP has been confirmed by *in vitro* studies of isolated mitochondria generated from many tissues. Consequently, the *in vivo* results presented in previous studies and in the work presented here make it reasonable to assume that the phenotypes observed in tissues and animals missing CyPD are due to its role in the regulation of the PTP. Thus, while it may appear unusual that diseases of different etiologies affecting different tissues can be altered by the absence of CyPD, one common player - mitochondrial PTP - can be implicated in all cases. However, the mitochondrial dysfunction associated with PTP is not proposed to be a common cause for the onset of these diseases. Rather it is proposed as a common “end-mechanism” when

pathologic extracellular and intracellular conditions brought on by a disease course favor the PTP opening and disrupt mitochondrial function. It is not unusual then to expect that the preservation of mitochondrial function in neurons in diseases of different etiologies will extend cellular lifespan and delay or prevent disease progression.

The key activators of PTP are mitochondrial $Ca^{2+}$ accumulation, oxidative stress, adenine nucleotide depletion, and uncouplers. Neurons rely on $Ca^{2+}$ fluxes for their primary functions – neuronal firing. Their vital dependence on $Ca^{2+}$ and $Ca^{2+}$ regulatory machinery can make $Ca^{2+}$ perturbation especially catastrophic in this type of cell. Therefore, understanding of the role of CyPD inactivation in the preservation of the mitochondrial function may be critical in the development of therapeutic interventions in the treatment of several leading neurodegenerative diseases. Prevention of the inappropriate PTP opening via CyPD inactivation in response to mitochondrial $Ca^{2+}$ accumulation and oxidative stress, two major players implicated in neurodegeneration, has been extensively studied and clearly demonstrated only in isolated mitochondria. It is not clear whether the prevention of the inappropriate PTP opening via CyPD inactivation is an underlying mechanism of neuroprotection, observed in animal models of neurodegeneration.

Our study investigated for the first time the role of CyPD in mitochondrial $Ca^{2+}$ dynamics and PTP in cortical neurons cultured from adult mice. The key activators of PTP, mitochondrial $Ca^{2+}$ accumulation and oxidative stress, were tested in this investigation. The results of this study demonstrate two novel findings on the role of CyPD in mitochondrial biology in cortical neurons. First, CyPD inactivation modulates mitochondrial $Ca^{2+}$ load capacity and PTP opening in neurons under elevated cytosolic

$Ca^{2+}$ levels. Second, CyPD inactivation modulates mitochondrial $Ca^{2+}$ and PTP opening in neurons under oxidative stress.

### 1.1. Calcium roles and regulation in neurons and mitochondria

Calcium is an essential ion in the development, functionality and plasticity of the nervous system. For example, calcium ions regulate synaptic vesicles fusion and release (Kandel 2000). During depolarization, neurons rapidly undergo a dramatic cytosolic $Ca^{2+}$ rise and decline that can also be followed by a slow $Ca^{2+}$ response phase that forms a plateau. This elevated $Ca^{2+}$ plateau phase, triggered by repetitive stimulation, creates a basis for posttetanic potentiation of synaptic transmission (Tang and Zucker 1997). Calcium also acts as a second messenger modulating the gating of ion channels, regulates key metabolic enzymes in mitochondria, controls cell cycle protein expression and promotes cell proliferation (Means 1994; Lu *et al.,* 1994; Hille 2001). However, the effect of changes in cytosolic $Ca^{2+}$ concentrations on mitochondrial $Ca^{2+}$ in neurons, specifically during neurodegeneration, has not been established. This thesis focuses on the shirt-term effects (1 to 9 min) of cytosolic $Ca^{2+}$ elevation and oxidative stress on mitochondrial $Ca^{2+}$ dynamics in neurons. Several systems that govern $Ca^{2+}$ homeostasis in neurons were engaged and activated in this study in order to experimentally regulate cytosolic $Ca^{2+}$ levels.

Multiple extracellular and intracellular systems are involved in neuronal calcium handling. Outside the cell, neurotransmitters, hormones, voltage-changes and sensory

inputs regulate $Ca^{2+}$ entry (Hille 2001). Calcium can enter neurons through several pathways along the plasma membrane: voltage-gated $Ca^{2+}$ channels, ligand-gated channels (NMDAR and AMPAR), receptor-operated channels, $Na^{+}$-$Ca^{2+}$ exchanger and plasma membrane $Ca^{2+}$ ATPase (Hille 2001). Upon entry, $Ca^{2+}$ ions are found in several cellular compartments, including cytosol and major intracellular $Ca^{2+}$ stores - endoplasmic reticulum (ER) and mitochondria. Notably, most $Ca^{2+}$ ions in neurons form complexes with $Ca^{2+}$-regulating factors such as $Ca^{2+}$-binding proteins (calmodulin, parvalbumin, calbindin and calretinin). Since resting extracellular $Ca^{2+}$ concentration (2 mM) is greater than resting intracellular levels (100 nM) by orders of magnitude, $Ca^{2+}$ influx into a neuron may dramatically change intracellular $Ca^{2+}$ concentration.

Changes in cytosolic $Ca^{2+}$ concentration are immediately reflected in the mitochondrial $Ca^{2+}$ level. Studies in isolated mitochondria have shown that they can rapidly take up $Ca^{2+}$ from the medium (Lucas *et al.,* 1978). The first evidence of mitochondrial $Ca^{2+}$ uptake in intact cells came from measurements of mitochondrial redox state in response to changes in cytosolic $Ca^{2+}$ (Duchen 1992). More recent studies using $Ca^{2+}$-sensitive indicators directly confirmed mitochondrial $Ca^{2+}$ uptake in a variety of intact cells (Szabadkai *et al.,* 2006). Initially, several theories on the role of mitochondrial $Ca^{2+}$ in cellular $Ca^{2+}$ homeostasis were proposed, including the role of mitochondria as $Ca^{2+}$ stores for rapid $Ca^{2+}$ mobilization and as a reserve pool where excess cellular $Ca^{2+}$ can accumulate following the release from the endoplasmic reticulum $Ca^{2+}$ (Lehninger 1970).

However, evidence also demonstrates that $Ca^{2+}$ plays an important role in the primary mitochondrial function - ATP production - via regulation of mitochondrial oxidative

phosphorylation (McCormack and Denton 1993). Increased mitochondrial calcium uptake has been observed in response to increased energy demand, which in turn stimulates ATP production via calcium-dependent upregulation of mitochondrial enzyme activity (Devin and Rigoulet 2007). Mitochondrial $Ca^{2+}$ activates key metabolic enzymes responsible for ATP production: pyruvate dehydrogenase via $Ca^{2+}$-dependent dephosphorylation and alpha-ketoglutarate and isocitrate dehydrogenases via direct binding of $Ca^{2+}$ to the enzyme complex (McCormack and Denton 1993). Mitochondrial $Ca^{2+}$ also stimulates ATP synthase, α-glycerophosphate dehydrogenase and adenine nucleotide translocase (ANT) and regulates activation of *N*-acetylglutamine synthase and its downstream effect on the urea cycle (McGivan *et al.,* 1976; Das and Harris 1990; Das and Harris 1990; Wernette *et al.,* 1981; Mildaziene *et al.,* 1995). Changes in cytosolic $Ca^{2+}$, specifically temporal changes in cytosolic dynamics, were shown to modulate mitochondrial $Ca^{2+}$ fluxes, thus modulating activation of $Ca^{2+}$-regulated enzymes (Duchen 1992). This suggests that mitochondrial $Ca^{2+}$ translates the level of neuronal activity into the adequate level of ATP production.

There are several important players in mitochondrial $Ca^{2+}$ uptake and extrusion. First, the mitochondrial transmembrane $H^{+}$ gradient creates an electrochemical driving force for $Ca^{2+}$ ion influx. Second, during neuronal activity when cytosolic $Ca^{2+}$ rises, $Ca^{2+}$ gradient between cytosol and the mitochondrial matrix also creates a driving force for $Ca^{2+}$ ions. The outer mitochondria membrane (OMM) has one identified regulator of $Ca^{2+}$ entry - mitochondrial voltage-dependent anion channel (VDAC) (Bernardi 1999). The inner mitochondria membrane (IMM) controls $Ca^{2+}$ entry via the mitochondrial $Ca^{2+}$ uniporter (MCU). The molecular structure of the MCU, the main $Ca^{2+}$ influx pathway,

remains unclear but its properties have been well studied. The MCU is characterized by a high $Ca^{2+}$ selectivity, a $Ca^{2+}$ influx rate of fast-gated pores and ruthenium red sensitivity (Kirichok *et al.,* 2004). Along with the MCU, another mitochondrial $Ca^{2+}$ influx pathway – the rapid uptake mode – has been shown, but its properties are not well characterized (Buntinas *et al.,* 2001). The rapid uptake mode allows for very rapid $Ca^{2+}$ influx into mitochondria during a cytosolic $Ca^{2+}$ increase.

The major pathway for $Ca^{2+}$ efflux from mitochondria is controlled by the $Na^{+}$-$Ca^{2+}$ exchanger. Its molecular properties are not fully defined, and its stoichiometry remains a matter of controversy (Jung *et al.,* 1995). Exchange of $3Na^{+}/Ca^{2+}$ was suggested instead of an initially proposed exchange of $2Na^{+}/Ca^{2+}$ (Jung *et al.,* 1995). Another pathway for $Ca^{2+}$ efflux from mitochondria is via the PTP, the formation of which has historically been associated with mitochondrial dysfunction. The non-transient PT leading to PTP formation in neurons and its regulation is the focus of this thesis work. Under normal conditions, small 'flickering' PTs are believed to transiently regulate mitochondrial $Ca^{2+}$ efflux without significant changes in mitochondrial homeostasis (Ichas *et al.,* 1997).

Figure 1 shows principal organelles that play role in cellular $Ca^{2+}$ handling and the pathways for mitochondrial $Ca^{2+}$ uptake. $Ca^{2+}$ released from the (ER) and $Ca^{2+}$ influx through plasma membrane are two major $Ca^{2+}$ sources for mitochondrial $Ca^{2+}$ (Figure 1) (Szabadkai and Duchen 2008), and this thesis focuses on studies that activate both of these pathways. The ER has its own $Ca^{2+}$-regulating machinery. ER calcium is accumulated by the action of SERCA, sarcoplasmic endoplasmic reticulum $Ca^{2+}$ ATPase.

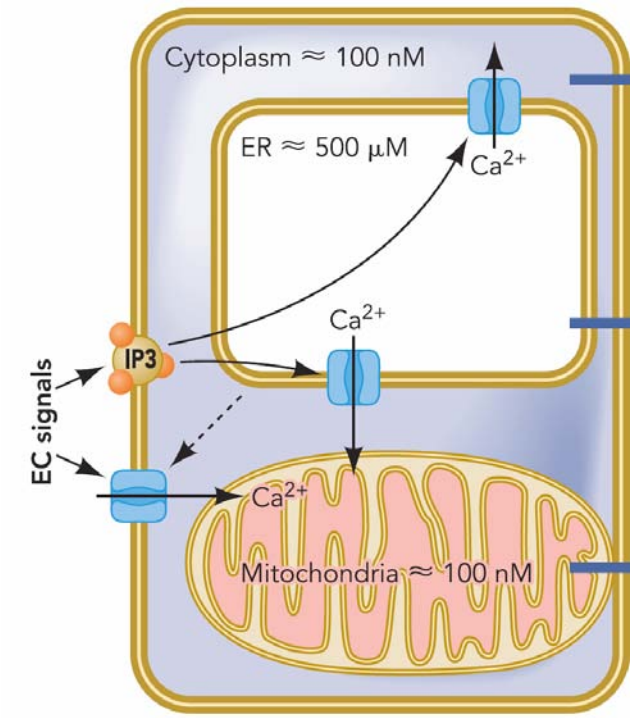


**Figure 1.** Model of the cell shows three principal organelles that play role in cellular $Ca^{2+}$ handling: mitochondria, endoplasmic reticulum (ER) and cytosol with $Ca^{2+}$ influx pathways via plasma membrane, and their resting $Ca^{2+}$ concentrations (Figure by György Szabadkai and Michael R. Duchen. 2008. Physiology, 23: 84–94).

$Ca^{2+}$ is released from the ER via two channels, inositol 1,4,5-trisphosphate receptors (IP3R), which were activated in this study, and ryanodine receptors (RyR) (Romagnoli *et al.*, 2007).

Formation of inositol 1,4,5-trisphosphate (IP3) (Figure 1) follows the activation of the large family of G-protein coupled receptors that activate the formation of IP3 in response to a wide variety of extracellular ligands; for example, P2Y-purinoceptors by purines (ATP and analogues). P2 nucleotide receptors are represented by two receptor subfamilies: G-protein coupled P2Y receptors and P2X receptors, which are ligand-gated ion channels. Activation of P2Y receptors by its agonists (ATP, UTP) increases the activity of phospholipase C leading to intracellular generation of IP3 from the plasma membrane phosphatidylinositol 4,5-bisphosphate ($PIP_2$). Activation of the ER's IP3R receptors by IP3 or RyR receptors by caffeine or other agents leads to rapid ER $Ca^{2+}$ release followed by mitochondrial $Ca^{2+}$ uptake.

Spatial proximity of mitochondria and ER ensures fast $Ca^{2+}$ signaling between these organelles. Domains of the ER are closely associated with mitochondria (Franzini-Armstrong 2007). The distribution of mitochondria within cells is regulated by mitochondria-ER communication, and mitochondria arrange in close association with $Ca^{2+}$ release sites of ER (Rizzuto *et al.*, 1993). Numerous data have confirmed that the $Ca^{2+}$ microenvironment determines mitochondrial uptake and in particular a fast and closely localized $Ca^{2+}$ release through activation of IP3Rs in the ER (Rizzuto *et al.*, 1993; Rizzuto *et al.*, 2004). Association between IP3R-containing ER membranes and mitochondria has been shown (Csordas *et al.*, 2006). Physical links - tethers- between mitochondria and ER have recently been clearly demonstrated. One study (de Brito and

Scorrano 2008) showed that a specific protein, mitofusin 2, tethers ER to mitochondria. Mitochondria are motile organelles, but the evidence of physical tethers suggests that they may stay in position at least for periods of time. Moreover, a recent study shows that $Ca^{2+}$ communication between mitochondria and ER can be controlled by the actual distance between the organelles via tethers (Csordas *et al.,* 2006).

### 1.2. What is mitochondrial permeability transition?

Mitochondrial dysfunction brought on by changes in mitochondrial $Ca^{2+}$ homeostasis is now being considered as a key player in cell death in multiple diseases. $Ca^{2+}$-driven PT is specifically implicated as an initial step in apoptotic and necrotic cell death stemming from mitochondrial dysfunction (Bernardi *et al.,* 2006) and mitochondrial $Ca^{2+}$ overload. PT is thought to occur following the formation of a non-specific pore in the inner mitochondrial membrane, the PTP (Zoratti and Szabo 1995; Bernardi *et al.,* 1999; Halestrap *et al.,* 2002; Brookes *et al.,* 2004; Forte and Bernardi 2005; Bernardi 1996; Bernardi *et al.,* 2006). Open–closed transitions of the PTP are regulated by multiple factors: mitochondrial $Ca^{2+}$ accumulation, adenine nucleotide depletion, oxidative stress and uncouplers. However, of these factors, mitochondrial $Ca^{2+}$ accumulation has been shown to most readily activate PT.

Unregulated, non-transient PT is defined by an increase of mitochondrial inner membrane permeability to molecules of less than 1500 daltons. It is characterized by the following mitochondrial events: depolarization of inner mitochondrial membrane, which

then leads to a collapse of mitochondrial respiration and ATP production, matrix swelling, outer membrane rupture and release of pro-apoptotic agents such as cytochrome c, Smac-Diablo, AIF and endonuclease G (Figure 2) (Zoratti and Szabo 1995; Bernardi *et al.*, 1999; Halestrap *et al.*, 2002; Brookes *et al.*, 2004; Forte and Bernardi 2005; Bernardi 1996; Bernardi *et al.*, 2006).

Permeability transition was demonstrated in isolated mitochondria over 40 years ago (Crofts and Chappell 1965). Initially, the PT was assayed in these isolated mitochondria by monitoring mitochondrial swelling, which follows the PT due to osmotic water flux across the membrane and by a decrease in absorbance measured spectrophotometrically (Forte and Bernardi 2005). However, in intact cells, mitochondrial swelling following the PT may not occur as readily since non-diffusible molecules in the cytosol can counterbalance the osmotic pressure created by the mitochondrial matrix proteins (Forte and Bernardi 2005). More recently, the PT has also been assayed by assessing a parameter defined as the $Ca^{2+}$ retention capacity (CRC) (Bopassa *et al.*, 2006). The CRC technique allows the assessment the PTP opening in isolated mitochondria following mitochondrial $Ca^{2+}$ overload. Here, isolated mitochondria are prepared in a standard reaction buffer containing a low-affinity fluorescent $Ca^{2+}$ indicator, such as Calcium Green-5N, which is not mitochondria-permeable. $Ca^{2+}$ pulses added to the buffer lead to increased fluorescence as reported by extramitochondrial Calcium Green. This fluorescence declines over time, representing $Ca^{2+}$ uptake by mitochondria from the buffer; mitochondria have a higher affinity for the added $Ca^{2+}$ than Calcium Green.

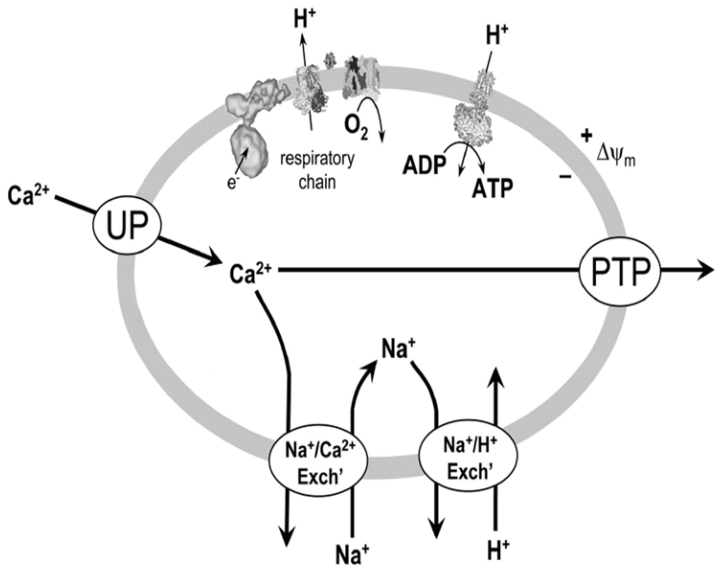


**Figure 2.** Model of inner mitochondria membrane (IMM) shows (1) calcium influx via $Ca^{2+}$ uniporter, UP, (2) calcium efflux via exchangers, (3) permeability transition pore, PTP, formation in response to high $Ca^{2+}$ concentration in the matrix and (3) respiratory chain complex and mitochondrial membrane potential along IMM (Figure by Brooks et al. 2004. Am J Physiol Cell Physiol 287).

With each additional $Ca^{2+}$ pulse, mitochondria accumulate more $Ca^{2+}$ until mitochondria reach their $Ca^{2+}$ retention capacity. When this capacity is reached, additional $Ca^{2+}$ pulses lead to the mitochondrial $Ca^{2+}$ overload and the PTP opening. The PTP opening is reported by a rapid, sudden and irreversible increase in Calcium Green fluorescence, reflecting both the inability of mitochondria to take up more $Ca^{2+}$ from the buffer and the mitochondrial $Ca^{2+}$ efflux via the PTP (an example is shown in Figure 3). Finally, assays of PT activity in intact cells have been based on loading cells with the fluorescent dye calcein-AM, which localizes to both cytosol and mitochondria. To selectively visualize calcein-AM in mitochondria, cytosolic calcein-AM fluorescence is quenched with $Co^{2+}$ (Petronilli et al., 1999). On the opening of the PTP, calcein-AM is released from the mitochondrial matrix. Corresponding decrease in calcein-AM fluorescence in mitochondria allows detection of the PTP opening in intact cells. This thesis study used more advanced, genetically encoded $Ca^{2+}$ indicators targeted to mitochondria of mouse embryonic fibroblasts and neurons, as described further in section 1.4.

### 1.3. Cyclophilin D is a regulator of the PTP

The discovery that the immunosuppressive drug cyclosporine A (CsA) inhibits PTP suggested that the cyclophilin isoform that specifically resides in mitochondria, cyclophilin D (CyPD), was a target molecule for CsA and in some way regulated the activity of the PTP (McGuinness *et al.*, 1990). CyPD is a member of the immunophilin family of proteins (Harding and Handschumacher 1988). Immunophilins are soluble cytosolic receptors capable of binding to immunosuppressant agents (McGuinness *et al.*,

1990). Immunophilins function as peptidyl prolyl cis-trans-isomerases that accelerate the folding of individual proteins by catalyzing the rearrangement of proline-containing protein segments. Immunophilin have two subgroups which include cyclophilins (CyPA, CyPB, CyPD) which bind cyclosporin A and FKBPs, which bind to a separate inhibitor, FK506. The immunophilin-immunosuppressant complexes cyclophilin-CsA and FKBP12-FK506 inhibit the phosphatase calcineurin to block T-cell activation.

CyPD is an 18 kDa cyclophilin isoform exclusively found in the mitochondrial matrix. Biochemical studies have established CyPD as a key regulator of PTP function by demonstrating that CsA inhibits the PTP by modulating CyPD-dependent activation of the pore complex (Zoratti and Szabo 1995; Halestrap *et al.,* 2002; Forte and Bernardi 2005). CyPD has high affinity for CsA, and the PTP can be inhibited even by low concentrations of the CsA (McGuinness *et al.,* 1990; Halestrap *et al.,* 1997). Increasing the amount of $Ca^{2+}$ in mitochondrial matrix has been shown to suppress CsA binding to PTP high-affinity binding sites (McGuinness *et al.,* 1990). However, increasing the concentrations of CsA under high $Ca^{2+}$ conditions prevents PTP opening, supporting the role of CyPD in PTP regulation (McGuinness *et al.,* 1990). $Ca^{2+}$-driven PTP activation can occur in the presence of CsA, though the $Ca^{2+}$ load must be significantly higher to trigger the PTP opening. Recently, studies using CyPD-null mice provided additional evidence for the regulation of the PTP by CyPD (Basso *et al.,* 2005; Baines *et al.,* 2005). These studies demonstrated that the elimination of CyPD dramatically increased mitochondrial $Ca^{2+}$ load and delayed PTP opening, and mitochondria prepared from CyPD-null mice were insensitive to CsA treatment.

Formation of the PTP in the inner mitochondrial membrane, its direct correlation with PT occurrence, and its nature as a "pore" was confirmed by two findings: (a) discovery of a high-conductance mitochondrial megachannel that regulates PT and is also inhibited by CsA and (b) demonstration that both PT and PTP are controlled by the proton electrochemical gradient (Broekemeier *et al.,* 1989; Szabo and Zoratti 1991; Bernardi *et al.,* 1992). Evidence defines the PTP as a CsA-sensitive, high-conductance, voltage-dependent channel of the inner mitochondrial membrane. However, the molecules forming the "pore" of the PTP have long been a matter of intense debate. Two candidate constituents of the PTP have been historically proposed, the voltage-dependent anion channel (VDAC) of the outer mitochondrial membrane and the adenine nucleotide translocator (ANT) of the inner membrane (Halestrap *et al.,* 2002; Bernardi *et al.,* 2006; Halestrap *et al.,* 2000; Halestrap and Brennerb 2003; Palmieri 2004). VDAC in the outer mitochondrial membrane plays an important role in the regulated flux of metabolites between the cytosol and mitochondrial compartments. Involvement of VDAC in the formation of PTP was suggested mainly on the evidence that (a) VDAC and PTP activity are regulated by the same conditions and (b) properties of purified VDAC in a lipid bilayer model are similar to properties of PTP in mitochondria (Zizi *et al.,* 1994; Gincel *et al.,* 2001; Szabo *et al.,* 1993). However, the direct involvement of VDAC in PTP function has not been demonstrated *in vivo* (Bernardi *et al.,* 2006). Moreover, a recent study using isolated mitochondria and fibroblasts from mice in which three mammalian *Vdac* genes were deleted demonstrated that activation of PTP opening in these mitochondria by $Ca^{2+}$ overload and oxidative stress was indistinguishable from WT mitochondria (Baines *et al.,* 2007). Therefore, PTP can form in the absence of VDAC.

ANT is a transporter of the inner mitochondrial membrane that catalyses the exchange of ATP and ADP across the inner membrane into the intermembrane space and eventual release into the cytosol. Based on the evidence that PTP can be modulated by ANT ligands (atractylate, bongkrekate) and reconstitution of ANT in liposomes shows $Ca^{2+}$-driven channel activity, it was suggested that formation of PTP requires ANT (Halestrap and Brennerb 2003; Rottenberg and Marbach - I 1990; Rottenberg and Marbach - II 1990). However, a study using mitochondria that lacks ANT isoforms conclusively demonstrated $Ca^{2+}$-driven PT occurrence in the absence of ANT (Kokoszka *et al.,* 2004). Therefore, CyPD, whose role is now well established through its inhibition by CsA, remains the only known regulator of the PTP.

Ablation of the nuclear *Ppif* gene, which encodes CyPD in a mouse, further confirmed the role of CyPD as a key regulator of PTP. Inactivation of CyPD in mice resulted in a significant increase in mitochondrial $Ca^{2+}$ load capacity (as measured by Calcium Green indicator) and the threshold level needed for the PTP opening (Baines *et al.,* 2005; Basso *et al.,* 2005). Figure 3 shows mitochondrial calcium uptake in isolated brain mitochondria from WT and CyPD-KO mice in response to $Ca^{2+}$ pulses as measured by the CRC assay outlined earlier. Retention capacity and the threshold for PTP opening in mitochondria prepared from CyPD-null mice were significantly higher when compared to mitochondria prepared from WT mice (Figure 3). Also, the retention capacity of WT mitochondria was increased by addition of CsA and was similar to that observed in CyPD-null mitochondria (Figure 3). Together these results demonstrate the essential role of CyPD as a major regulator if the PTP.

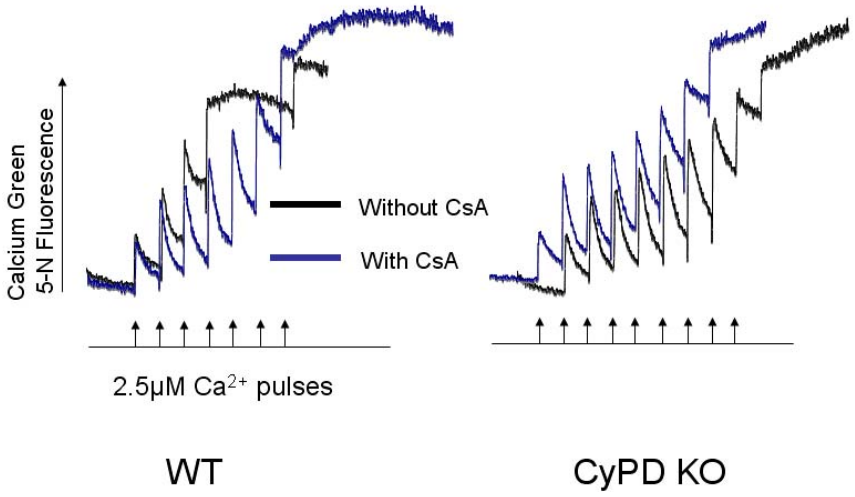


**Figure 3.** Calcium uptake in isolated brain mitochondria from WT and CyPD-KO mice in response to $Ca^{2+}$ pulses. Inactivation of *Ppif* gene (CyPD KO) or CyPD inactivation by CsA (WT with CsA) resulted in a significant increase in mitochondrial $Ca^{2+}$ load capacity and the threshold level needed for the PTP opening (Figure by Forte et al. 2007. PNAS 104:18).

In addition to $Ca^{2+}$ overload, oxidative stress can also trigger PTP opening can also be activated in isolated mitochondria preparations in response to. Mitochondria are a significant source of reactive oxygen species (ROS), a known cause of oxidative stress (Inoue *et al.,* 2003). Previously ROS were considered to be by-products of mitochondrial respiration, leading to oxidative damage and contributing to aging (Harman 2003). However, more recent evidence has shown that mitochondrially derived ROS are important for multiple cell signaling processes such as cell cycle, proliferation, enzyme function, and apoptosis (Brookes *et al.,* 2004). Perturbations in mitochondrial ROS production have been linked to changes in mitochondrial $Ca^{2+}$ homeostasis. Studies on isolated mitochondria showed that ROS generation coincides with PT pore opening in response to $Ca^{2+}$ (Castilho *et al.,* 1995).

However, it remains unclear whether ROS generation is an activator or a consequence of PT pore opening. One set of studies support the idea that ROS is a consequence of PTP. Their data demonstrate that antioxidants are able to inhibit $Ca^{2+}$-induced PTP pore opening and that $Ca^{2+}$-induced PTP opening is sensitive to the concentration of $O_2\cdot$, suggesting $H_2O_2$ generation (Castilho *et al.,* 1995). On the contrary, another set of studies showed that exogenously added ROS can trigger the PTP, supporting the idea that ROS are activators of the PTP (Castilho *et al.,* 1995; Packer and Murphy 1994). The presence of ROS in the nervous system, such as microglia-derived nitric oxide, in neurodegenerative diseases also confirms that exogenous ROS takes place in neurodegeneration (Block *et al.,* 2007). Therefore exogenous ROS is likely to be a trigger of PTP opening *in vivo*. This thesis investigates the effects of exogenously added ROS on mitochondrial $Ca^{2+}$ and PTP opening in cultured cortical neurons neurons.

### 1.4. Mitochondrial $Ca^{2+}$ imaging in live cells

The increasing evidence that mitochondrial $Ca^{2+}$ imbalance, ROS and PT are underlying causes of cell death in many diseases led to the development of new imaging tools for investigating mitochondrial $Ca^{2+}$ dynamics and PT in live cells. Visualization and quantitative analysis of mitochondrial $Ca^{2+}$ in neurons was made possible by advances in development of fluorescent $Ca^{2+}$ indicators. Detection of $Ca^{2+}$ changes by such indicators is based on the alteration of their fluorescent properties when they are bound to $Ca^{2+}$. Currently there are two classes of fluorescent $Ca^{2+}$ indicators – chemically-engineered and genetically-encoded. The advantage of chemical indicators over genetically encoded fluorescent indicators is their broad range of $Ca^{2+}$ affinities, but their major disadvantage is their limitations in targeting to organelles, specific cells or tissues (Palmer *et al.*, 2006; Paredes *et al.*, 2008). Mitochondria-specific $Ca^{2+}$-chelating chemical indicators, such as rhod-2, are widely used. These indicators, in acetoxymethyl ester form, are membrane-permeable and readily accumulate in mitochondria due to their positively charged nature (Palmer *et al.*, 2006; Paredes *et al.*, 2008). However, rhod-2 has a few drawbacks. Rhod-2 is an intensity-based $Ca^{2+}$ sensor. Therefore distribution of the indicator within mitochondria and mitochondrial movement may lead to artifacts in its signal (Pozzan and Rudolf 2008). Rhod-2 becomes fluorescent and $Ca^{2+}$- sensitive after cleavage of the ester bond. This creates another rhod-2 drawback since the cleavage of the ester bond occurs in cytosol; therefore, the rhod-2 signal has both mitochondrial and cytosolic components (Kann and Kovacs 2007).

Genetically-encoded $Ca^{2+}$ indicators available today have a smaller range of $Ca^{2+}$ binding affinities than chemical indicators, but their major advantage is their targeting specificity. These probes have been targeted to mitochondria, nucleus, Golgi, endoplasmic reticulum, the plasma membrane of cells and have also been expressed in whole animals (Griesbeck *et al.,* 2001; Miyawaki *et al.,* 1997; Filippin *et al.,* 2005; Palmer *et al.,* 2006). The first genetically-encoded $Ca^{2+}$ indicator was aequorin, a photoprotein responsible for green bioluminescence, which has become one of most reliable indicators used for mitochondrial $Ca^{2+}$ measurements (Pozzan and Rudolf 2008). Aequorin can be efficiently directed to any location inside a cell with an appropriate targeting sequence (Brini *et al.,* 1999). Other advantages of aequorin are that it efficiently folds into a fully functional protein in most cell types, its light production is highly quantitative, and it produces light upon binding of calcium, which eliminates a need for excitation light (Pozzan and Rudolf 2008). A disadvantage of aequorin is the low amount of light it produces upon binding to $Ca^{2+}$ (Bell *et al.,* 2006; Pozzan and Rudolf 2008). Therefore it is best suited for imaging populations of cells or for whole-animal imaging. A recent in vivo study showed that aequorin could to be localized in the mitochondrial compartment, but the technique requires an application of coelenterazine, a light-emitting luciferin, for successful imaging (Curie *et al.,* 2007). In a single cell, especially when imaging subcellular compartments, aequorin's signal is not detectable.

This thesis used two genetically encoded $Ca^{2+}$ indicators - a GFP-based mitochondrially-targeted inverse and ratiometric pericams. There are two major groups of genetically encoded indicators that allow measurement of either inducible changes in fluorescence intensity or in FRET (fluorescence resonance energy transfer). Examples of

the indicators that are targeted to mitochondria are pericams (used in this study), camgaroo and cameleon (Baird *et al.,* 1999; Filippin *et al.,* 2005). These indicators are easily targeted to subcellular compartments but their targeting efficiency varies depending on the peptide sequence. Generally, to target genetically encoded $Ca^{2+}$ indicators to mitochondria, a tandemly duplicated mitochondrial targeting sequence encoding the N-terminal of subunit IV of cytochrome *c* oxidase is used to improve the delivery of the indicator the organelle's matrix (Filippin *et al.,* 2005). Duplication of the targeting sequence also results in the three-fold increase in excitation ratio of the ratiometric pericam in response to a common mitochondrial $Ca^{2+}$ uptake stimulus, histamine, when compared to a non-duplicated sequence (Filippin *et al.,* 2005).

Ratiometric and inverse pericams were designed by fusing circularly permuted green fluorescent protein to two $Ca^{2+}$-sensing protein domains taken from calmodulin (CaM) and M13, a 26-residue peptide derived from the CaM-binding region of the skeletal muscle myosin light-chain kinase (Nagai *et al.,* 2001). In this design, conversion of the interaction between two protein domains into a change in the electrostatic potential of the fluorophore upon binding to $Ca^{2+}$ allows detection of changes in free $Ca^{2+}$ fluxes (Nagai *et al.,* 2001). Three types of pericam were developed: flash pericam, which becomes brighter upon binding to $Ca^{2+}$; inverse pericam, which becomes dimmer; and ratiometric pericam, with dual excitation wavelengths, in which excitation wavelengths respond in an opposite manner upon binding to $Ca^{2+}$ (Nagai *et al.,* 2001)**.** The advantage of ratiometric probes, such as ratiometric pericam, over single wavelength probes is that they reduce recording errors by obtaining a ratio signal that is not affected by artifacts such as a dye concentration, illumination intensity or thickness of a specimen. Ratiometric pericam's

properties, such as organelle specificity, wide dynamic range of $Ca^{2+}$ response, ratiometric property and fluorophore stability, make it a reliable tool for imaging mitochondrial $Ca^{2+}$ in live cells (Nagai *et al.,* 2001).

### 1.5. Alteration of $Ca^{2+}$ homeostasis in neurodegenerative diseases

Studies of major neurological diseases affecting a large percentage of the human population support the involvement of $Ca^{2+}$-driven mitochondrial dysfunction in the pathogenesis of these diseases. For example, studies of brain tissue from Alzheimer's disease (AD) patients showed an increase in free intracellular $Ca^{2+}$, protein-bound $Ca^{2+}$ and an increase in activity of $Ca^{2+}$-dependent proteases in neurons containing neurofibrillary tangles (Nixon 2003). Amyloid beta-peptide in AD was implicated in the increase of intracellular $Ca^{2+}$ levels, by altering the function of plasma membrane ion ATPases (Mattson *et al.,* 1992). Amyloid beta oligomers were also implicated in the disruption of intracellular $Ca^{2+}$ homeostasis by generation of ROS and by formation of $Ca^{2+}$-conducting pores in cell membranes (Kawahara and Kuroda 2000).

Moreover, the analysis of brain tissue from patients with Parkinson's disease (PD), Huntington's disease (HD) and amyotrophic lateral sclerosis (ALS) also demonstrated cellular $Ca^{2+}$ overload (Mattson 2007). In Parkinson's disease studies, down-regulation of intracellular $Ca^{2+}$ by over-expression of $Ca^{2+}$-binding proteins calbindin and calretinin showed neuroprotection in dopaminergic neurons (Yamada *et al.,* 1990). In mouse models of Huntington's disease, medium spiny neurons expressing mutant huntingtin

demonstrated mitochondrial $Ca^{2+}$ overload in response to glutamate (Tang *et al.,* 2005). In ALS, motor neurons of patients exhibited significant increase in the intracellular $Ca^{2+}$ (Alexianu *et al.,* 1994). Studies in animal and cell culture models of ischemic stroke demonstrated intracellular $Ca^{2+}$ overload in neurons as a key consequence of the ischemic damage (Kristian and Siesjo 1998).

Importantly for the studies outlined in this thesis, recent studies also demonstrate that neuronal mitochondria undergo changes in MS. Tissue from MS patients and animal models of MS – EAE (experimental autoimmune encephalomyelitis) and Theiler's encephalomyelitis - show structural changes in mitochondria, as well as alteration of mitochondrial proteins and function (Sathornsumetee *et al.,* 2000). Demyelinated regions of axons have greater numbers of mitochondria (Mutsaers and Carroll 1998). Tissue derived from chronic active MS lesions has reduced activity of the mitochondrial respiratory complex I (Dutta *et al.,* 2006). A significant decrease in COX-1 reactivity, the main catalytic subunit of mitochondrial respiratory complex IV, was demonstrated in axons of acute MS lesions (Mahad *et al.,* 2008). The motor cortex without lesions also shows a reduction in mitochondrial respiratory complex I and complex III activities (Dutta *et al.,* 2006).

### 1.6. CyPD and neuroprotection in a multiple sclerosis model

A link between CyPD inactivation and neuroprotection has now been demonstrated in animal models of several neurodegenerative diseases: MS, ALS, AD and ischemic brain

injury (Schinzel *et al.,* 2005; Forte *et al.,* 2007; Du *et al.,* 2008; Martin *et al.,* 2009). Previous studies established that inhibition of CyPD by CsA or *Ppif* gene ablation results in resistance of neurons, as well as hepatocytes, myocytes and myocardiocytes to cell death caused by oxidative stress (Griffiths and Halestrap 1993; Forte *et al.,* 2007; Baines *et al.,* 2005; Halestrap 2009). The work presented in this thesis began with a focus on the role of mitochondrial dysfunction in multiple sclerosis, specifically on CyPD as a therapeutic target for prevention of disability in multiple sclerosis. A collaborative study between Dr. Michael Forte, Vollum Institute, OHSU, and Dr. Dennis Bourdette, Department of Neurology, OHSU, showed a striking resistance of CyPD-null mice to EAE – a mouse model of multiple sclerosis (Forte *et al.,* 2007). Based on that work and the work done by other groups, mitochondrial $Ca^{2+}$ regulation and specifically the prevention of the PTP opening under mitochondrial $Ca^{2+}$ overload via CyPD inactivation was suggested as a mechanism of neuroprotection (Brookes *et al.,* 2004; Bernardi *et al.,* 2006; Forte *et al.,* 2007).

Several events can lead to a cellular $Ca^{2+}$ overload in neurodegenerative diseases which in turn will create mitochondrial $Ca^{2+}$ overload; excitotoxicity is one possible mechanism. During excitotoxicity, overexposure to excitatory amino acids such as glutamate leads to a prolonged activation of the *N*-methyl-D-aspartate (NMDA) receptors resulting in cytosolic $Ca^{2+}$ overload and cell death (Sattler and Tymianski 2001). Direct involvement of mitochondrial $Ca^{2+}$ accumulation in the excitotoxic cell death is supported by the fact that pretreatment of neurons with protonophore FCCP, a mitochondrial uncoupler that abolishes mitochondrial $Ca^{2+}$ uptake and therefore $Ca^{2+}$ overload, prevents cell death (Stout *et al.,* 1998). Alteration in sodium channels in

diseases such as MS is another event that can trigger axonal $Ca^{2+}$ overload (Mahad *et al.*, 2008). Axonal $Na^{+}$ overload and consequent depolarization will lead to excessive $Ca^{2+}$ entry via voltage-sensitive $Ca^{2+}$ channel activation and stimulation of reverse $Na^{+}/Ca^{2+}$ exchange, further increasing $Ca^{2+}$ entry and prompting to mitochondrial $Ca^{2+}$ overload (Kornek *et al.*, 2001). Interestingly, sodium channel blockers show promising results in several neurodegenerative conditions (Tarnawa *et al.*, 2007).

Along with ischemic brain injury, reactive oxygen species (ROS) and nitric oxide are strongly implicated in pathologies of MS, ALS, AD and PD (Kadowaki *et al.*, 2005; Trapp *et al.*, 1999; Mitsumoto *et al.*, 2008; Hureau and Faller 2009). For instance, ROS and reactive nitrogen species can modify a critical residue of RyR receptor, activating the channel and enhancing $Ca^{2+}$ release from ER, which could then lead to mitochondrial $Ca^{2+}$ overload. Although the evidence clearly demonstrates that exogenously added ROS can trigger the PTP opening (Brookes *et al.*, 2004; Castilho *et al.*, 1995) no data show how ROS affects mitochondrial $Ca^{2+}$ in neurons.

### 1.7. Adult mouse cortical culture model

In contrast to previous studies on isolated mitochondria, the imaging technique used in the work presented here investigated for the first time mitochondrial $Ca^{2+}$ dynamics in the context of primary neurons cultured from adult mice. Our focus was on the role of CyPD on mitochondrial $Ca^{2+}$ load capacity and PTP opening in adult neurons. CyPD-KO and WT mice were used to establish primary cultures for live cell imaging. Mice in which

the *Ppif* gene is absent are not distinguishable from the wild type (WT) mice and are born at the expected Mendelian ratios. The culture model used in this work - adult mouse primary cortical culture - was chosen since many neurodegenerative diseases primarily affect mature, adult systems. In contrast to brain slice culture, AMC culture is a dissociated culture, which allows for easy visualization and analysis of mitochondrial dynamics within a single neuron or its compartments – soma, axon, dendrites and synapses (Figure 4).

Adult mouse culture may be a reliable model for investigating mitochondrial dysfunction in neurodegenerative diseases, the onset of which often occurs during adulthood. Cultured cortical neurons prepared from adult mice are more susceptible to oxidative stress (Figure 22, Results). Culture preparation procedure may affect the biology of neurons from both young and adult animals; however it is important to consider the age-related differences that may be conserved in the culture. Evidence from animal models and human subjects demonstrates significant difference in neuronal and mitochondrial biology between different ages. Studies demonstrate age-related changes in expression of the inositol trisphosphate receptors, ryanodine receptors, AMPA receptors, NMDA receptors, metabotropic glutamate receptors, subtypes of G-protein-gated inward rectifying potassium channels and estrogen receptors in cortical and other regions of the brain in mice, rats, primates and humans. All of these above factors play a central role in neuronal $Ca^{2+}$ regulation. Moreover, a recent study demonstrates that neuroprotection stemming from *Ppif* gene ablation is also age-dependant.

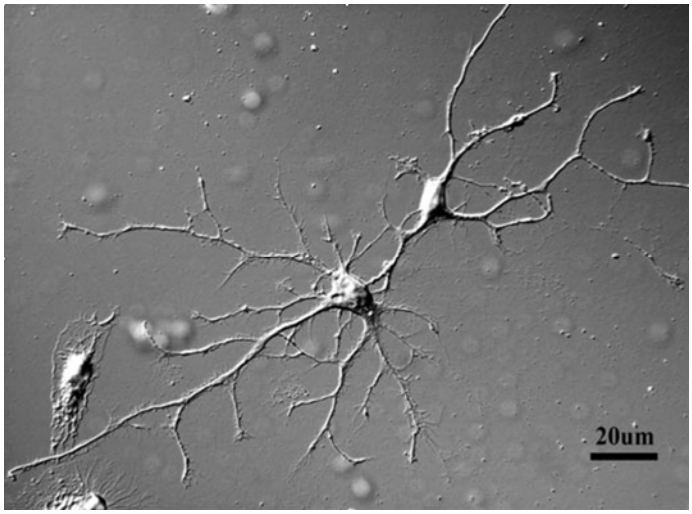


**Figure 4.** Image of cortical neurons in AMC culture from WT mice, 60x oil.

Adult CyPD-null mice (postnatal day 60) had a significant reduction in hypoxic-ischemic brain injury when compared to the WT, whereas young CyPD-null (postnatal day 9) mice exhibited more severe injury than the WT (Wang *et al.*, 2009). Therefore, if the age-related differences are conserved *in vitro*, adult culture model may more accurately present mitochondrial $Ca^{2+}$ dynamics physiologically significant for adult stages.

Moreover, the evidence showed that cytosolic $Ca^{2+}$ response in neurons is age-related. A study showed no cytoplasmic $Ca^{2+}$ transients in postnatal (P14) neurons in response to caffeine, which acts via the ryanodine receptor RyR, whereas the majority of P30 neurons showed considerable cytosolic response (Lalo and Kostyuk 1998). The amplitude of transients induced by application of ATP, which acts via metabotropic P2Y receptors, was significantly smaller in P30 neurons than in P14 neurons (Lalo and Kostyuk 1998). Intracellular calcium release channels, inositol trisphosphate receptor (IP3R-1) and RyR-2 were first detected at embryonic day 11 in mouse neocortex and expression of these proteins was shown to increase progressively throughout brain development (Faure *et al.*, 2001). When compared with RyR-1 and RyR-3 isoforms, RyR-2 was shown to be the predominant isoform in many brain regions after postnatal day 7 in mice (Mori *et al.*, 2000).

Evidence also demonstrates age-related changes in the level of calcium-binding proteins in neurons. Expression of calbindin D28k in the rat cerebral cortex and in the striatum increases between postnatal P0 and P10 stages and decreases between P28 and P120 stages in the striatum (Litwinowicz *et al.*, 2003). Expression of calmodulin genes (CaM I, II, III) changes in rat brain between embryonic E19 and postnatal P20. CaM II expression is highest during early age and then it gradually decreases by P20 in the layer

1 of cerebral cortex (Kortvely *et al.*, 2002). Calcium influx causes large fractions of calmodulin in both the cytosol and nucleus to bind calcium (Zimprich *et al.*, 1995). Increased levels of calcineurin immunoreactivity were demonstrated in the mouse hippocampal CA1 region during aging processes (Eto *et al.*, 2008). Along with age-related changes in $Ca^{2+}$ regulation in neurons, the normal aging process in the nervous system is associated with increased amounts of oxidative stress and impaired mitochondrial function (Hyun *et al.*, 2006; Drew and Leeuwenburgh 2004).

Taken together, these studies demonstrate that factors regulating neuronal $Ca^{2+}$ are age-dependent. Therefore the age of an animal may affect cytosolic, and thus mitochondrial, $Ca^{2+}$ dynamics. Choosing an adult mouse cortical culture for this thesis work allowed us to control for the age-related CyPD inactivation affect in response to oxidative stress and possibly for other differences in $Ca^{2+}$ regulation between adulthood and early age.

### 1.8. Thesis Rationale

Previous studies identified a novel mechanism of neurodegeneration. Further identification of this mechanism's key players may greatly empower clinical neuroprotective strategies. These studies show that the cause of neuronal death could be due to mechanisms related to mitochondrial dysfunction, in particular to regulation of mitochondrial $Ca^{2+}$ . Mitochondrial $Ca^{2+}$ fluctuations within a normal range reflect neuronal activity level and regulate ATP production via key metabolic enzymes. High

levels of cytosolic $Ca^{2+}$ may lead to mitochondrial $Ca^{2+}$ overload and dysfunction. A key event that leads to $Ca^{2+}$-driven mitochondrial dysfunction is the unregulated activation of permeability transition (PT), which eliminates the mitochondrion's ability to make ATP, depletes mitochondrial $Ca^{2+}$ stores, elevates cytosolic $Ca^{2+}$ and generates ROS. Occurrence of PT depends on the opening of an inner membrane channel, the mitochondrial permeability transition pore (PTP). Opening of the PTP in isolated mitochondria disrupts the inner mitochondrial transmembrane potential and releases the apoptogenic proteins such as cytochrome *c*; therefore the PTP may have an important role in cell death control. Mitochondrial $Ca^{2+}$ overload is not the only condition that has been identified to trigger PTP in mitochondria. Oxidative stress can also readily activate PTP opening. Previous studies identified a molecular player that regulates PTP. CyPD, a protein found exclusively in mitochondrial matrix, has been shown to be a key regulator of PTP opening. Studies using neurodegenerative diseases models showed that inactivation of CyPD provides neuroprotection and this affect is age-dependent.

The evidence that we have at this point is that pharmacological inactivation or genetic ablation of CyPD (a) modulates mitochondrial $Ca^{2+}$ load capacity and the PTP opening in isolated mitochondria, (b) results in resistance of neurons to cell death caused by oxidative stress *in vitro* and *in vivo* and (c) results in neuroprotection in animal models of MS, ALS and AD. CyPD inactivation may affect multiple intra-mitochondrial and intra-cellular processes, modulation of which leads to the observed neuroprotection. Currently two effects of CyPD inactivation have been established in isolated mitochondria: modulation of mitochondrial $Ca^{2+}$ load capacity and the PTP opening. These effects may be a key underlying mechanism or a partial underlying mechanism of neuroprotection

observed in animal models of MS, ALS, AD and oxidative stress. However, no one has yet shown that such modulation, observed in isolated mitochondria, occurs in intact cells. The effect of CyPD inactivation on mitochondrial $Ca^{2+}$ load capacity and the PTP opening observed in isolated mitochondria may not be present in intact cells where multiple $Ca^{2+}$-buffering systems control $Ca^{2+}$ dynamics. Investigation of the underlying mechanism of neuroprotection via CyPD inactivation is necessary for developing neuroprotective therapeutics that target CyPD. Therefore the goals of this thesis were to establish whether CyPD inactivation modulates mitochondrial $Ca^{2+}$ and PTP in live cortical neurons cultured from adult mice in response to elevated cytosolic $Ca^{2+}$ and oxidative stress.

Chapter 2 describes in more detail the adult mouse neuronal culture, pericam constructs and their delivery to mitochondria and $Ca^{2+}$ imaging in neurons. Chapter 3 presents the results of our investigation. Major findings of this thesis - CyPD-dependent modulation of mitochondrial $Ca^{2+}$ and PTP in cortical neurons - are discussed in Chapter 4. Chapter 5 details the conclusions derived from this work.

## 2. METHODS

### 2.1. Animals

CyPD-null mice in which the nuclear *Ppif* gene has been ablated were generated and backcrossed eight times into the C57BL/6 background as described by Basso *et al.* (Basso *et al.*, 2005). The *Ppif*-null mouse colonies were maintained homozygotes. CyPD-null mice are not distinguishable from the wild type (WT) mice and are born at the expected Mendelian ratios.

### 2.2. Pericam constructs

For mitochondrial $Ca^{2+}$ imaging, cultures were transfected with either inverse pericam (mitoIP) or ratiometric pericam (mitoRP), a GFP-based genetically encoded $Ca^{2+}$ indicator. Inverse pericam is a single wavelength indicator (excitation 490 nm, emission 515 nm) with a $K_d$ = 0.2 μM, whereas ratiometric pericam is a dual excitation wavelength indicator (ex 415/494 nm, em 513 nm) with a $K_d$ = 1.7 μM (Nagai *et al.*, 2001). These pericams contain duplicated mitochondrial targeting sequences encoding the N-terminal of subunit IV of cytochrome *c* oxidase and driven by the mouse actin promoter (Nagai *et al.*, 2001). The calcium-sensing property of pericams is based on the fusion of circularly permuted YFP to calmodulin (CaM) and M13, a peptide derived from the CaM-binding

region of the skeletal muscle myosin light-chain kinase. The fluorescence properties of the pericams change in $Ca^{2+}$-dependent manner upon interaction between CaM and M13. The pericams were kindly provided by Dr. Atsushi Miyawaki, Institute of Physical and Chemical Research, Japan (Nagai *et al.*, 2001).

### 2.3. Mouse embryonic cell culture and transfection

Mouse embryonic fibroblast cultures from WT and CyPD-null mice were grown in DMEM media (Invitrogen) supplemented with 10% FBS in humidified incubator at 37°C and 5% $CO_2$. When cultures reached 60–80% confluence they were transfected with 1.5 μg of mitoIP plasmid using the Lipofectamine-2000 reagent (Invitrogen). Cells were imaged 48 hours after the transfection. To confirm mitoIR localization to the mitochondria, cells were loaded with the mitochondria-selective dye Mitotracker (200 nM) (Invitrogen) for 30 minutes.

### 2.4. Neuronal cell culture and transfection

For each experiment, two-to-four month-old WT and CyPD-KO mice matched by gender were used. The cerebral cortex was dissected and placed in 2 ml Hibernate A medium supplemented with B-27 (B27, HA, Invitrogen) and with 0.5 mM glutamine (Sigma) at 4°C. The cortex was sliced and transferred to a 50-ml tube containing 5ml

B27/HA. After warming for 8 min at 30°C, slices were digested with 6 ml of a 2 mg/ml papain (Sigma) solution in B27/HA for 30 min at 30°C in a gyrating water bath. The slices were transferred to 2 ml B27/HA. After 2 min at room temperature, the slices were triturated 10 times and allowed to settle for 1 min. Approximately 2 ml of the supernatant were transferred to another tube, and the sediment re-suspended in 2 ml B27/HA. The above step was repeated twice, and a total of 6 ml collected. The resultant supernatant was subjected to density gradient centrifugation at 2000 rpm for 15 min. The density gradient was prepared in four 1-ml layers of 35, 25, 20, and 15% Optiprep (Invitrogen) in B27/HA medium (vol/vol). Debris above 7ml was discarded. The rest of the fractions, excluding the bottom pellet, were collected and diluted in 5 ml of B27/HA. After centrifuging twice at 1000 rpm for 2 min, the cell pellets were re-suspended in 100 µl of nucleofection solution with 3 µg/ml of mitoRP construct and electroporated following Amaxa electroporation system protocol for neurons (Amaxa). Cells were resuspended in 1 ml of $Ca^{2+}$-free DMEM and incubated for 15 min at 37°C. After centrifuging at 1000 rpm for 2 min, the cell pellets were suspended in B27/Neurobasal A medium with 0.5 mm glutamine and counted. Aliquots of $30\times10^3$ cells were plated on glass cover slips (25 mm diameter) that were coated overnight with 10 µM poly-d-lysine (Sigma). After 1 hour incubation in a humidified incubator at 37°C and 5% $CO_2$, cover slips were rinsed with B27/HA then transferred to 6-well plates containing 1 ml of B27/neurobasal A medium. After 24 hours the medium was changed to B27/Neurobasal A medium (Invitrogen) with 5 ng/ml fibroblast growth factor 2 (Invitrogen) and 0.01 mg/ml gentamicin (Sigma). Immunocytochemistry was carried out with antibodies for neurons (β-tubulin III, Molecular Probes), astrocytes (glial fibrillary acidic protein, Molecular

Probes), oligodendrocytes (myelin basic protein, Molecular Probes) and microglia (BS lectin 1, Sigma). Cultures were routinely found to consist of 70% neurons and 30% glia. Neuronal viability was assessed by using the Calcein AM cell viability assay kit (Biotium).

Since assessment of mitochondrial $Ca^{2+}$ levels using genetically-encoded $Ca^{2+}$ probes in adult neurons has not been previously reported, several methods of mitoRP delivery to adult neurons were tested, including delivery by lipofectamine and other reagents. Delivery of mitoRP to neuronal mitochondria by electroporation using the Amaxa system was routinely successful. However, the protocol recommended by Amaxa, developed for embryonic and early postnatal neurons, required a modification in case of adult neurons. Immediately after the electroporation step, which forms pores in plasma membrane, adult neurons need to be suspended in a $Ca^{2+}$-free buffer to prevent neuronal death. Suspending adult neurons in $Ca^{2+}$-containing buffer, which is suitable for embryonic/postnanal neurons, results in a complete loss of viability. Therefore, using a $Ca^{2+}$-free buffer immediately after the electroporation allowed to successfully deliver mitoRP to adult neurons. Using this system, the mitoRP signal is detectable 48 hours post transfection and gradually decreases in intensity starting on day 6 post transfection.

**2.5. Fura-FF and TMRM**

For cytosolic $Ca^{2+}$ measurements, cells were loaded with 5 µM or fura-2AM or fura-FF (Molecular Probes) in imaging buffer (142 mM NaCl, 4 mM $NaHCO_3$, 10 mM Na-

Hepes, 2.5 mM KCl, 1.2 mM $MgCl_2$, 2 mM CaCl2, and 10 mM glucose, pH 7.4) containing 2% BSA (Sigma) for 15–20 min at 37°C. Cells were washed with ECM containing 0.25% BSA for 10 min at 37°C before recording. Neurons in which cytosolic $Ca^{2+}$ was evaluated were from the same culture preparation as the ones plated for mitochondrial $Ca^{2+}$ evaluation, however these neurons were not transfected with mitoRP. Closeness of 380 nm and 415 nm excitation wavelengths between fura-2AM (340/380 nm) and ratiometric pericam (415/494 nm) did not allow for a successful simultaneous imaging of both probes in the same neuron. For mitochondrial membrane potential measurements cells were loaded with 10 nM tetramethyl rhodamine methyl ester (TMRM, Sigma) and 1.6 μM cyclosporin H (Alexis Biochemicals) for 30 min at 37°C and imaged in ECM containing 10 nM TMRM (Sigma). To depolarize mitochondrial membrane potential, 450 nM carbonyl cyanide 4-(trifluoromethoxy) phenylhydrazone (FCCP, Sigma) was used.

**2.6. Fluorescence imaging**

Imaging was carried out after days 4-5 in culture. Mitochondrial and cytosolic $Ca^{2+}$ responses were stimulated with adenosine triphosphate (ATP, Sigma), (*S*)-3,5-dihydroxyphenylglycine (DHPG, Sigma), potassium chloride (KCl, Sigma) and hyndrogen peroxide ($H_2O_2$, Fisher). Imaging of mitochondrial or cytosolic $Ca^{2+}$ and mitochondrial membrane potential in primary neuronal cultures from adult mice were carried out by using an inverted microscope (Olympus IX81, 60×, UPIanSApo340, NA

1.35) equipped with a cooled CCD camera (Cascade II; Intelligent Imaging Innovations) and a high speed wavelength switcher (Lambda DG-5, Sutter Instruments) controlled by SlideBook software (Intelligent Imaging Innovations). Mitochondrial $Ca^{2+}$ was evaluated by using ratiometric pericam construct (415 and 494 nm excitation, 515 nm emission, Chroma filters). Cytosolic $Ca^{2+}$ was evaluated by ratiometric fura-FF (340 and 380 nm excitation, 505 nm emission, Chroma filters). Mitochondrial membrane potential was evaluated by TMRM (535 nm excitation, 575 nm emission, Chroma filters). For imaging, cells were transferred to ECM at 37°C (heated stage, Warner Instruments). During imaging cells were perfused at 2 ml/min with ECM at 37°C supplied with 5% $CO_2$ air mixture. Exposure time was 100-200 msec, frames were taken every 0.5-2 sec. After stimulation cells were not re-used for a recoding with a different stimulus.

**2.7. Image analysis**

Cytosolic or mitochondrial $Ca^{2+}$ and mitochondrial membrane potential were measured in cytosol and mitochondria, respectively, of neuronal soma only. Mitochondrial $Ca^{2+}$ was evaluated by mitoIP or mito RP in 3-5 clusters of mitochondria (2-5 $\mu m^2$) per cell. Mitochondrial membrane potential was evaluated by TMRM probe in 3-5 clusters of mitochondria (2-5 $\mu m^2$) per cell. The data obtained from 3-5 clusters of mitochondria was averaged to represent mitochondrial $Ca^{2+}$ or the membrane potential response per cell. Cytosolic $Ca^{2+}$ was evaluated by fura-2AM or fura-FF in the perinuclear region of a cell. Fluorescence change in mitochondria or cytosol was

evaluated using SlideBook software (Intelligent Imaing Innovations) by subtracting the background fluorescence. The background fluorescence was determined as fluorescence outside the cells. The response data from each cell was then normalized to the baseline value before stimulation using Excel software.

### 2.8. Statistical analysis

Each experiment was replicated three times by using three different animals per genotype (n=3). The data from all evaluated cells from three animals per genotype were used for the statistical analysis. There was no significant difference in responses within a genotype from animal to animal. Data from each experiment were analyzed by one-way ANOVA with SPSS statistical software followed by Bonferroni post-hoc test when needed to analyze data between two or more groups. The data from all evaluated cells from three animals per genotype are presented as mean ± SED in the Results section bar graphs.

# 3. RESULTS

## 3.1. Mitochondrial $Ca^{2+}$ in mouse embryonic fibroblasts

To investigate the role of CyPD in mitochondrial $Ca^{2+}$ dynamics in intact cells, mouse embryonic fibroblast (MEFs) were used as an initial model. MEF cultures were established from WT and CyPD-null mice as described in Methods. MEFs were transfected with mitochondrially-targeted $Ca^{2+}$ indicator inverse pericam (mitoIP) ($K_d$ = 0.2 μM ) by lipofectamine, as described in Methods, and imaged 48-72 hours after transfection. Co-localization using mitoIP and Mitotracker, a mitochondria-selective dye, confirmed that mitoIP localizes specifically to the mitochondria (Figure 5). The signal from this particular form of pericam, inverse, becomes dimmer when bound to $Ca^{2+}$. Mitochondrial $Ca^{2+}$ was evaluated by mitoIP in 3-5 clusters of mitochondria (2-5 $\mu m^2$) per cell. Response values of clusters were averaged to evaluate the mitochondrial $Ca^{2+}$ response per single cell. Mitochondrial $Ca^{2+}$ uptake in MEFs was stimulated via IP3 production following P2Y receptor activation by ATP (100 μM). ATP was applied in a single pulse and remained in the medium until the end of the recording. To simultaneously image mitochondrial and cytosolic $Ca^{2+}$, MEFs were loaded with cytosolic ratiometric indicator fura-2AM. Cytosolic $Ca^{2+}$ was measured in the MEFs perinuclear region where fura-2AM has a stable bright signal.

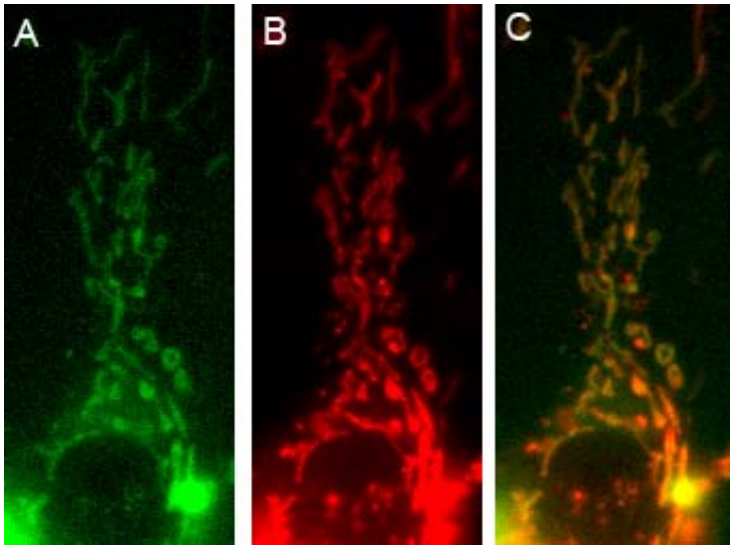


**Figure 5.** Images of mitochondria in a live mouse embryonic fibroblast transfected with mitochondrially-targeted $Ca^{2+}$ indicator inverse pericam (**A**, green) and loaded with Mitotracker, a mitochondria-selective dye (**B**, red), 60x oil. **C**. Merging images of mitoIP signal (A) and Mitotracker signal (B) confirms localization of mitoIP to mitochondria.

A

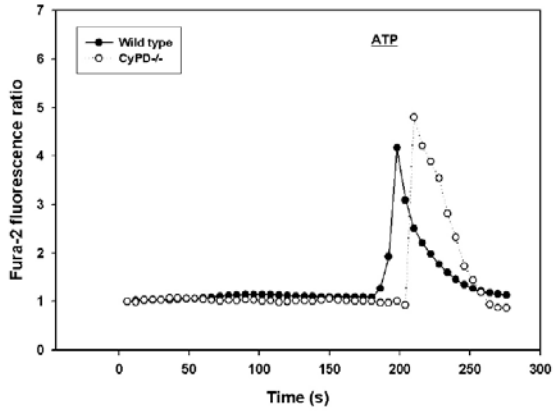


B

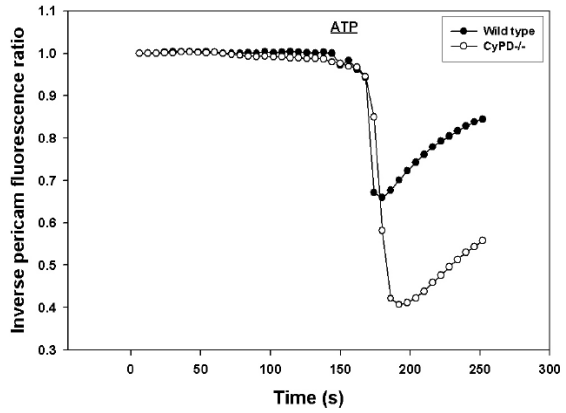


**Figure 6. A.** Representative traces of cytosolic $Ca^{2+}$ responses following stimulation with ATP of MEFs prepared from adult WT and CyPD-null mice (WT, n=45 cells; CyPD-null=47 cells). Statistical analysis by one-way ANOVA; $p > 0.05$. Levels of cytosolic $Ca^{2+}$ were assessed following pre-incubation of neurons with fura-2AM. **B.** Representative traces of mitochondrial $Ca^{2+}$ responses in MEFs prepared from adult WT and CyPD-null mice following stimulation with ATP (WT, n=45 cells; CyPD-null=47 cells). Statistical analysis by one-way ANOVA; $p < 0.01$. Levels of mitochondrial $Ca^{2+}$ were assessed following transfection of neurons with mitochondrially-targeted inverse pericam. Decrease in the inverse pericam fluorescence represents an increase in mitochondrial $Ca^{2+}$ level. MEFs were stimulated with 100 μM ATP which remained in the imaging buffer after the addition.

Following the application of ATP, there was no significant difference in cytosolic $Ca^{2+}$ response between WT and CyPD-null MEFs (Figure 6A), suggesting that CyPD inactivation does not alter IP3-dependent ER $Ca^{2+}$ release. Analysis of mitochondrial $Ca^{2+}$ in response to ATP reported by mitoIP showed that in cultured MEFs, mitochondria devoid of CyPD can take up significantly more $Ca^{2+}$ (Figure 6B). When compared to the results from the previous studies in isolated mitochondria absence of CyPD leads to the same modulation of mitochondrial $Ca^{2+}$ in response in MEFs.

### 3.2. Mitochondrial $Ca^{2+}$ in neurons in response to a single stimulus

The pilot experiment using MEFs created an experimental basis for further investigating the role of CyPD in mitochondrial $Ca^{2+}$ dynamics in excitable cells - neurons. Mitochondrially-targeted ratiometric pericam (mitoRP), instead of inverse pericam, was used in these studies. As outlined in the Introduction, ratiometric probes, like mitoRP, have several advantages over probes that can only report the extent of $Ca^{2+}$ uptake, like mitoIP. MitoRP ($K_d$ = 1.7 μM) is directed to mitochondria by a duplicated mitochondrial targeting sequence, as outlined in the Introduction, and its ratiometric property allows for control of the imaging artifacts (Figure 7A).

Changes in mitochondrial $Ca^{2+}$ reported by mitoRP were evaluated in 3-5 clusters of mitochondria (2-5 $\mu m^2$) in neuronal somata (Figure 7B).

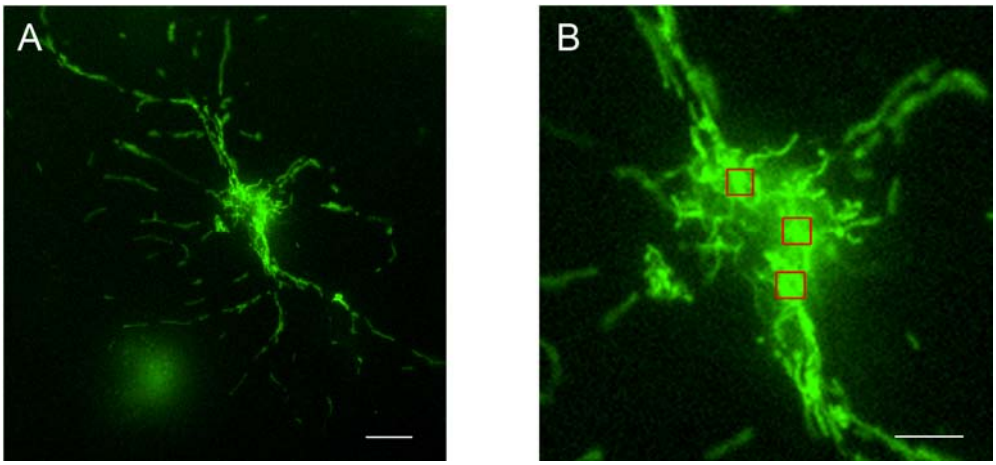


**Figure 7. A,** Image of a live adult cultured cortical neuron transfected with mitochondrially-targeted $Ca^{2+}$ indicator ratiometric pericam, 60x oil. Scale=10 μm. **B**, Magnified image of the soma region in the same neuron. Red boxes represent the areas of mitochondrial populations analyzed in neuronal soma. Three to five areas were chosen per each neuronal soma. Scale=5 μm.

Response values of clusters were averaged to represent mitochondrial $Ca^{2+}$ response per single neuron. Since mitochondria are motile organelles, only clusters in which no mitochondria moved out of the squares during a recording (Figure 7B) were chosen for evaluation.

As described in Methods, immunocytochemical analysis of adult cortical culture shows that 70% of the culture is represented by neurons and 30% of the culture by glia. Since adult cortical culture is a dispersed culture it is easy to visualize and identify single neurons. Neurons were identified morphologically (presence of processes of 100 μM or longer) for mitochondrial or cytosolic $Ca^{2+}$ recordings.

Mitochondrial $Ca^{2+}$ uptake in neurons was stimulated via IP3 production following P2Y receptor activation, as in the case of MEFs, and also via cell depolarization. Both pathways were investigated by perfusing the cultures with an appropriate stimulus. First, ATP (100 μM) was used to stimulate IP3 production and subsequent $Ca^{2+}$ release from ER. To ensure that the absence of CyPD does not alter ER $Ca^{2+}$ release in neurons, cytosolic $Ca^{2+}$ response to ATP was evaluated in WT and CyPD-null cultures using fura-2AM as described in Methods. Cytosolic $Ca^{2+}$ response to ATP was identical in WT and CyPD-null neurons at the peak values (2.2 fold increase) and during the decline to the baseline (Figures 8 A-B).

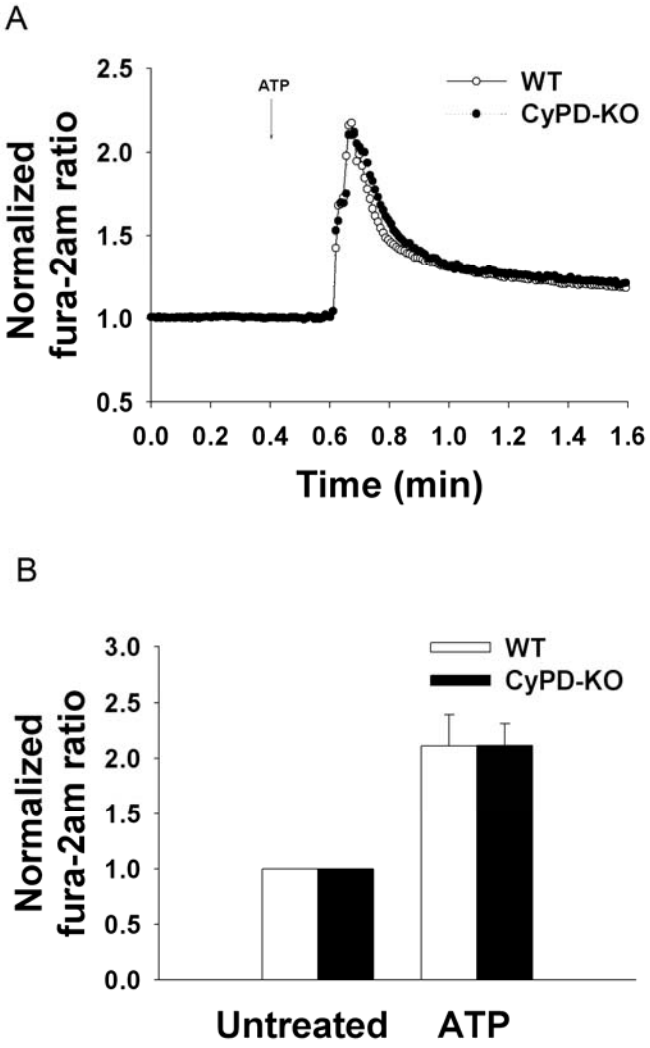


**Figure 8. A.** Representative traces of cytosolic $Ca^{2+}$ responses following perfusion with ATP of neurons prepared from adult WT and CyPD-null mice. **B.** Quantification of cytosolic $Ca^{2+}$ levels of adult WT and CyPD-null neurons at baseline (Untreated) and at peak following stimulation with ATP. (WT, n=35 neurons; CyPD-null, n=34 neurons). Levels of cytosolic $Ca^{2+}$ were assessed following pre-incubation of neurons with fura-2AM. Neurons were stimulated with 100 μM ATP for 30 sec. One-way ANOVA analysis demonstrated no significant difference between cytosolic $Ca^{2+}$ levels in neurons prepared from WT and CyPD-null animals following ATP stimulation.

Analysis of the mitochondrial $Ca^{2+}$ response showed that following the perfusion with ATP there was no significant difference in mitochondrial $Ca^{2+}$ accumulation, peak $Ca^{2+}$ levels attained or $Ca^{2+}$ decline to baseline between WT and CyPD-null neurons (Figures 9 A-B).

To confirm that mitoRP reports $Ca^{2+}$ influx into mitochondria, neurons were pretreated with p-trifluoromethoxy carbonyl cyanide phenyl hydrazone (FCCP), a protonophore that uncouples mitochondrial membrane potential, thereby removing the driving force for $Ca^{2+}$ accumulation into the mitochondrial matrix. Pretreatment with FCCP abolished mitochondrial $Ca^{2+}$ uptake in response to ATP (Figure 9C).

A separate class of IP3-coupled receptors was activated to compare mitochondrial $Ca^{2+}$ uptake between the two genotypes. Metabotropic glutamate receptors (mGluRs) modulate several G-protein-related signal transduction pathways including intracellular calcium. Two of these receptors, mGluR1 and mGluR5, are coupled to IP3 signal transduction. Neurons were perfused with a mGluR1 agonist (*S*)-3,5-dihydroxyphenylglycine (DHPG) (50 μM). As with ATP, cytosolic $Ca^{2+}$ rise in response to DHPG was evaluated to confirm equal ER $Ca^{2+}$ release in neurons of both genotypes. There was no significant difference in cytosolic $Ca^{2+}$ rise (2.2 fold increase) between WT and CyPD-null neurons in response to DHPG (Figures 10 A-B). There was also no significant difference in mitochondrial $Ca^{2+}$ uptake between WT and CyPD-null in response to this stimulus (Figures 11 A-B).

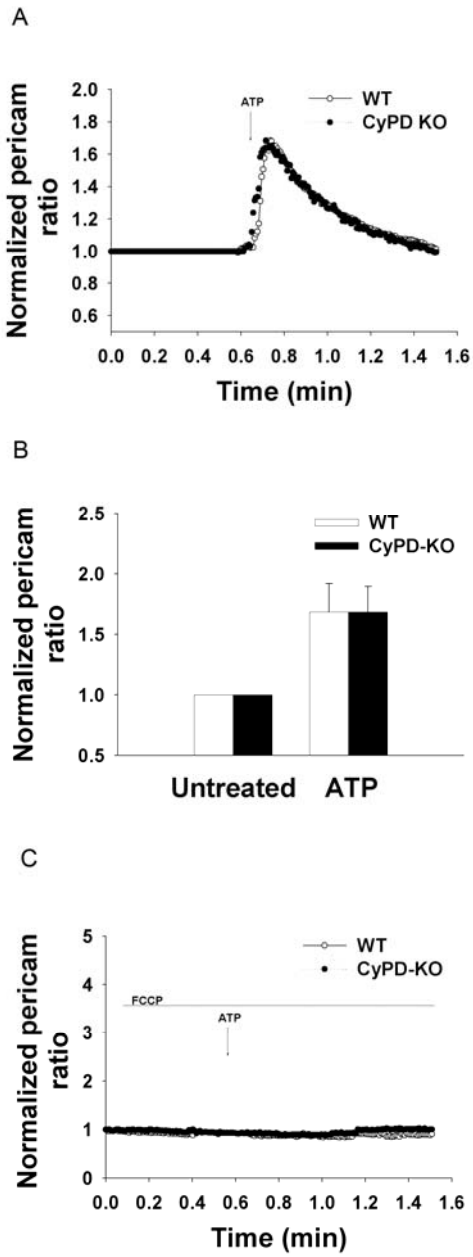


**Figure 9. A.** Representative traces of mitochondrial $Ca^{2+}$ responses in neurons prepared from adult WT and CyPD-null mice following perfusion with ATP. **B.** Quantification of mitochondrial $Ca^{2+}$ changes in adult WT and CyPD-null neurons at baseline (Untreated) and at peak following stimulation with ATP (WT, n=55 neurons; CyPD-null=57). **C.** Pretreatment with mitochondrial uncoupler FCCP (450 nM) for 3 min abolishes mitochondrial $Ca^{2+}$ in neurons following perfusion with ATP. Levels of mitochondrial $Ca^{2+}$ were assessed following transfection of neurons with mitoRP. Neurons were stimulated with 100 μM ATP for 30 sec. One-way ANOVA analysis demonstrated no significant difference between mitochondrial $Ca^{2+}$ levels in neurons prepared from WT and CyPD-null animals following ATP stimulation.

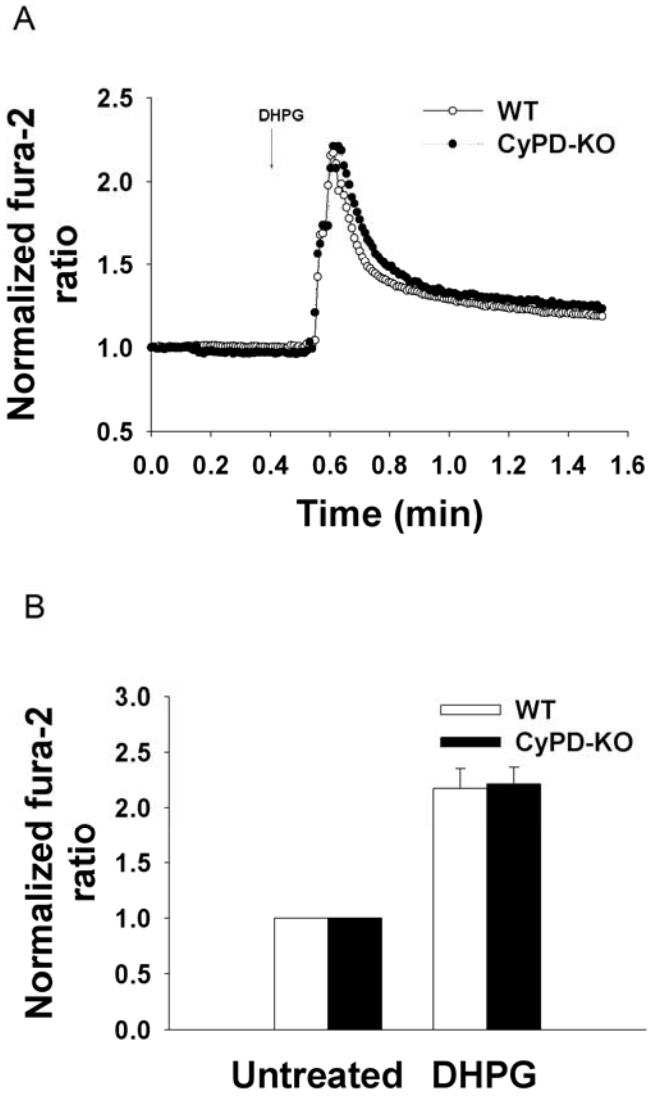


**Figure 10. A.** Representative traces of cytosolic $Ca^{2+}$ responses following perfusion with DHPG of neurons prepared from adult WT and CyPD-null mice. **B.** Quantification of cytosolic $Ca^{2+}$ levels of adult WT and CyPD-null neurons at baseline (Untreated) and at peak following stimulation with DHPG (WT, n=40 neurons; CyPD-null=42 neurons). Levels of cytosolic $Ca^{2+}$ were assessed following pre-incubation of neurons with fura-2AM. Neurons were stimulated with 50 μM DHPG for 30 sec. One-way ANOVA analysis demonstrated no significant difference between cytosolic $Ca^{2+}$ levels in neurons prepared from WT and CyPD-null animals following DHPG stimulation.

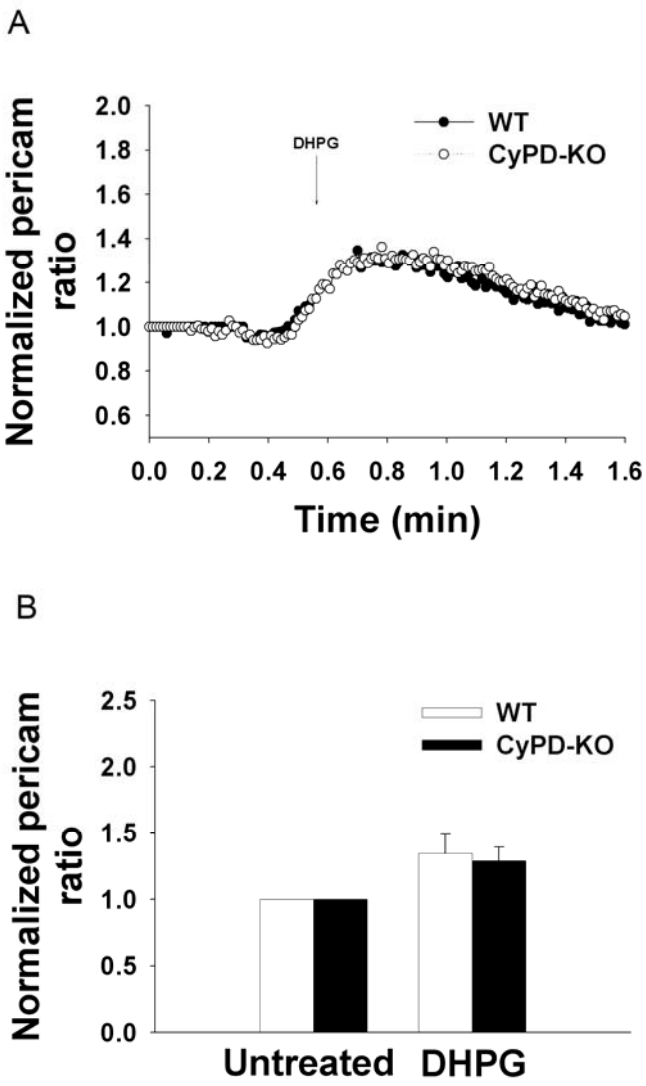


**Figure 11. A.** Representative traces of mitochondrial $Ca^{2+}$ responses in neurons prepared from adult WT and CyPD-null mice following perfusion with DHPG. **B.** Quantification of mitochondrial $Ca^{2+}$ changes in adult WT and CyPD-null neurons at baseline and at peak following stimulation with DHPG (WT, n=48 neurons; CyPD-null=42). Levels of mitochondrial $Ca^{2+}$ were assessed following transfection of neurons with mitoRP. Neurons were stimulated with 50 μM DHPG for 30 sec. One-way ANOVA analysis demonstrated no significant difference between mitochondrial $Ca^{2+}$ levels in neurons prepared from WT and CyPD-null animals following DHPG stimulation.

Extracellular $Ca^{2+}$ entry via $Ca^{2+}$ channels also readily stimulates mitochondrial $Ca^{2+}$ uptake. This separate pathway for $Ca^{2+}$ influx was tested next. Plasma membrane voltage-dependent $Ca^{2+}$ channels were activated by depolarizing neurons with KCl (90 mM). Perfusion with KCl resulted in identical cytosolic $Ca^{2+}$ response in WT and CyPD-null neurons (Figures 12 A-B). Again, there was no significant difference in mitochondrial $Ca^{2+}$ uptake, $Ca^{2+}$ peak value or return to the baseline in response to depolarization (Figures 13 A-B). Mitochondrial $Ca^{2+}$ uptake in response to KCl was abolished when a $Ca^{2+}$-free imaging buffer was used (Figure 13C) or when cells were treated with FCCP (not shown). Taken together these data suggest that CyPD elimination does not alter mitochondrial $Ca^{2+}$ uptake in adult cortical neurons in response to the intracellular $Ca^{2+}$ rise triggered by ER $Ca^{2+}$ release or depolarization.

Elevation in cytosolic calcium caused by the activation of the NMDA receptor is the main cause of glutamate excitotoxicity and elevation in cytosolic $Ca^{2+}$ persists even after the removal of glutamate (Deshpande *et al.*, 2007). Therefore the effect of glutamate was tested in WT and CyPD-null neurons to compare mitochondrial $Ca^{2+}$ uptake. Several glutamate concentrations were used and only high concentration of glutamate (500 μM) elicited mitochondrial $Ca^{2+}$ uptake in neurons. There was no significant difference in mitochondrial $Ca^{2+}$ uptake, $Ca^{2+}$ peak value or return to the baseline in WT or CyPD-null neurons in response to glutamate. Since the neuronal cultures were imaged on day 4-5, prior to the formation of functional synapses under these culture conditions, it is not clear whether the results were affected by the young age of the culture.

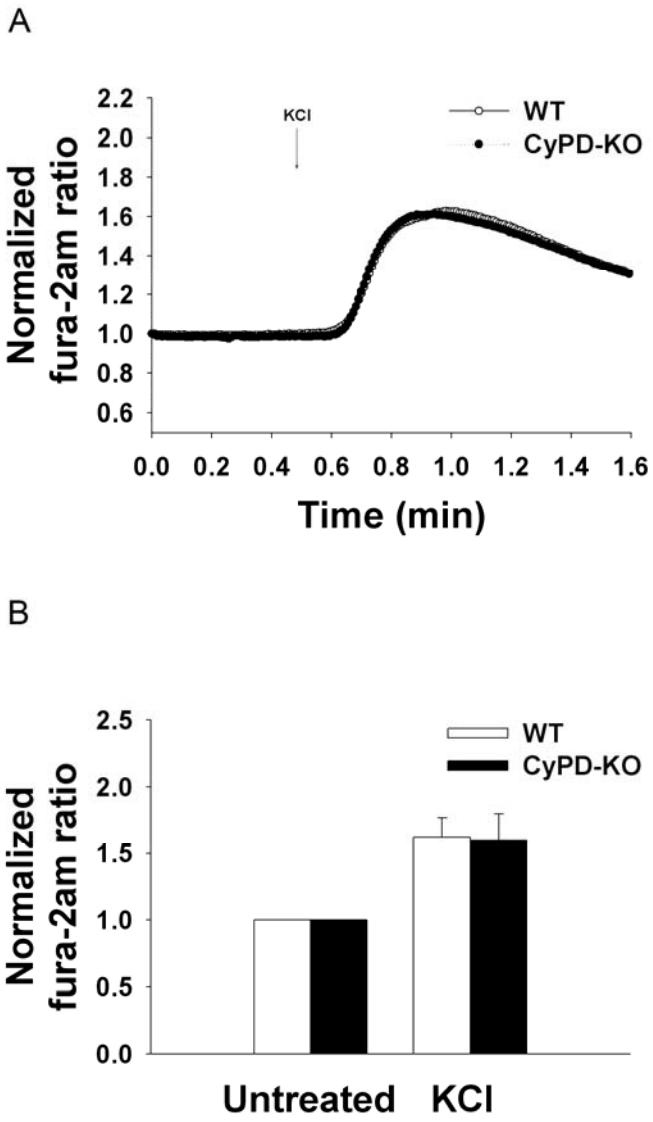


**Figure 12. A.** Representative traces of cytosolic $Ca^{2+}$ responses of neurons prepared from adult WT and CyPD-null mice following perfusion with KCl. **B.** Quantification of cytosolic $Ca^{2+}$ levels of adult WT and CyPD-null neurons at baseline (Untreated) and at peak following stimulation with KCl (WT, n=36 neurons; CyPD-null, n=32 neurons). Levels of cytosolic $Ca^{2+}$ were assessed following pre-incubation of neurons with fura-2AM. Neurons were stimulated with 90 mM KCl for 30 sec. One-way ANOVA analysis demonstrated no significant difference between cytosolic $Ca^{2+}$ levels in neurons prepared from WT and CyPD-null animals following KCl stimulation.

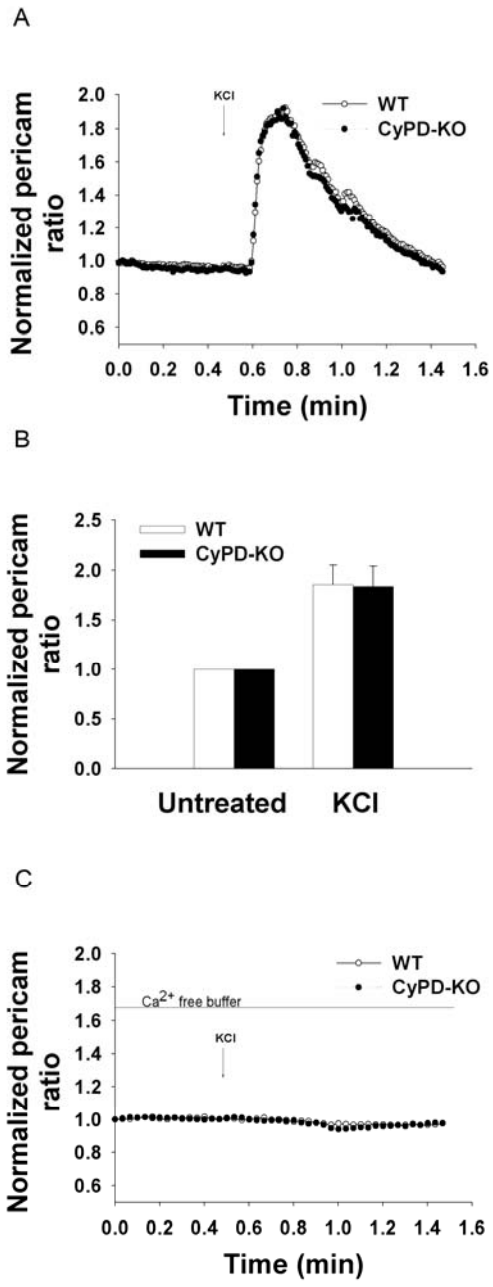


**Figure 13. A.** Representative traces of mitochondrial $Ca^{2+}$ in neurons prepared from adult WT and CyPD-null mice following stimulation with KCl. **B.** Quantification of mitochondrial $Ca^{2+}$ changes in adult WT and CyPD-null neurons at baseline (untreated) and at peak following stimulation with KCl (WT, n=42 neurons; CyPD-null, n=40 neurons). **C.** Absence of mitochondrial $Ca^{2+}$ responses to KCl stimulation in neurons of each genotype in the absence of extracellular $Ca^{2+}$. Levels of mitochondrial $Ca^{2+}$ were assessed following transfection of neurons with mitoRP. Neurons were stimulated with 90 mM KCl for 30 sec. One-way ANOVA analysis demonstrated no significant difference between mitochondrial $Ca^{2+}$ levels in neurons prepared from WT and CyPD-null animals following KCl stimulation.

Recording of mitoRP at the older age of the culture (8-10 days) was not possible due to the absence of mitoRP signal at this stage. Therefore this experimental model using mitoRP was not suitable for investigating mitochondrial $Ca^{2+}$ response to glutamate.

### 3.3. Mitochondrial $Ca^{2+}$ in neurons in response to dual stimuli

Onset of PT in mitochondria is thought to occur when mitochondrial matrix $Ca^{2+}$ reaches a threshold level at which $Ca^{2+}$ extrusion pathways ($Na^{+}/Ca^{2+}$ exchanger) cannot eliminate accumulated $Ca^{2+}$. Physiologic stimuli tested here (ATP, DHPG, KCl) lead to a significant cytosolic $Ca^{2+}$ and mitochondrial $Ca^{2+}$ rise in neurons in both WT and CyPD-null neurons (Figures 9A, 11A, 13A). However, it remains unclear whether the cytosolic $Ca^{2+}$ rise achieved in those experiments led to levels of mitochondrial matrix $Ca^{2+}$ beyond the capacity of the resident $Ca^{2+}$ exchangers, and thereby driving activation of the PTP, during which inactivation of CyPD may reveal its role. To achieve a critical $Ca^{2+}$ level in mitochondria which may trigger PTP opening, the mitochondrial $Ca^{2+}$ response to dual stimuli was tested by simultaneous activation of ER $Ca^{2+}$ release and depolarization. To achieve this ATP (100 μM) and KCl (90 mM) were perfused simultaneously for 30 seconds. Assessment of the cytosolic $Ca^{2+}$ rise in response to dual stimuli with fura-2AM showed no significant difference between WT and CyPD-null. Since elevation of cytosolic $Ca^{2+}$ triggered by dual stimuli may lead to $Ca^{2+}$ levels that are outside of the dynamic range fura-2AM ($K_d$=145 nM), cytosolic $Ca^{2+}$ was also assessed with fura-FF, an indicator that works in a wider range of cytosolic $Ca^{2+}$ levels ($K_d$=5.5 μM).

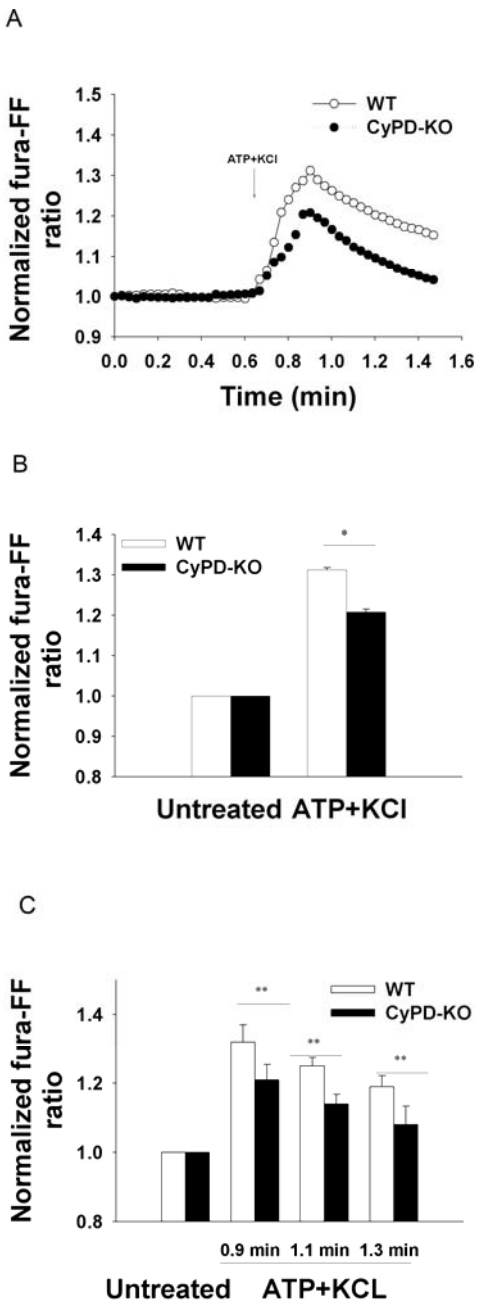


**Figure 14. A.** Representative traces of cytosolic $Ca^{2+}$ responses following simultaneous perfusion of neurons prepared from adult WT and CyPD-null mice with KCl and ATP. **B.** Quantification of cytosolic $Ca^{2+}$ levels of adult WT and CyPD-null neurons at baseline (untreated) and at peak following stimulation with KCl and ATP. (WT, n=56, CyPD-null, n=50). **C.** Cytosolic $Ca^{2+}$ retention following ATP and KCl stimulation. Bars represent cytosolic $Ca^{2+}$ levels at 0.9 min, 1.1 min and 1.3 min (WT, n=56 neurons; CyPD-null, n=50 neurons). Levels of cytosolic $Ca^{2+}$ were assessed following pre-incubation of neurons with fura-FF. Neurons were stimulated with 90 mM KCl and 100 μM ATP for 30 sec. Statistical analysis by one-way ANOVA; * $p < 0.05$, ** $p < 0.01$.

Measurements using fura-FF showed a significantly higher cytosolic $Ca^{2+}$ level in WT neurons than in CyPD-null neurons at peak value (Figures 14 A-B) and a slower decline to the baseline (Figure 14 C) in response to dual stimuli.

Mitochondrial $Ca^{2+}$ response to dual stimuli in WT and CyPD-null neurons inversely corresponded to the cytosolic $Ca^{2+}$ response in these genotypes. Mitochondrial $Ca^{2+}$ uptake in CyPD-null neurons (3.9 fold increase) was significantly higher than in WT neurons (2.2 fold increase) in response to a combined treatment of ATP and KCl (Figures 15 A-B). Mitochondrial $Ca^{2+}$ decline to the baseline was significantly slower in CyPD-null neurons than in WT neurons (Figure 16A). Mitochondrial morphology and neuronal viability were also assessed following application of the combined stimuli. Mitochondrial morphology appeared unchanged in WT and CyPD-null neurons during and immediately after the recording (Figure 17). Mitochondria retained a rod shape and did not form aggregates indicative of mitochondrial degradation (Karbowski and Youle 2003). In addition, there was no significant difference in neuronal viability between the genotypes 24 hours following the treatment, as assessed by Calcein AM (Figure 16B). Inside the cells, Calcein AM is hydrolyzed by endogenous esterase into the highly negatively charged green fluorescent calcein, which is retained in the cytoplasm of live cells. Pretreatment with FCCP eliminated mitochondrial $Ca^{2+}$ responses to a combined treatment of ATP and KCl. These data show that elevation of cytosolic $Ca^{2+}$ by dual stimuli results in higher mitochondrial $Ca^{2+}$ levels in neurons of both genotypes when compared to an activation of a single pathway (Figures 9A, 11A, 13A and 15A).

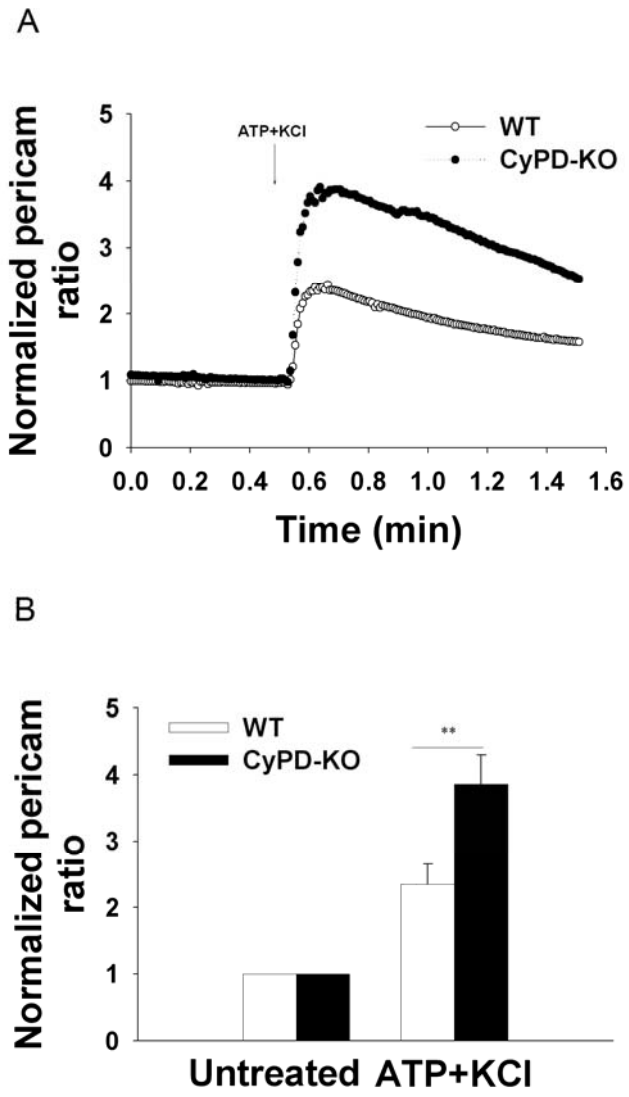


**Figure 15. A.** Representative traces of mitochondrial $Ca^{2+}$ in neurons prepared from adult WT and CyPD-null mice following stimulation with KCl and ATP. **B.** Quantification of mitochondrial $Ca^{2+}$ changes in adult WT and CyPD-null neurons at baseline (untreated) and at peak following stimulation with KCl and ATP (WT, n=51 neurons; CyPD-null, n=48 neurons). Levels of mitochondrial $Ca^{2+}$ were assessed following transfection of neurons with mitoRP. Neurons were stimulated with 90 mM KCl and 100 μM ATP for 30 sec. Statistical analysis by one-way ANOVA; ** $p < 0.01$.

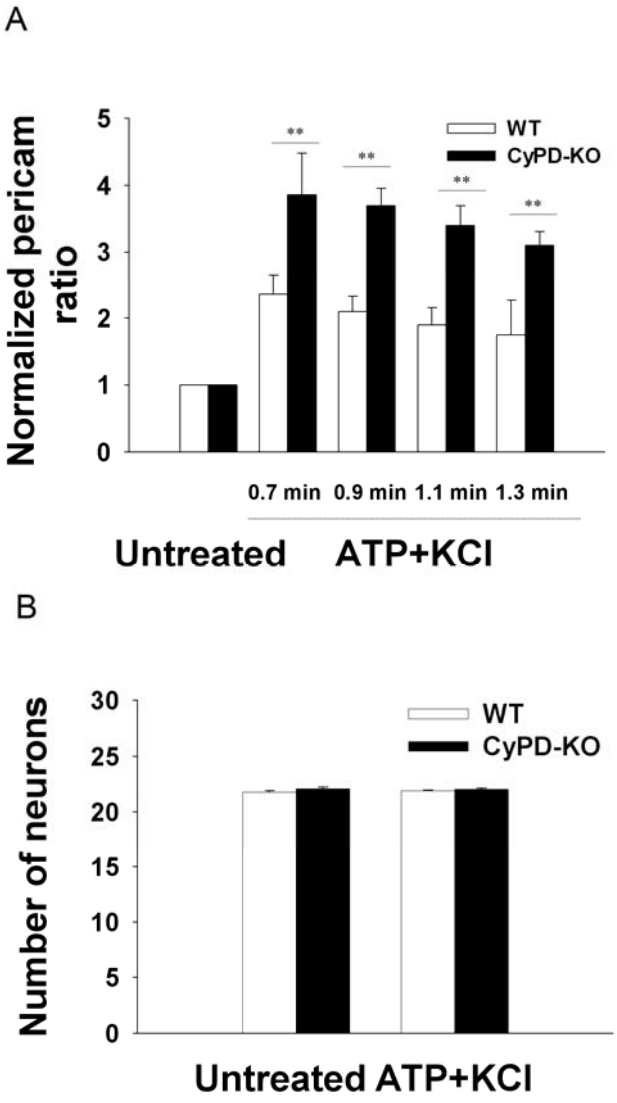


**Figure 16. A.** Mitochondrial $Ca^{2+}$ retention following ATP and KCl stimulation. Bars represent mitochondrial $Ca^{2+}$ levels at 0.7 min, 0.9 min, 1.1 min and 1.3 min (WT, n=51 neurons; CyPD-null, n=48 neurons)**. B.** Neuronal viability following ATP and KCl stimulation. Bars represent a total number of live neurons in five random fields of view per cover slip with WT or CyPD-null cultures using 20x objective. Neuronal viability was assessed with Calcein AM dye 24 hours after ATP and KCl stimulation (WT, n=15 cover slips; CyPD-null, n=15 cover slips). Statistical analysis by one-way ANOVA; ** $p < 0.01$.

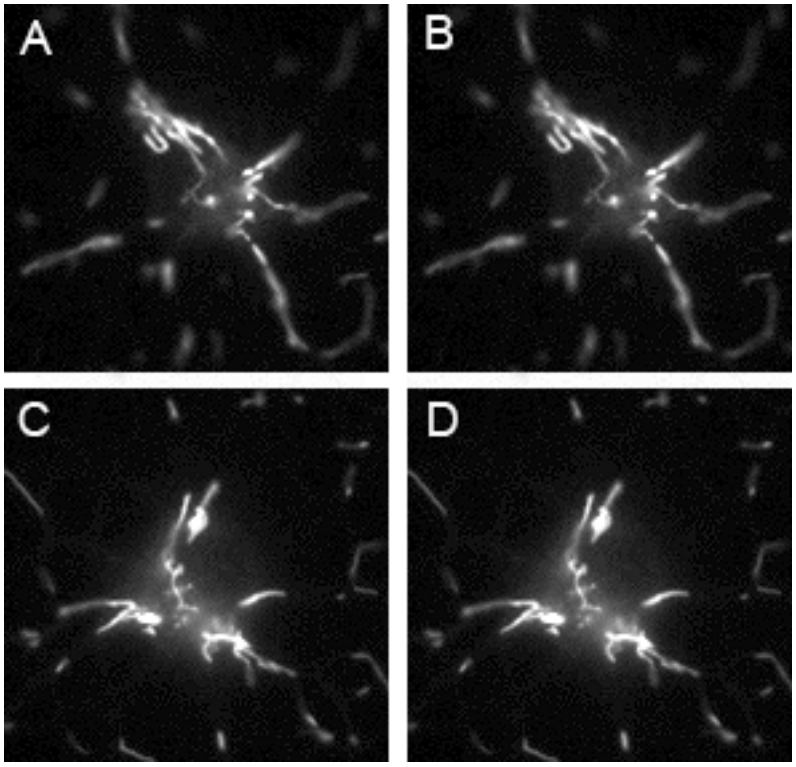


F**igure 17. A-B.** Representative images of mitochondrial morphology in soma of an adult cortical neuron from WT mice transfected with mitoRP before (A) and after (B) the stimulation with $ATP^{+}KCl$. **C-D**. Representative images of mitochondrial morphology in soma of an adult cortical neuron from CyPD-null mice transfected with mitoRP before (C) and after (D) the stimulation with $ATP^{+}KCl$. The images were converted from fluorescent green to a grayscale for easy visualization of mitochondrial morphology. 60x, oil.

Moreover, under these conditions mitochondrial $Ca^{2+}$ uptake in CyPD-null neurons is significantly higher and the $Ca^{2+}$ return to the baseline is significantly slower than in WT, suggesting that higher mitochondrial and cytosolic $Ca^{2+}$ level in neurons than can be obtained with single stimulus is required to activate the PTP opening. Therefore, CyPD inactivation appears to modulate PTP opening in neurons under elevated cytosolic $Ca^{2+}$ level resulting in a larger mitochondrial $Ca^{2+}$ uptake load and longer retention of $Ca^{2+}$ in the mitochondrial matrix.

### 3.4. Mitochondrial $Ca^{2+}$ in neurons pretreated with cyclosporine A in response to dual stimuli

A different experimental approach was used to confirm that modulation of mitochondrial $Ca^{2+}$ and PTP opening in neurons under high $Ca^{2+}$ conditions stems from CyPD inactivation. Instead of genetic inactivation of CyPD, pharmacological inactivation of CyPD in WT neurons by cyclosporine A (CsA), a classic inhibitor of the PTP, was investigated after application of the same two stimuli. In response to a single stimulus (ATP or KCl) there was no significant difference in mitochondrial $Ca^{2+}$ uptake in WT neurons pretreated with CsA when compared to untreated WT neurons, which is similar to the results obtained when comparing WT and CyPD-null neurons under the same single stimulus.

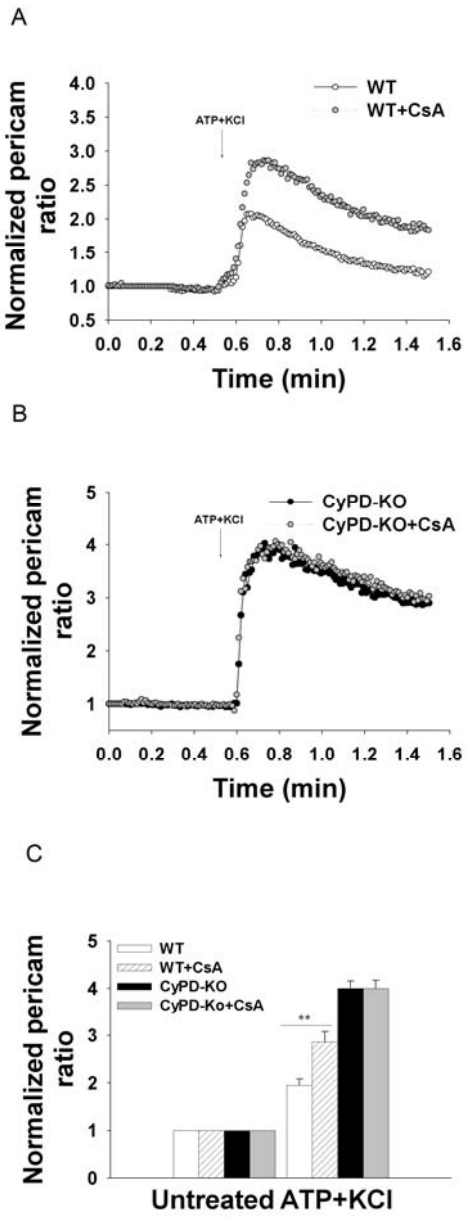


**Figure 18. A.** Representative traces of mitochondrial $Ca^{2+}$ responses in WT neurons and WT neurons pretreated with CsA in response to ATP and KCl. **B.** Representative traces of mitochondrial $Ca^{2+}$ responses in CyPD-null neurons and CyPD-null neurons pretreated with CsA in response to ATP and KCl. **C.** Quantification of mitochondrial $Ca^{2+}$ changes in adult WT and CyPD-null neurons following pretreatment with CsA at baseline (untreated) and at peak following stimulation with KCl and ATP (WT, n=30; WT+CsA, n=33; CyPD-null, n=32; CyPD-null +CsA, n= 35). Levels of mitochondrial $Ca^{2+}$ were assessed following transfection of neurons with mitoRP. Neurons were pretreated with CsA (10 μM) for 30 min. Neurons were subsequently stimulated with 90 mM KCl and 100 μM ATP for 30 sec. Statistical analysis by one-way ANOVA; **p<0.01.

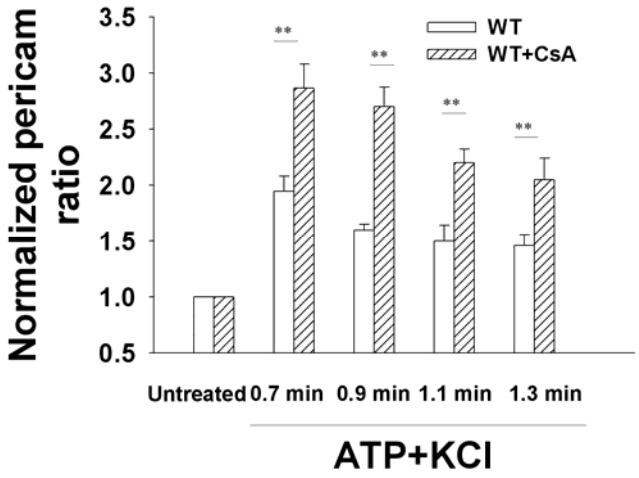


**Figure 19.** Mitochondrial $Ca^{2+}$ retention following ATP and KCl stimulation. Bars represent mitochondrial $Ca^{2+}$ levels at 0.7 min, 0.9 min, 1.1 min and 1.3 min (WT, n=30; WT+CsA, n=33). Statistical analysis by one-way ANOVA; **p<0.01.

When dual stimuli were applied (ATP and KCl), mitochondrial $Ca^{2+}$ uptake in WT neurons pretreated with CsA was significantly higher than in untreated WT neurons (Figures 18 A,C) and the decline to the baseline was significantly slower (Figure 19), mimicking the affect of a genetic ablation of CyPD. However, following application of dual stimuli, the magnitude of the response in WT neurons pretreated with CsA was smaller than in neurons in which CyPD was genetically inactivated (Figures 18 A-B). Pretreatment of CyPD-null neurons with CsA had no effect on mitochondrial $Ca^{2+}$ uptake in response to dual stimuli (Figures 18 B-C), confirming the previous findings that CyPD is the target of CsA action in the regulation of mitochondrial $Ca^{2+}$ dynamics. These results demonstrate that pharmacological inactivation of CyPD leads to the similar changes in mitochondrial $Ca^{2+}$ dynamics as observed following genetic oblation of CyPD.

### 3.5. Mitochondrial membrane potential in neurons in response to dual stimuli

Inner mitochondrial membrane potential ($\Delta\Psi$) dissipates following PTP opening. Consequently, the opening of the pore can be independently assessed by measuring $\Delta\Psi$ in neurons. To investigate the PTP opening in response to high $Ca^{2+}$ conditions in neurons cultured from adult mice, a potentiometric fluorescent dye tetramethylrhodamine methyl ester (TMRM) was used. TMRM's positive charge and lipophilic solubility allows it to be membrane-permeable and penetrate cells (Ehrenberg *et al.,* 1988). The dye redistributes across IMM according to the Nernst equation in a voltage dependent manner

(Ehrenberg *et al.,* 1988). Collapse of TMRM fluorescence indicates dissipation of $\Delta\Psi$ and PTP opening.

Initially, a simultaneous recording of mitoRP and TMRM in a same neuron was tested. However, a co-localization of both probes in the neuronal mitochondria abolished mitoRP response to any stimuli, such as ATP or KCl. Therefore measurements of $\Delta\Psi$ in neurons were carried out independently from the mitochondrial $Ca^{2+}$ measurements. Similar to the mitochondrial $Ca^{2+}$ measurements, $\Delta\Psi$ reported by TMRM was evaluated in 3-5 clusters of mitochondria (2-5 $\mu m^2$) in neuronal soma. Response values of clusters were averaged to present $\Delta\Psi$ per single neuron. To confirm that genetic CyPD inactivation modulates PTP opening, neurons were also pretreated with CsA, a pharmacological CyPD inhibitor. Again, to create elevated cytosolic $Ca^{2+}$ level, neuronal cultures were simultaneously perfused with ATP (100 μM) and KCl (90 mM). At the end of the experiment, FCCP was added to fully depolarize the membrane. Following the treatment, a significant decline in $\Delta\Psi$ occurred in WT neurons, as expected following opening of the PTP (Figures 20 A-B). There was no change in $\Delta\Psi$ in WT neurons pretreated with CsA, CyPD-null neurons or in CyPD-null neurons pretreated with CsA (Figure 20 A-B, previous page) in response to dual stimuli, suggesting that PTP opening was prevented. Treatment with FCCP dissipated $\Delta\Psi$ in all groups, as expected if TMRM accurately reports mitochondrial $\Delta\Psi$ (Figure 20A, previous page). In a separate experiment, $\Delta\Psi$ was assessed in WT and CyPD-null neurons in response to a single stimulus, ATP (Figure 21). A slight non-significant increase in $\Delta\Psi$ followed by a return to the baseline occurred in neurons of both genotypes in response to ATP, confirming the absence of the PTP opening in response to a single stimulus.

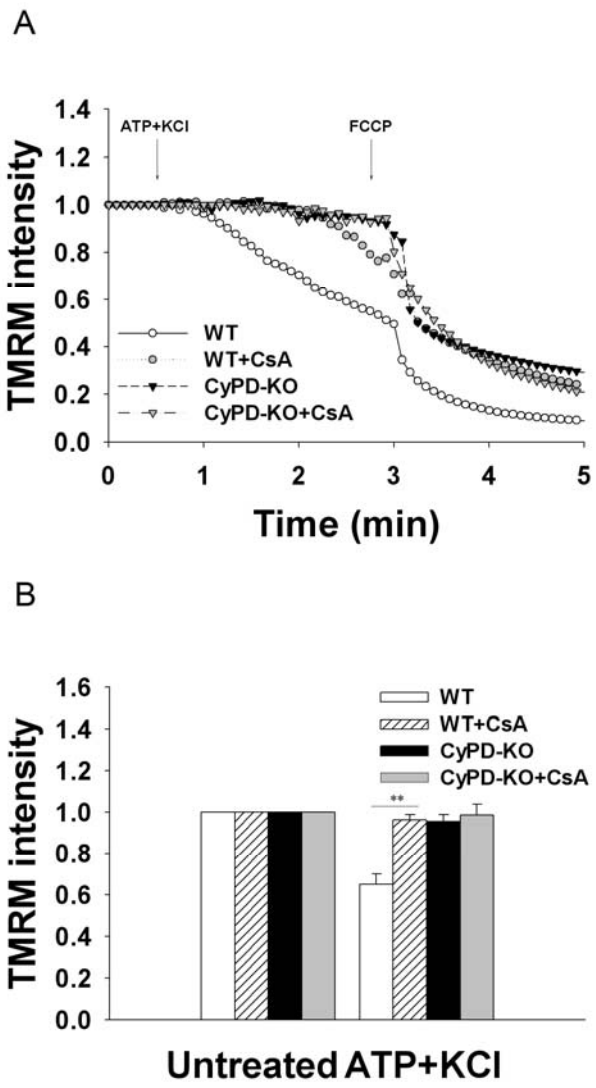


**Figure 20. A.** Representative traces of $\Delta\psi$ in neurons from adult WT and CyPD-null mice in response to ATP and KCl. ATP (100 μM) and KCl (90 mM) were applied simultaneously for 30 seconds then washed out. Application of mitochondrial uncoupler FCCP (450 nM) collapses $\Delta\psi$. **B.** Quantification of the $\Delta\psi$ at baseline and at 2 min point in response to ATP and KCl (WT, n=44 cells; WT+CsA, n=32; CyPD-null, n=48 cells; CyPD-null+CsA, n=33), *$p<0.01$, one-way ANOVA.

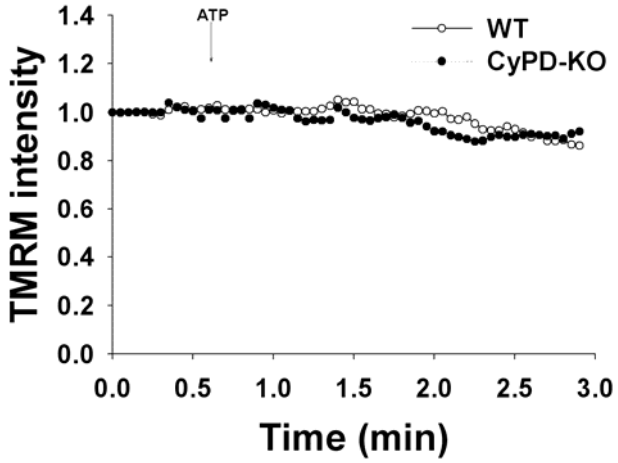


**Figure 21.** Representative traces of mitochondrial membrane potential in neurons from adult WT and CyPD-null mice in response to ATP. ATP (100 μM) was applied for 30 seconds then washed out (WT, n=16 cells; CyPD-null, n=15 cells). One-way ANOVA analysis demonstrated no significant difference between $\Delta\psi$ in neurons prepared from WT and CyPD-null animals following ATP stimulation.

Taken together, these data confirm that CyPD inactivation delays PTP opening in adult neurons in response to elevated levels of cytosolic $Ca^{2+}$ created by simultaneous ER $Ca^{2+}$ release and depolarization.

### 3.6. Mitochondrial $Ca^{2+}$ in neurons in response to oxidative stress

As described in the Introduction, previous studies established that oxidative stress, similarly to high cytosolic $Ca^{2+}$, also readily triggers PTP opening in isolated mitochondria. However, the effect of oxidative stress on mitochondrial $Ca^{2+}$ in the intact cells has never been demonstrated. Studies using CyPD-null mice established that neurons in these animals are resistant to the oxidative stress brought on by ischemia-reperfusion. Here hydrogen peroxide, a classical oxidative stress agent, was used to assess the resistance of cortical neurons from adult WT and CyPD-null mice to oxidative stress. Cortical neurons were routinely grown in a serum-free Neurobasal A medium optimized for neurons and supplemented with a B-27 cocktail. This medium includes components which protect neurons from the oxidative stress. Therefore cultures were transferred to a B27-free medium 12 hours prior to hydrogen peroxide treatment. WT and CyPD-null neurons were treated for 15 minutes with 100 μM and 200 μM $H_2O_2$ and their viability was assessed 24 hours after the treatment using Calcein AM dye as previously described. Quantification of viable neurons showed that adult CyPD-null neurons are significantly more resistant to oxidative stress than adult WT neurons in the $H_2O_2$ concentration-dependant manner (Figure 22).

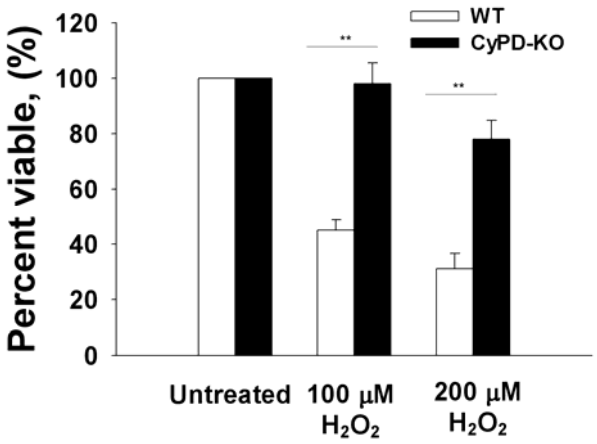


**Figure 22**. Neuronal viability following hydrogen peroxide treatment. WT and CyPD-null neurons were treated with 100 μM or 200 μM $H_2O_2$ for 15 minutes. Live neurons were counted 24 hours after the treatment in five random fields of view per cover slip using 20x objective. Neuronal viability was assessed with Calcein AM dye (WT, n=18 cover slips; CyPD-null, n=18 cover slips). The viability data from $H_2O_2$ treatments were normalized to the viability of the untreated culture. Statistical analysis by one-way ANOVA; ** $p < 0.01$.

It should be noted that previous studies have shown that glia, particularly astrocytes, provide neuroprotection in response to hydrogen peroxide (Desagher *et al.*, 1996). However, the neuronal culture used here contains only 15% astrocytes and 15% microglia, as described in Methods. Therefore it is safe to conclude that CyPD inactivation in adult neurons provides neuroprotection under oxidative stress.

To assess mitochondrial $Ca^{2+}$ in response to the oxidative stress, WT and CyPD-null neurons were transfected with mitoRP. To assess cytosolic $Ca^{2+}$, cultures were loaded with fura-2AM. Neurons were continuously perfused with 20 μM or 100 μM $H_2O_2$ for 9.5 minutes. Cytosolic $Ca^{2+}$ began to increase within 30 sec upon the application of $H_2O_2$ (20 μM and 100 μM) in both WT and CyPD-null neurons and continued to rise for the next nine minutes (Figures 23A, 24A). Observed cytosolic $Ca^{2+}$ rise is consistent with the previous studies that showed cytosolic $Ca^{2+}$ increases in response to $H_2O_2$ using WT postnatal neuronal cultures (Annunziato *et al.*, 2003). However, cytosolic $Ca^{2+}$ level in WT neurons was significantly higher than in CyPD-null neurons at the 5 min point in response to 100 μM $H_2O_2$ (Figure 23A), the time point at which the difference between two genotypes began to be apparent, and continued to be significantly higher until 9.5 min in response (Figure 24A).

Based on these results on the cytosolic $Ca^{2+}$ responses to $H_2O_2$, it was expected that $H_2O_2$ treatment would lead to an increase in mitochondrial $Ca^{2+}$ in WT and CyPD-null neurons. On the contrary, in both genotypes, the $H_2O_2$ treatment led to a >20% decrease in the mitochondrial $Ca^{2+}$ during the first 5 minutes in response to both 20 μM $H_2O_2$ (Figure 25A) and 100 μM $H_2O_2$ (Figure 26A).

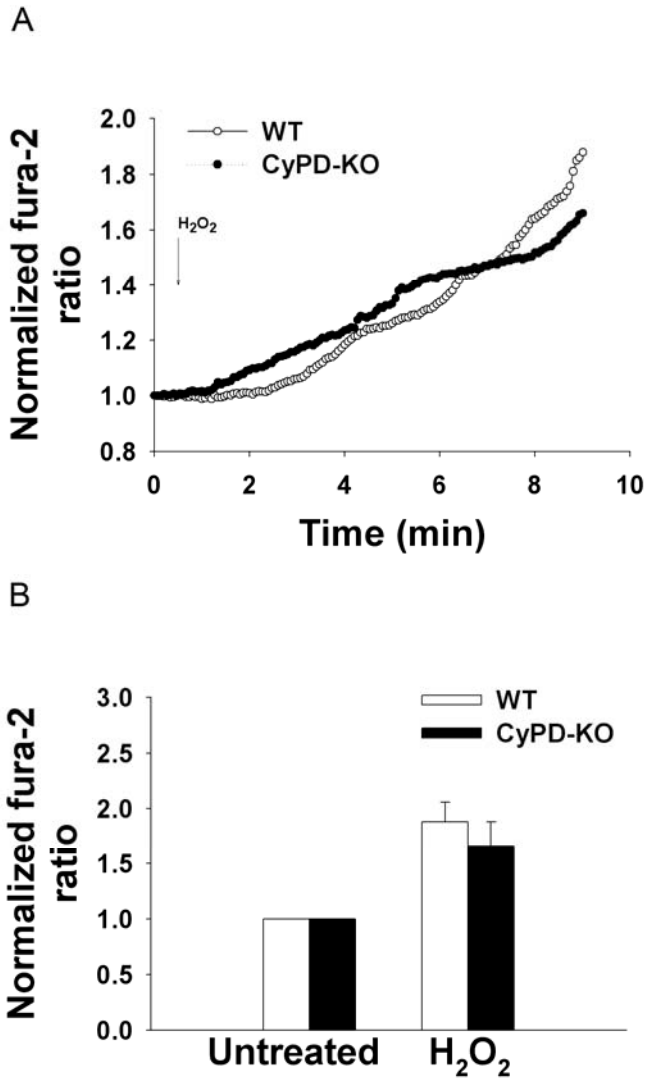


**Figure 23. A.** Representative traces of cytosolic $Ca^{2+}$ responses following perfusion of neurons prepared from adult WT and CyPD-null mice with 20 μM hydrogen peroxide. **B.** Quantification of cytosolic $Ca^{2+}$ levels in adult WT and CyPD-null neurons at baseline (untreated) and 9 min following treatment with 20 μM $H_2O_2$. (WT, n=47; CyPD-null, n=51). Levels of cytosolic $Ca^{2+}$ were assessed following pre-incubation of neurons with fura-2AM. Neurons were treated with 20 μM $H_2O_2$ for 9.5 min.

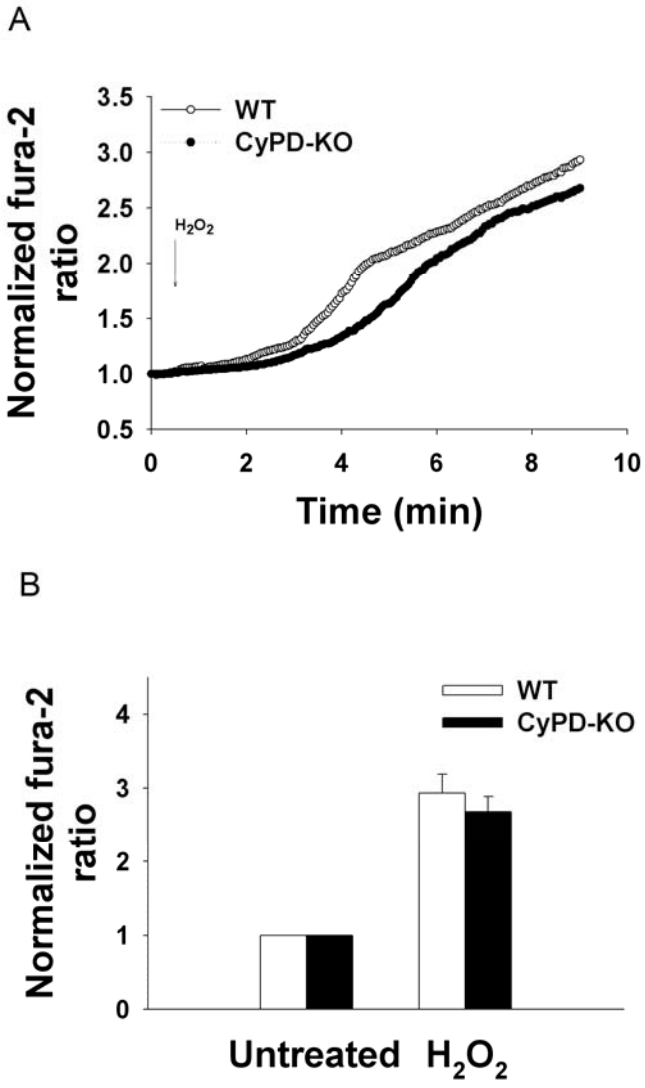


**Figure 24. A.** Representative traces of cytosolic $Ca^{2+}$ responses following perfusion of neurons prepared from adult WT and CyPD-null mice with 100 μM hydrogen peroxide. **B.** Quantification of cytosolic $Ca^{2+}$ levels of adult WT and CyPD-null neurons at baseline (untreated) and at 9 min point following treatment with 100 μM $H_2O_2$. (WT, n=30, CyPD-null, n=31), *$p<0.01$, one-way ANOVA. Levels of cytosolic $Ca^{2+}$ were assessed following pre-incubation of neurons with fura-2AM. Neurons were treated with 100 μM $H_2O_2$ for 9.5 min.

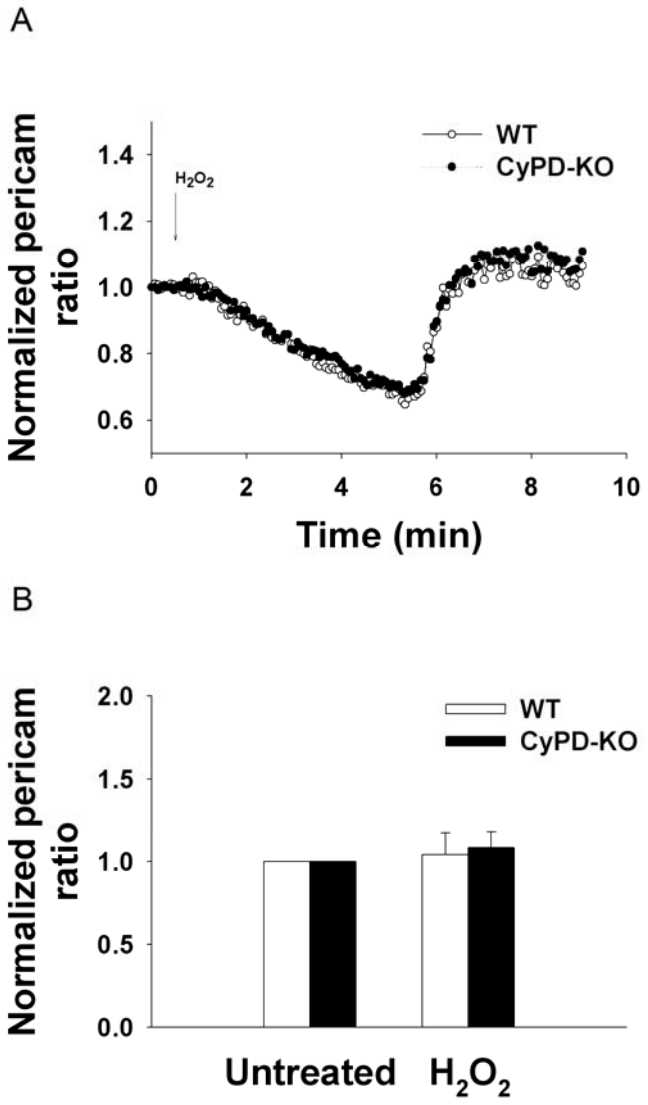


**Figure 25. A.** Representative traces of mitochondrial $Ca^{2+}$ responses following perfusion of neurons prepared from adult WT and CyPD-null mice with 20 μM hydrogen peroxide. **B.** Quantification of mitochondrial $Ca^{2+}$ levels of adult WT and CyPD-null neurons at baseline (untreated) and at 9 min point following treatment with $H_2O_2$ (WT, n=45, CyPD-null, n=40). Levels of mitochondrial $Ca^{2+}$ were assessed following transfection of neurons with mitoRP. Neurons were treated with 20 μM $H_2O_2$ for 9.5 min.

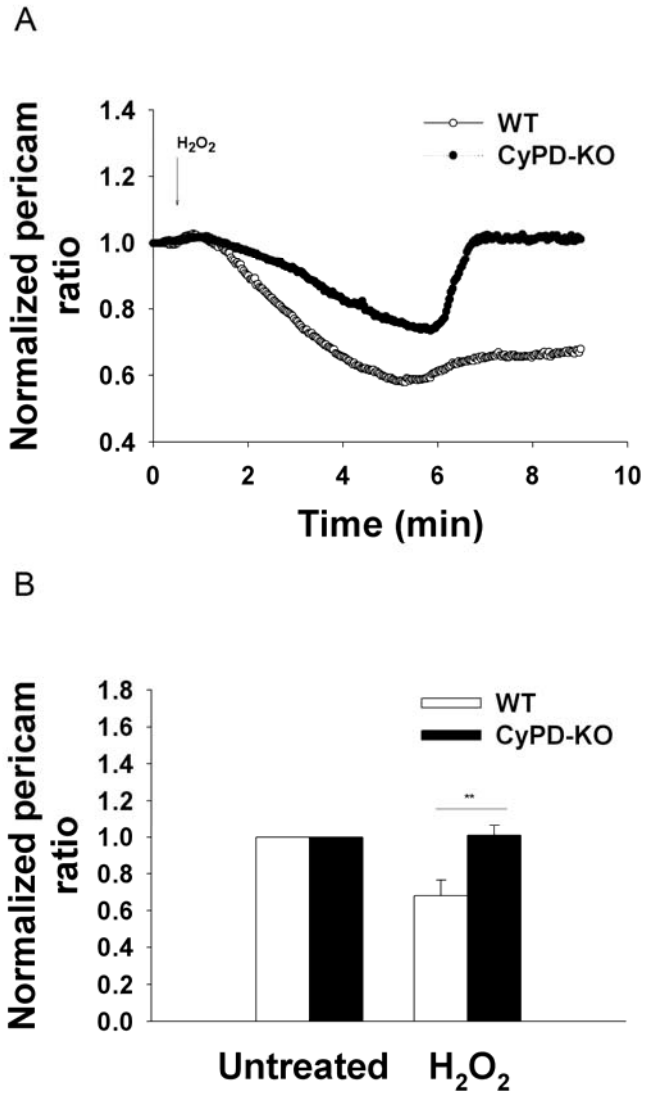


**Figure 26. A.** Representative traces of mitochondrial $Ca^{2+}$ responses following perfusion of neurons prepared from adult WT and CyPD-null mice with 100 μM hydrogen peroxide. **B.** Quantification of mitochondrial $Ca^{2+}$ levels of adult WT and CyPD-null neurons at baseline (untreated) and at 9 min point following treatment with $H_2O_2$. (WT, n=48, CyPD-null, n=49). Levels of mitochondrial $Ca^{2+}$ were assessed following transfection of neurons with mitoRP. Neurons were treated with 100 μM $H_2O_2$ for 9.5 min.

Around 5 minutes after the start of $H_2O_2$ perfusion mitochondrial $Ca^{2+}$ had a steep return to the baseline in WT and CyPD-null neurons in response to 20 μM $H_2O_2$ (Figure 25A, previous page). There was no significant difference in mitochondrial $Ca^{2+}$ levels between WT and CyPD-null neurons after 9 min of exposure to 20 μM $H_2O_2$ (Figure 25B, previous page). However, mitochondrial $Ca^{2+}$ in WT neurons failed to return to the baseline in response to 100 μM $H_2O_2$ (Figure 26A, previous page). The mitochondrial $Ca^{2+}$ level in WT neurons was significantly lower than in CyPD-null neurons after 9 min of exposure to 100 μM $H_2O_2$ (Figure 26B, previous page). The lower mitochondrial $Ca^{2+}$ level in WT neurons in response to 100 μM $H_2O_2$ at 5 min and 9 min corresponds with the higher cytosolic $Ca^{2+}$ level in WT neurons under the same treatment. These data suggests that the cytosolic $Ca^{2+}$ rise that occurs under oxidative stress in neurons does not lead to the mitochondrial $Ca^{2+}$ overload in the absence of any mitochondrial $Ca^{2+}$ uptake stimuli. On the contrary, mitochondrial $Ca^{2+}$ dumping may contribute to the cytosolic $Ca^{2+}$ increase under oxidative stress. These data also shows that CyPD inactivation modulates mitochondrial $Ca^{2+}$ release in adult neurons under oxidative stress and eventually stabilizes mitochondrial $Ca^{2+}$ level at the baseline.

### 3.7. Mitochondrial $Ca^{2+}$ in neurons pretreated with CsA in response to oxidative stress

In order to confirm the role of CyPD inactivation in modulating mitochondrial $Ca^{2+}$ dynamics under oxidative stress, pharmacological inactivation of CyPD by CsA was also tested. WT and CyPD-null neurons were pretreated with CsA and perfused with 100 μM $H_2O_2$ for 9.5 min. Mitochondrial $Ca^{2+}$ decreased in both WT neurons pretreated with CsA and untreated WT neurons during the first 5 minutes of exposure (Figure 27A). However, mitochondrial $Ca^{2+}$ in untreated WT neurons failed to return to the baseline, whereas mitochondrial $Ca^{2+}$ in WT neurons pretreated with CsA returned to the baseline by the 6 min point (Figure 27A). Mitochondrial $Ca^{2+}$ was significantly lower in untreated WT neurons at 9 min after the beginning of the $H_2O_2$ treatment than in WT neurons pretreated with CsA (Figure 27C) thus mimicking the difference in responses between WT and CyPD-null neurons under the same treatment. Pretreatment of CyPD-null neurons with CsA had no affect on mitochondrial $Ca^{2+}$ dynamics under oxidative stress in this genotype (Figure 27B). Again, these data confirms that the interaction of CsA with CyPD is required for the modulation of the PTP opening and mitochondrial $Ca^{2+}$ dynamics. These data confirms that inactivation of CyPD, by genetic or pharmacological means, modulates mitochondrial $Ca^{2+}$ release in adult neurons under oxidative stress and stabilizes mitochondrial $Ca^{2+}$ levels.

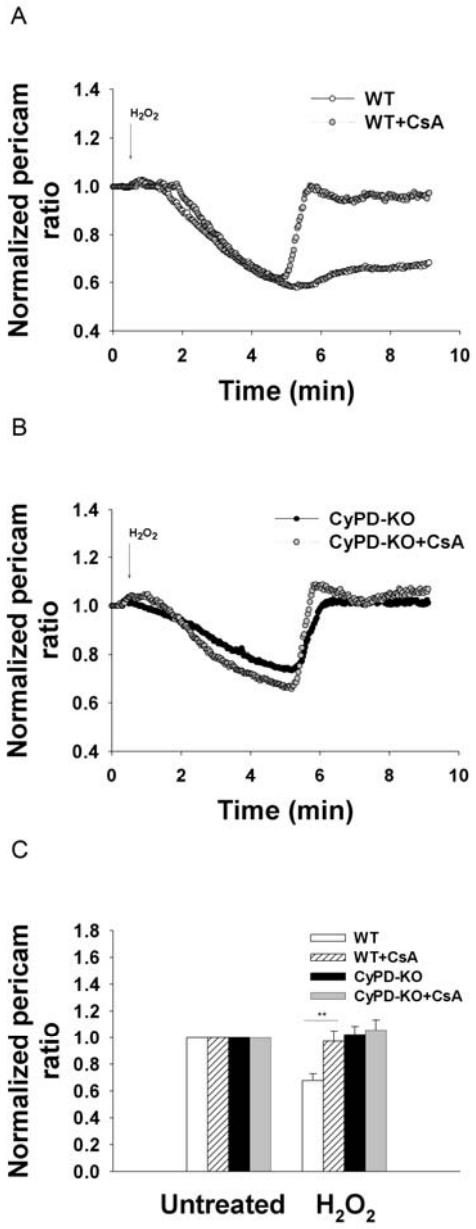


**Figure 27. A.** Representative traces of mitochondrial $Ca^{2+}$ responses in WT neurons and WT neurons pretreated with CsA in response to $H_2O_2$. **B.** Representative traces of mitochondrial $Ca^{2+}$ responses in CyPD-null neurons and CyPD-null neurons pretreated with CsA in response to $H_2O_2$. **C.** Quantification of mitochondrial $Ca^{2+}$ changes in adult WT and CyPD-null neurons following pretreatment with CsA at baseline (untreated) and at 9 min point following treatment with 100 μM $H_2O_2$ (WT, n=48; WT+CsA, n=30; CyPD-null, n=49; CyPD-null +CsA, n=23). Levels of mitochondrial $Ca^{2+}$ were assessed following transfection of neurons with mitoRP. Neurons were pretreated with CsA (10 μM) for 30 min. Neurons were subsequently treated with 100 μM $H_2O_2$ for 9.5 min. Statistical analysis by one-way ANOVA; **p<0.01.

### 3.8. Mitochondrial membrane potential in neurons in response to oxidative stress

To independently assess the PTP opening in WT and CyPD-null neurons under oxidative stress conditions, cultures were loaded with TMRM to measure the changes in mitochondrial membrane potential $\Delta\Psi$. Again the cultures were perfused with 100 μM $H_2O_2$ for 9.5 min. A fast decrease of >20% in $\Delta\Psi$ occurred in the first two minutes in both WT and CyPD-null neurons (Figure 28A). This result is consistent with the previous findings that showed $\Delta\Psi$ decrease in postnatal retinal ganglion cells neurons in response to the oxidative stress and the prevention of depolarization by pretreatment with CsA (Lieven *et al.*, 2003). In the next 7.5 minutes $\Delta\Psi$ continued to decrease gradually in WT neurons whereas in CyPD-null neurons made a slight return towards the baseline at 5 min but then continued to decline (Figure 28A). At 5 min, $\Delta\Psi$ in CyPD-null neurons was significantly higher than in WT neurons (Figure 28B). These data show that CyPD inactivation in adult neurons results in an inappropriate PTP opening, when compared to WT, under oxidative stress in the absence of mitochondrial $Ca^{2+}$ uptake stimuli.

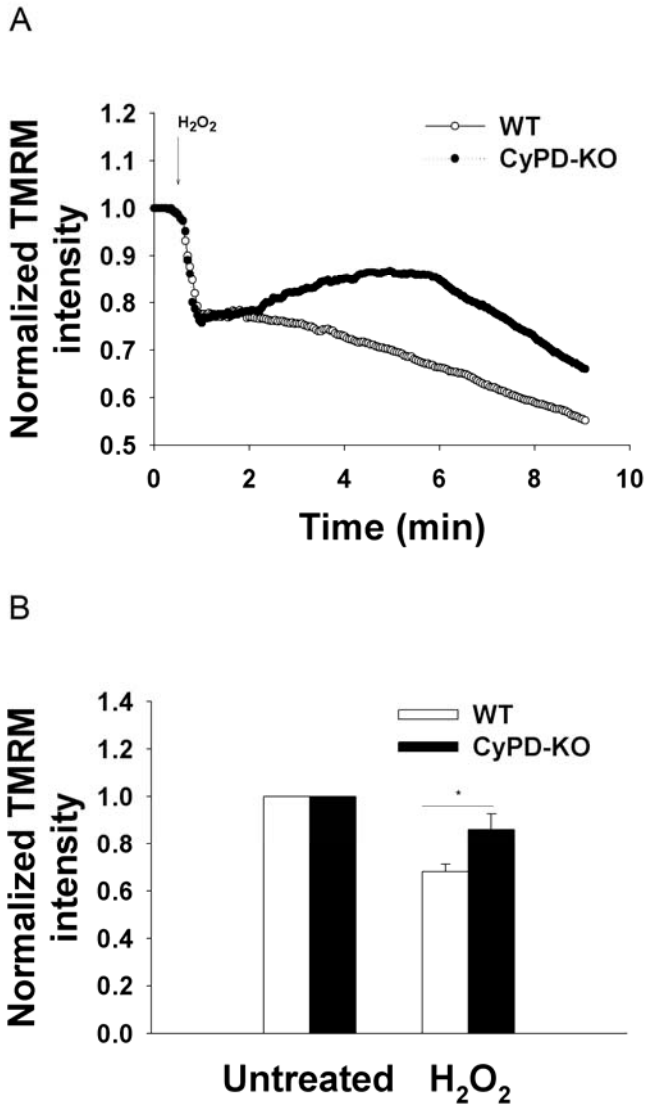


**Figure 28. A.** Representative traces of $\Delta\psi$ in neurons from adult WT and CyPD-null mice in response to 100 $H_2O_2$. **B.** $\Delta\psi$ at baseline (untreated) and at 5 min point in response to 100 $H_2O_2$ (WT, n=35; CyPD-null, n=36). Neurons were treated with 100 μM $H_2O_2$ for 9.5 min. Statistical analysis by one-way ANOVA; *$p<0.05$.

# 4. DISCUSSION

## 4.1. No PTP formed in neurons in response to a single stimulus

Previously, modulation of mitochondrial $Ca^{2+}$ uptake following inhibition of CyPD by CsA or by CyPD gene ablation had been demonstrated only in isolated mitochondria. Based on these *in vitro* results, it was initially predicted that in the intact cells CyPD inactivation would modulate mitochondrial $Ca^{2+}$ homeostasis and delay PTP opening in response to various stimuli that raise cytoplasmic $Ca^{2+}$ and, therefore, mitochondrial $Ca^{2+}$ levels. Indeed, genetic ablation of CyPD in MEFs resulted in higher mitochondrial $Ca^{2+}$ uptake in response to ER $Ca^{2+}$ release, suggesting that the PTP opening in CyPD-null MEFs was delayed. In contrast, however, genetic ablation of CyPD in adult neurons did not result in higher mitochondrial $Ca^{2+}$ uptake in response to ER $Ca^{2+}$ release. We extended these results to show that activation of IP3-dependant ER $Ca^{2+}$ release or depolarization of neurons individually resulted in the same mitochondrial $Ca^{2+}$ dynamics in CyPD-null neurons as in WT neurons. This suggests that the elevation of cytosolic $Ca^{2+}$ levels in response to a single stimulus does not result in mitochondrial $Ca^{2+}$ levels high enough to activate the PTP opening.

Since the core components forming the PTP have not been clearly defined, the direct assessment of the PTP formation and opening in mitochondria, for instance by fluorescently tagging the pore components and tracking their dynamics, is not yet feasible. Therefore, mitochondrial $Ca^{2+}$ accumulation as investigated in this study, played a dual role in the permeability transition both as a trigger for the PTP opening and as a

reporter of the PTP opening by the characterization of mitochondrial $Ca^{2+}$ accumulation in WT and CyPD-null neurons. It was predicted that, first, the sufficiently elevated cytosolic $Ca^{2+}$ level in neurons would lead to mitochondrial $Ca^{2+}$ overload and PTP opening. The PTP opening would be reflected in the inability of the neuronal mitochondria to take up $Ca^{2+}$ upon re-stimulation, similarly to the inability of isolated mitochondria to take up $Ca^{2+}$ after the PTP opening as described in the Introduction. Second, inactivation of CyPD would result in a delay in the PTP opening, and therefore higher mitochondrial $Ca^{2+}$ uptake and retention would occur, since normal $Ca^{2+}$ extrusion pathways ($Na^{+}/Ca^{2+}$ exchanger) would not be able to efficiently extrude $Ca^{2+}$ during $Ca^{2+}$ overload. However, the mitochondrial $Ca^{2+}$ uptake data suggest that the mitochondrial $Ca^{2+}$ overload and the PTP opening did not occur in response to ER $Ca^{2+}$ release alone or to depolarization alone. Contrary to our predictions, mitochondria in WT and CyPD-null neurons treated with a single stimulus (ATP) were able to take up $Ca^{2+}$ again when re-stimulated (Figure 29). Moreover, these results established that CyPD ablation does not modulate mitochondrial $Ca^{2+}$ dynamics in the absence of the PTP.

We also predicted that inactivation of CyPD would result in different levels of mitochondrial $Ca^{2+}$ accumulation in WT and CyPD-null neurons and in a modulation of the PTP opening in CyPD-null neurons . The absence of this difference in neuronal cultures, when compared to MEF cultures and isolated mitochondria preparation, may result from the conditions required to activate the PTP opening. In isolated mitochondria, the absence of $Ca^{2+}$ regulatory machinery such as ER, plasma membrane and $Ca^{2+}$-binding proteins, eliminates buffering of $Ca^{2+}$ influx into the mitochondria.

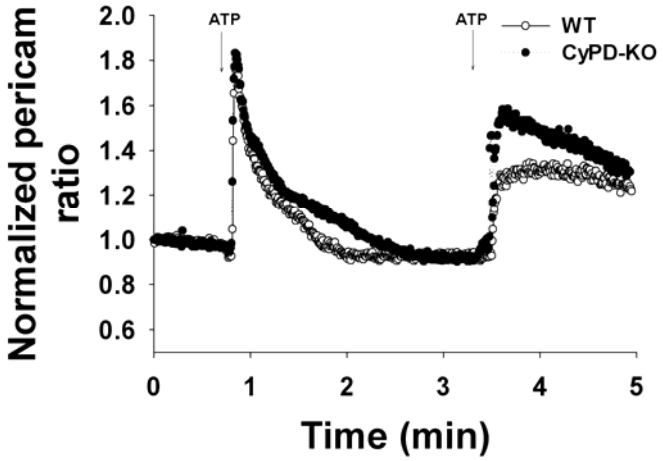


**Figure 29**. Representative traces of mitochondrial $Ca^{2+}$ responses following perfusion with ATP of neurons prepared from adult WT and CyPD-null mice (WT, n=35 neurons; CyPD-null, n=34 neurons). Levels of mitochondrial $Ca^{2+}$ were assessed by transfecting neurons with mitoRP. Neurons were stimulated with 100 μM ATP for 30 sec each time.

Continuous application of extra-mitochondrial $Ca^{2+}$ pulses easily triggers PTP opening in isolated mitochondria, which is detected by the inability of the mitochondria to accumulate more $Ca^{2+}$ (Figure 3, page 15, Introduction). In intact non-excitable cells such as MEFs, stimulation of ER $Ca^{2+}$ release appeared to result in PTP opening, since mitochondrial $Ca^{2+}$ uptake was significantly higher in CyPD-null MEFs than in WT (Figure 6B, page 38, Results). However, the requirements for PTP activation in different cell types may be different.

The results obtained from neurons suggest that cytosolic $Ca^{2+}$ levels following ER $Ca^{2+}$ release or depolarization did not lead to a mitochondrial $Ca^{2+}$ overload and a PTP formation. This data may also explain why CyPD-null mice are indistinguishable from the WT mice in breeding, development and lifespan. Under normal cytosolic $Ca^{2+}$ fluctuations, which do not lead to mitochondrial $Ca^{2+}$ overload, CyPD inactivation does not appear to affect normal animal development and neuronal functioning. Based on the evidence that PTP plays a key role in apoptosis and necrosis, and that adult neurons do not regenerate, the inability of neuronal mitochondria to readily form PTP may be a part of a survival mechanism for post-mitotic cells such as neurons.

### 4.2. PTP opening was activated in neurons by dual stimuli

High $Ca^{2+}$ levels have been shown to trigger PTP in isolated mitochondria. One of the techniques to achieve such level is to permeabilize cells and then modify extracellular $Ca^{2+}$ concentration with $CaCl_2$ applications. For this study, however, a ‘non-invasive’

approach was used to preserve the integrity of neuronal membrane. This approach involved simultaneously stimulating ER $Ca^{2+}$ release and $Ca^{2+}$ influx via voltage-gated $Ca^{2+}$ channels by depolarization of neurons. Under these conditions, mitochondrial $Ca^{+}$ uptake in WT neurons significantly increased when compared to stimulation with a single stimulus, suggesting that the PTP was formed. Measurement of $\Delta\Psi$ in WT neurons by using TMRM was also consistent with PTP opening. A significant decrease in TMRM fluorescence in response to dual stimuli was indicative of the $\Delta\Psi$ dissipation associated with the PTP opening (Figure 20A, page 60, Results).

How would activation of ER $Ca^{2+}$ release combined with depolarization lead to a $Ca^{2+}$ level sufficient to activate PTP opening? Previous studies have shown that in neurons, ER can modulate depolarization-induced cytosolic $Ca^{2+}$ elevations (Simpson *et al.,* 1995; Rose and Konnerth 2001). Depending on the strength of depolarization, ER may act either in $Ca^{2+}$ uptake mode or $Ca^{2+}$ release mode (Simpson *et al.,* 1995; Rose and Konnerth 2001). Data from sympathetic neurons show that as depolarization-induced cytosolic $Ca^{2+}$ elevations become larger, the ER switches from a $Ca^{2+}$ uptake mode to a $Ca^{2+}$ release mode (Albrecht *et al.,* 2001; Hongpaisan *et al.,* 2001). Specifically, these data show that during weak depolarization, when cytosolic $Ca^{2+}$ approached 350 nM, the ER accumulated $Ca^{2+}$. However, during strong depolarization (under 50 mM $K^{+}$), when cytosolic $Ca^{2+}$ was raised above 800 nM or during inhibition of mitochondrial $Ca^{2+}$ uptake, the ER released $Ca^{2+}$.

Several ER $Ca^{2+}$ release mechanisms are known: the IP3R-dependent mechanism, the RyR-dependent mechanism, and the ryanodine-sensitive $Ca^{2+}$-induced $Ca^{2+}$ release mechanism (CICR). The RyR-dependent mechanism, readily activated by caffeine, was

not tested in the present study. However, the IP3R-dependent mechanism was activated in the present study via ATP stimulation. Further, the mechanism of CICR from ryanodine-sensitive $Ca^{2+}$ stores, which is known to amplify and propagate a transient increase in intracellular $Ca^{2+}$ concentration (Jackson and Thayer 2006), might have been co-activated by depolarization. In neurons, RyR might be activated independently from caffeine via the CICR after $Ca^{2+}$ entry through voltage-dependent $Ca^{2+}$ channels. A study using adrenal chromaffin cells showed that CICR was elicited by the activation of plasma membrane $Ca^{2+}$ channels through the same RyR activated by caffeine (Alonso *et al.*, 1999). Therefore, simultaneous stimulation of two $Ca^{2+}$ sources (IP3-dependent ER $Ca^{2+}$ and extracellular $Ca^{2+}$ influx) used in the present study to activate PTP opening in neurons may, in fact, have led to the activation of more than one ER $Ca^{2+}$ release mechanisms. Along with the IP3-dependant mechanism, the RyR-sensitive CICR mechanism also could have been activated in neurons by strong depolarization using 90 mM KCl. Even though ER $Ca^{2+}$ dynamics were not evaluated in the present study, evidence from previous studies supports the idea that then combination of strong depolarization and IP3-dependant ER $Ca^{2+}$ release in neurons would increase the rate of ER $Ca^{2+}$ release, resulting in higher $Ca^{2+}$ influx into mitochondria.

### 4.3. Role of CyPD inactivation in PTP opening in neurons in response to dual stimuli

Mitochondria in CyPD-null neurons were able to take up and retain significantly more $Ca^{2+}$ than mitochondria in WT neurons under elevated cytosolic $Ca^{2+}$ levels triggered by dual stimuli (ATP and KCl). This significantly higher accumulation and retention suggests two scenarios of mitochondrial $Ca^{2+}$ accumulation-retention dynamics. First, ablation of CyPD in these cells completely prevented appropriate PTP formation in response to dual stimuli, resulting in a high mitochondrial $Ca^{2+}$ uptake in CyPD-null neurons and then a slow $Ca^{2+}$ efflux via the $Na^{+}/Ca^{2+}$ exchanger. While we consider this interpretation the most parsimonious, we recognize that alternatives are possible. For example, ablation of CyPD inefficiently activate the PTP. Inefficient activation implies at least two possibilities: (a) PTPs may have formed but in fewer number than in WT neurons; (b) the same number of PTPs have formed as in WT neurons, but their conduction dynamics may be altered. While the results presented here cannot distinguish between these alternatives, imaging mitochondrial $Ca^{2+}$ responses in single neuronal mitochondrion following combined stimuli may provide means for assessing the potential for variation in individual responses at the level of single mitochondrion.

The mitochondrial membrane potential data (Figure 20, page 60, Results) support the first scenario, in which CyPD inactivation completely prevented the PTP opening in CyPD-null neurons under elevated cytosolic $Ca^{2+}$. Dissipation of $\Delta\Psi$ in WT neurons but not in CyPD-null neurons in response to dual stimuli strongly suggests the absence of the PTP opening in CyPD-null neurons. In addition, two observations do not support the

second scenario, inefficient activation of PTPs: first, the absence of $\Delta\Psi$ dissipation, and, second, unusual dynamics of mitochondrial $Ca^{2+}$ decline after the stimuli. If an inefficient PTP activation occurred in CyPD-null neurons when mitochondrial $Ca^{2+}$ reached its threshold, it would be expected that mitochondrial $Ca^{2+}$ would eventually return to the baseline, similarly to WT neurons. $Ca^{2+}$ efflux from mitochondria in CyPD-null neurons would take place via $Na^{+}/Ca^{2+}$ exchanger and also via the inefficiently activated PTPs. Interestingly, even though mitochondrial $Ca^{2+}$ in CyPD-null neurons showed a decline towards the baseline, $Ca^{2+}$ level did not return to the baseline during the first nine minutes following the 30 sec stimulation with dual stimuli (Figure 30A). Mitochondrial $Ca^{2+}$ levels in CyPD-null neurons at 9.5 min (9 min after the stimuli addition) were significantly higher than the baseline value (Figure 30B). This suggests that the $Ca^{2+}$ efflux in CyPD-null neurons appears to be relatively slow even with the open PTPs.

Mitochondrial $Ca^{2+}$ extrusion was also prolonged in WT neurons under high $Ca^{2+}$ conditions; however, it returned to baseline within six minutes. This extrusion in CyPD-null neurons was 9 times slower (9 minutes$^{+}$) than under lower cytosolic $Ca^{2+}$ triggered by a single stimulus (within 1 min). The kinetic parameters for $Ca^{2+}$ efflux have been previously shown to vary in mitochondria from different sources. In isolated mitochondria, the *V*max of $Ca^{2+}$ efflux from liver mitochondria was higher than from heart mitochondria (Bernardi 1999). However the parameters for $Ca^{2+}$ efflux for neuronal mitochondria in intact cells have not yet been fully investigated. Previous evidence suggests that $Ca^{2+}$ efflux via the $Na^{+}/Ca^{2+}$ exchanger may be favored by the transmembrane potential (Bernardi 1999).

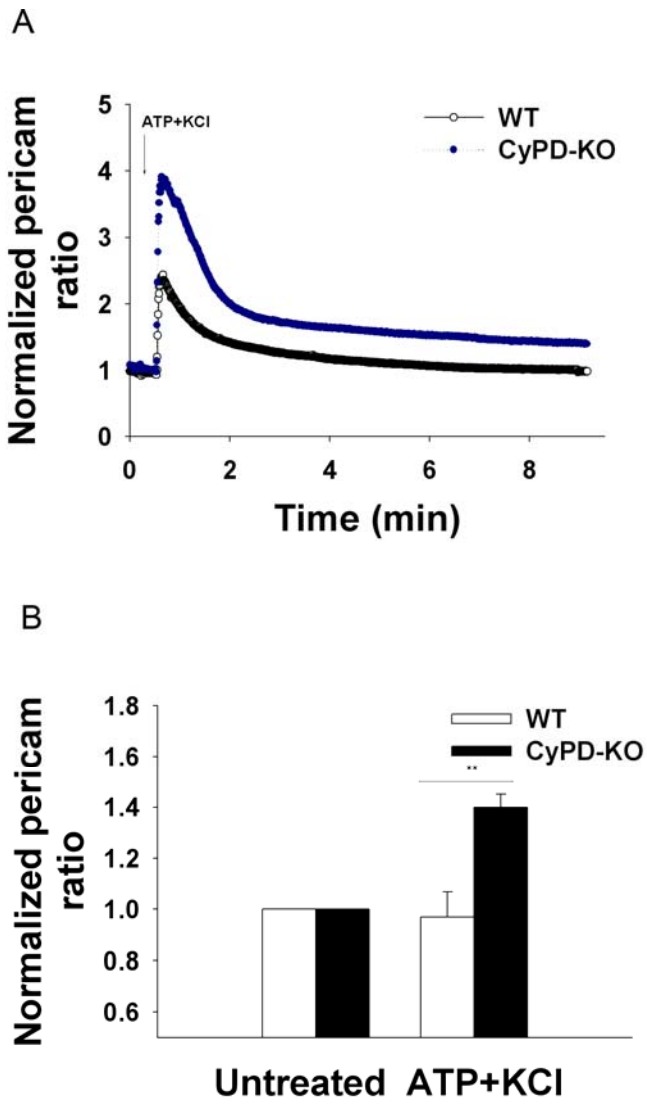


**Figure 30. A.** Representative traces of mitochondrial $Ca^{2+}$ in neurons prepared from adult WT and CyPD-null mice following stimulation with ATP and KCl. Neurons were stimulated with 90 mM KCl and 100 μM ATP for 30 sec. **B.** Quantification of mitochondrial $Ca^{2+}$ changes in adult WT and CyPD-null neurons at baseline (untreated) and at 9.5 min time point following stimulation with ATP and KCl (WT, n=51 neurons; CyPD-null, n=48 neurons). Levels of mitochondrial $Ca^{2+}$ were assessed following transfection of neurons with mitoRP. Statistical analysis by one-way ANOVA; ** $p < 0.01$.

Yet, no significant changes in the ΔΨ in CyPD-null neurons were detected in response to high $Ca^{2+}$ conditions. This suggests that ΔΨ did not affect the kinetic parameters for $Ca^{2+}$ efflux via the $Na^{+}/Ca^{2+}$ exchanger.

A possible explanation for the prolonged retention of $Ca^{2+}$ in CyPD-null neurons in response to high $Ca^{2+}$ conditions is the increased rate of ATP production triggered by high level of $Ca^{2+}$ in mitochondrial matrix. This explanation is plausible because $Ca^{2+}$ ions regulate three major metabolic enzymes responsible for ATP production, and higher mitochondrial $Ca^{2+}$ was shown to correlate with higher energy demands by cells. The higher rate of ATP production and release could act as a continuous stimulus on P2Y receptors until mitochondrial $Ca^{2+}$ reaches the base level. Previously, ATP release was demonstrated from rat dorsal root ganglia in response to KCl treatment (Matsuka *et al.*, 2008). Continuous $Ca^{2+}$ uptake by mitochondria in CyPD-null neurons stimulated by ATP would suggest that the mitochondria are functional and the appropriate PTP opening did not occur. Taken together, the unusual dynamics of mitochondrial $Ca^{2+}$ decline in CyPD-null neurons after dual stimuli do not support any PTP opening taking place.

It should be noted that assessment of ΔΨ, and therefore PTP opening, by TMRM has limitations. Inefficient PTP activation may not result in a dramatic ΔΨ dissipation and therefore would not be reported by TMRM. Such a possibility could support the alternative scenario, in which $Ca^{2+}$ efflux in CyPD-null neurons after dual stimuli takes place via the $Na^{+}/Ca^{2+}$ exchanger and inefficiently activated PTPs.

Other results confirm the major finding that mitochondria in WT and CyPD-null respond differently to elevated $Ca^{2+}$. The cytosolic $Ca^{2+}$ response data confirmed the difference in mitochondrial $Ca^{2+}$ uptake and retention in WT and CyPD-null neurons,

showing significantly lower cytosolic $Ca^{2+}$ level in CyPD-null neurons than in WT neurons. Since $Ca^{2+}$ response was assessed in large clusters of mitochondria in neuronal somata, it was expected that fluctuations in such a $Ca^{2+}$ pool would have a measurable effect on cytosolic $Ca^{2+}$ levels.

Modulation of mitochondrial $Ca^{2+}$ uptake and retention in response to high $Ca^{2+}$ conditions were also observed in WT neurons pretreated with CsA. Pharmacological inhibition of CyPD by CsA resulted in significantly higher mitochondrial $Ca^{2+}$ uptake and retention, suggesting that there was a modulation in PTP opening in these cells. However, the magnitude of the response was smaller with CsA treatment than with genetic CyPD ablation, suggesting that pharmacological inactivation is less effective. This again raises the question about the currently unknown elements of the permeability transition, such as the number or conduction properties of PTPs triggered by high mitochondrial $Ca^{2+}$. Since CyPD inactivation by CsA resulted in smaller $Ca^{2+}$ load than in CyPD-null neurons under high $Ca^{2+}$, more appropriate PTP opening may have occurred due to the incomplete inactivation of CyPD. Most importantly, pharmacological inactivation of CyPD in adult neurons confirmed the role of CyPD in mitochondrial $Ca^{2+}$ dynamics in adult neurons. Taken together, these data suggest that complete (genetic) CyPD inactivation prevents PTP opening in adult neurons under elevated cytosolic $Ca^{2+}$ levels triggered by ER $Ca^{2+}$ release and depolarization, and thus this inactivation modulates mitochondrial $Ca^{2+}$ dynamics.

### 4.4. Role of CyPD inactivation in PTP opening in neurons under oxidative stress

Investigation of the role of CyPD inactivation in a variety of cell types from CyPD-KO mice has demonstrated that these cells show increased resistance to both high $Ca^{2+}$ conditions (Nakagawa *et al.,* 2005; Baines *et al.,* 2005) and oxidative stress (Schinzel *et al.,* 2005). In addition, whole animal studies have demonstrated a striking resistance of CyPD-null mice to heart ischemia-reperfusion injury (Nakagawa *et al.,* 2005; Baines *et al.,* 2005) and focal brain ischemia (Schinzel *et al.,* 2005), in which the generation of ROS has been implicated in cell death. The present study tested the role of CyPD inactivation in PTP formation in neurons cultured from adult mice in response to oxidative stress, another well described activator of the PTP in isolated mitochondria. Our study confirms previous findings on the neuroprotective effect of CyPD ablation under oxidative stress and demonstrates that cortical neurons cultured from adult CyPD-null mice are significantly more resistant to $H_2O_2$-induced death than WT neurons. Our study also examined, for the first time, the responses to oxidative stress of mitochondrial $Ca^{2+}$ dynamics in primary neurons and of PTP induction. Results from mitochondrial membrane potential measurements confirmed PTP formation in neurons under oxidative stress. However, our results do not support the previously proposed model in which oxidative stress leads to the elevation of mitochondrial $Ca^{2+}$ levels.

Extensive evidence on isolated mitochondria demonstrates that exogenously added ROS can trigger PTP opening (Brookes *et al.,* 2004; Castilho *et al.,* 1995; Packer and Murphy 1994). Previous studies, using mitochondrially-target aequorin, also show that exogenously added $H_2O_2$ induces mitochondrial $Ca^{2+}$ rise in intact cells, such as in an

endothelial cell line (Doan *et al.*, 1994; Jornot *et al.*, 1999). These studies in intact cells suggest the following interpretations: short term exposure to $H_2O_2$ leads to sustained elevation of mitochondrial $Ca^{2+}$; elevation of mitochondrial $Ca^{2+}$ is secondary to the cytosolic $Ca^{2+}$ rise triggered by $Ca^{2+}$ release from intracellular stores; elevation of mitochondrial $Ca^{2+}$ depends on $Ca^{2+}$ uptake via the uniporter and results from the inhibition of the $Na^+/Ca^{2+}$ exchanger, and finally the increase in cytosolic calcium triggered by $H_2O_2$ cannot be attributed to a release of $Ca^{2+}$ from the mitochondrial matrix, as had been previously proposed (Doan *et al.*, 1994; Jornot *et al.*, 1999).

Based on this idea, the following model of oxidative stress in cultured cells as mediated by $H_20_2$ treatment (1 mM for 5 min) was proposed: $H_2O_2$ treatment $\rightarrow$ production of superoxide radicals $\rightarrow$ release of $Ca^{2+}$ from intracellular stores (ER) $\rightarrow$ elevation of cytosolic $Ca^{2+}$ $\rightarrow$ elevation of mitochondrial $Ca^{2+}$ $\rightarrow$ unregulated activation of the PTP $\rightarrow$ cell death. However, our data obtained following the assessment of mitochondrial $Ca^{2+}$ levels in primary neurons in response to $H_2O_2$ treatment did not support this model. Treatment of neurons with either 20 μM or 100 μM $H_2O_2$ results in the release, not the uptake, of mitochondrial $Ca^{2+}$ in both WT and CyPD-null neurons, during the first five minutes of exposure. This is especially interesting because ER $Ca^{2+}$ release was shown to occur in neurons under oxidative stress (Ermak and Davies 2002), which would normally trigger mitochondrial $Ca^{2+}$ uptake. Since ER $Ca^{2+}$ was not evaluated in our study, the role of the ER $Ca^{2+}$ in response to oxidative stress in neurons has not yet been established. However, my findings suggest that the initial phase of $H_2O_2$ treatment (the first 5 minutes) strongly depolarizes the IMM, thus abolishing the driving force for $Ca^{2+}$ released by ER.

Another interesting finding of this study is that at the 5-minute time point during continuous treatment of neurons with $H_2O_2$, mitochondrial $Ca^{2+}$ release switches to $Ca^{2+}$ uptake - though the mechanism for this switch is not entirely clear. It may be that that re-polarization of the IMM occurs at about this time point, creating a driving force for $Ca^{2+}$ influx. Another possibility is that significant $Ca^{2+}$ efflux from mitochondria during the first 5 minutes leads to the 'minimum mitochondrial $Ca^{2+}$ threshold,' which reverses the mode of the $Na^+/Ca^{2+}$ exchanger and brings in $Ca^{2+}$. This switch brought the mitochondrial $Ca^{2+}$ back to the baseline in both WT and CyPD-null neurons when treated with 20 μM $H_2O_2$. However, following treatment with 100 μM $H_2O_2$ only CyPD-null neurons showed that mitochondrial $Ca^{2+}$ had returned to baseline. This finding demonstrates that CyPD inactivation modulates mitochondrial $Ca^{2+}$ under strong oxidative stress (100 μM $H_2O_2$) in neurons and allows it to return to the baseline. Thus, recovery of mitochondrial $Ca^{2+}$ under oxidative stress in CyPD-null neurons may preserve the functionality of mitochondria and ensure ATP production.

The partial recovery of mitochondrial membrane potential in CyPD-null neurons under strong oxidative stress (100 μM $H_2O_2$), which showed the same temporal pattern as mitochondrial $Ca^{2+}$, supports the hypothesized preservation of mitochondrial function in CyPD-null neurons compared to WT neurons. The fast initial drop in $\Delta\Psi$ in WT and CyPD-null neurons indicates PTP opening in neurons of both genotypes under strong oxidative stress. Remarkably, the absence of CyPD appeared to slow down $\Delta\Psi$ dissipation under strong oxidative stress. In CyPD-null neurons, $\Delta\Psi$ began to increase toward baseline between 2 and 6 min whereas in WT neurons, $\Delta\Psi$ steadily decreased (Figure 28, page 74, Results). This observation suggests that the absence of CyPD

modulates PTP opening under oxidative stress. Previous studies have already described such a mechanism of PTP formation under oxidative stress and shown that the PTP is modulated by dithiol cross-linking or oxidation and by pyridine nucleotide oxidation, which increases PTP sensitivity to $Ca^{2+}$ (Costantini *et al.*, 1996; Chernyak and Bernardi 1996).

Cytosolic $Ca^{2+}$ measurements reflected the difference in mitochondrial $Ca^{2+}$ dynamics in WT and CyPD-null neurons under strong oxidative stress. Cytosolic $Ca^{2+}$ was significantly higher in WT neurons at 5 min and 9 min points (100 μM $H_2O_2$), corresponding with lower mitochondrial $Ca^{2+}$ in this genotype at these time points. Therefore during the first five minutes of exposure to strong oxidative stress, mitochondrial $Ca^{2+}$ may be one of the major $Ca^{2+}$-contributing pools to the observed cytosolic $Ca^{2+}$ increase. After five minutes, mitochondria devoid of CyPD may re-establish homeostatic levels by taking $Ca^{2+}$ from the cytosol, which is reflected in the lower cytosolic $Ca^{2+}$ levels in CyPD-null neurons compared with WT neurons. Cytosolic $Ca^{2+}$ levels were highly elevated in both genotypes in response to oxidative stress (a 3-fold increase by minute 9). However, the cell death in WT cultures associated with strong oxidative stress (Figure 22, page 64, Results) may primarily stem from the initial insult, resulting in global PTPs opening (by minute 1) which is then followed by high cytosolic $Ca^{2+}$ levels in neurons (by minute 9).

Although $H_2O_2$ was shown by this study to lead to changes in mitochondrial membrane potential and mitochondrial permeability, the exact site affected by $H_2O_2$ within mitochondria remains to be established. Previous investigations have reported a defect at the electron transport chain (Geshi *et al.*, 1988). Studies also show lipid

peroxidation of mitochondrial membrane (Paradies *et al.,* 1999) and a decrease in cardiolipin content (Paradies *et al.,* 2004) as a consequence of oxidative stress. These changes have been shown to alter mitochondrial respiration and oxidative phosphorylation. Exposure of mitochondria to $H_2O_2$ was also shown to inactivate various mitochondrial proteins (Zhang *et al.,* 1990). Therefore, $H_2O_2$ treatment may have either a direct or an indirect effect on mitochondrial membrane potential and mitochondrial permeability - it could either modify the electrochemical gradient due to its charge or it could alter oxidative phosphorylation, mitochondrial proteins and lipids.

In animal models of neurodegeneration, such as the EAE model, mitochondrial dysfunction and ATP depletion due to oxidative stress may have broader consequences, such as deregulated ionic balance. Under normal conditions, $Ca^{2+}$, $Na^{+}$ and $K^{+}$ gradients in axons are controlled by ATP-dependent pumps (Bernardi 1999). Previous studies suggest that both high energy demand associated with conduction along demyelinated axons and limited cellular energy supply due to mitochondrial dysfunction can lead to ionic gradient collapse and axonal $Ca^{2+}$ overload (Kruman and Mattson 1999; Zhu *et al.,* 2000). This overload can result from $Na^{+}$ pump dysfunction, allowing $Na^{+}$ to enter axons through non-inactivating $Na^{+}$ channels, leading to axonal $Na^{+}$ overload. Axonal $Na^{+}$ overload and consequent depolarization will in turn create excessive $Ca^{2+}$ entry via voltage-sensitive $Ca^{2+}$ channel activation and stimulation of reverse $Na^{+}/Ca^{2+}$ exchange. Since $Ca^{2+}$ regulates ATP production, increases in energy demand will therefore also stimulate excess intracellular $Ca^{2+}$ via release of intracellular stores (Cortassa *et al.,* 2003). Cytosolic $Ca^{2+}$ overload can engage multiple $Ca^{2+}$-dependent enzymes, including calpains (Sanvicens *et al.,* 2004) and also consequently lead to mitochondrial $Ca^{2+}$

overload. This overload, however, as we have shown, does not take place initially in response to oxidative stress.

As this study shows, PTP opening took place in CyPD-null neurons under strong oxidative stress, but mitochondrial $Ca^{2+}$ dynamics were none-the-less modulated. Together these observations suggest that inefficient activation of the PTPs occurred in CyPD-null neurons. Thus, inefficient activation of the PTPs in CyPD-null neurons may be a key neuroprotective event under oxidative stress. Pharmacological inactivation of CyPD demonstrated the same recovery of mitochondrial $Ca^{2+}$ under strong oxidative stress as that observed in CyPD-null neurons. This finding confirms the role of CyPD inactivation in PTP opening and mitochondrial $Ca^{2+}$ modulation under oxidative stress. Taken together, these results suggest that CyPD inactivation modulates PTP opening and mitochondrial $Ca^{2+}$ dynamics under oxidative stress in cortical neurons cultured from adult mice.

## 5. CONCLUSIONS

The present study showed for the first time mitochondrial $Ca^{2+}$ dynamics in live cortical neurons from adult mice in response to different cytosolic $Ca^{2+}$ levels and to oxidative stress. The study demonstrated that elevated cytosolic $Ca^{2+}$ and oxidative stress can lead to the PTP opening in neurons and established that CyPD in the mitochondrial matrix acts as a modulator of PTP opening and mitochondrial $Ca^{2+}$ in cortical neurons cultured from adult mice. These findings lead to several conclusions. First, genetic and

pharmacological inactivation of CyPD in cortical neurons cultured from adult mice prevents PTP formation under elevated cytosolic $Ca^{2+}$ triggered by simultaneous ER $Ca^{2+}$ release and depolarization. Second, genetic and pharmacological inactivation of CyPD in adult cortical neurons modulates PTP opening and mitochondrial $Ca^{2+}$ under oxidative stress. Third, genetic inactivation of CyPD is neuroprotective under oxidative stress in adult cortical neurons. Finally, genetic inactivation of CyPD does not modulate mitochondrial $Ca^{2+}$ dynamics in the absence of the PTP.

The results of this study have important clinical implications. Activation of mitochondrial PTP is increasingly considered a final common mechanism of cell death in the leading neurodegenerative diseases, in which $Ca^{2+}$ overload and oxidative stress have been implicated. Therefore regulation of PTP via CyPD inactivation may become a key neuroprotective target in the development of therapies for neurodegenerative diseases.

Much work remains in order to develop such therapies. Elucidation of the PTP components is an essential next step towards better understanding how to prevent the PTP in neurodegeneration. As described in the Introduction, no components of the PTP have been firmly identified. It may be that some of the PTP components are already known and are a part of the $Ca^{2+}$-regulating machinery. For instance, elevated $Ca^{2+}$ may trigger the reverse mode of the mitochondrial $Ca^{2+}$ uniporter, which would create an additional extrusion pathway for $Ca^{2+}$, similar to the PTP opening. A previous study suggests that during $Ca^{2+}$ accumulation in isolated liver mitochondria, reverse uniport via a mitochondrial $Ca^{2+}$ uniporter appears to be the pathway of $Ca^{2+}$ release (Riley and Pfeiffer 1986). That study demonstrated that if an excess of a calcium chelator, EGTA, is added to the medium during mitochondrial $Ca^{2+}$ accumulation, a substantial fraction of

the previously accumulated $Ca^{2+}$ is released rapidly, and the reverse uniport appears to be the pathway of release. However, that study did not suggest that the reverse uniport leads to changes in permeability. Thus, reverse uniport alone may not account for the events associated with the non-transient PTP opening. Investigation of the reverse uniport in intact cells using mitochondrially-targeted $Ca^{2+}$ indicators such as pericam, as well as using mitochondrial $Ca^{2+}$ uptake and extrusion inhibitors, would allow further understanding of mitochondrial $Ca^{2+}$ dynamics in cells and possibly the PTP.

Although the role of CyPD as a key regulator of the PTP has been firmly established in isolated mitochondria and demonstrated in the present study using intact cells, it has not been demonstrated *in vivo*. Imaging mitochondrial $Ca^{2+}$ dynamics in neurons *in vivo* would establish whether CyPD inactivation modulates mitochondrial $Ca^{2+}$ and the PTP opening in the whole animal. Currently, imaging techniques using genetically modified mice expressing fluorescent indicators targeted to organelles are emerging and would allow for an *in vivo* investigation (Misgeld *et al.*, 2007).

Another aspects of CyPD inactivation that remains unclear are the long-term effects of its absence on cellular biology and whether compensatory mechanisms are activated in CyPD-null animals. In mice, ablation of CyPD does not result in a distinguishable phenotype. The present study demonstrated that CyPD ablation modulates mitochondrial $Ca^{2+}$ dynamics under elevated $Ca^{2+}$ and oxidative stress. Therefore ATP production may also be modulated via $Ca^{2+}$-dependent mitochondrial enzymes that regulate oxidative phosphorylation. However, it is of interest to establish whether CyPD ablation modulates primary mitochondrial functions - respiratory chain function and ATP production - in a $Ca^{2+}$-independent manner. Increased ATP production in CyPD-null neurons could be a

part of a neuroprotective mechanism providing a larger ATP pool for cellular functions during stress. Detection of local ATP release from CyPD-null cells can be carried out by using surface-attached firefly luciferase.

Investigation of the effect of CyPD inactivation on mitochondrial $Ca^{2+}$ dynamics and the PTP opening in a different subset of neuronal mitochondria would be another important step. The present study investigated mitochondrial $Ca^{2+}$ dynamics and the PTP opening in somata, but not in axons or synapses, of neurons cultured from adult CyPD-null mice. Previous studies have shown that synaptic mitochondria are more susceptible to the PTP opening in response to the elevated $Ca^{2+}$ (Brown *et al.,* 2006). Axonal or synaptic mitochondria are less numerous than mitochondria in a soma, therefore imaging these mitochondria requires a high magnification lens, such as 100x or 150x, which allows detection of $Ca^{2+}$ fluxes in a single mitochondrion. Such future studies are critical for advancing both the therapeutic potential of targeting the PTP and the understanding of the biology of mitochondrial calcium dynamics in neurons.

**REFERENCES**

Albrecht, M. A., S. L. Colegrove, J. Hongpaisan, N. B. Pivovarova, S. B. Andrews and D. D. Friel (2001). Multiple modes of calcium-induced calcium release in sympathetic neurons I: attenuation of endoplasmic reticulum Ca2+ accumulation at low [Ca2+](i) during weak depolarization. J Gen Physiol 118(1): 83-100.

Alexianu, M. E., B. K. Ho, A. H. Mohamed, V. La Bella, R. G. Smith and S. H. Appel (1994). The role of calcium-binding proteins in selective motoneuron vulnerability in amyotrophic lateral sclerosis. Ann Neurol 36(6): 846-58.

Alonso, M. T., M. J. Barrero, P. Michelena, E. Carnicero, I. Cuchillo, A. G. Garcia, J. Garcia-Sancho, M. Montero and J. Alvarez (1999). Ca2+-induced Ca2+ release in chromaffin cells seen from inside the ER with targeted aequorin. J Cell Biol 144(2): 241-54.

Annunziato, L., S. Amoroso, A. Pannaccione, M. Cataldi, G. Pignataro, A. D'Alessio, R. Sirabella, A. Secondo, L. Sibaud and G. F. Di Renzo (2003). Apoptosis induced in neuronal cells by oxidative stress: role played by caspases and intracellular calcium ions. Toxicol Lett 139(2-3): 125-33.

Baines, C. P., R. A. Kaiser, N. H. Purcell, N. S. Blair, H. Osinska, M. A. Hambleton, E. W. Brunskill, M. R. Sayen, R. A. Gottlieb, G. W. Dorn, J. Robbins and J. D. Molkentin (2005). Loss of cyclophilin D reveals a critical role for mitochondrial permeability transition in cell death. Nature 434(7033): 658-62.

Baines, C. P., R. A. Kaiser, T. Sheiko, W. J. Craigen and J. D. Molkentin (2007). Voltage-dependent anion channels are dispensable for mitochondrial-dependent cell death. Nat Cell Biol 9(5): 550-5.

Baird, G. S., D. A. Zacharias and R. Y. Tsien (1999). Circular permutation and receptor insertion within green fluorescent proteins. Proc Natl Acad Sci U S A 96(20): 11241-6.

Basso, E., L. Fante, J. Fowlkes, V. Petronilli, M. A. Forte and P. Bernardi (2005). Properties of the permeability transition pore in mitochondria devoid of cyclophilin D. J Biol Chem.

Bell, C. J., N. A. Bright, G. A. Rutter and E. J. Griffiths (2006). ATP regulation in adult rat cardiomyocytes: time-resolved decoding of rapid mitochondrial calcium spiking imaged with targeted photoproteins. J Biol Chem 281(38): 28058-67.

Bernardi, P. (1996). The permeability transition pore. Control points of a cyclosporin A-sensitive mitochondrial channel involved in cell death. Biochim Biophys Acta 1275(1-2): 5-9.

Bernardi, P. (1999). Mitochondrial transport of cations: channels, exchangers, and permeability transition. Physiol Rev 79(4): 1127-55.

Bernardi, P., A. Krauskopf, E. Basso, V. Petronilli, E. Blachly-dyson, F. De Lisa and M. Forte (2006). The mitochondrial permeability transition from in vitro artifact to disease target. FEBS J. 273(10): 2077-2099.

Bernardi, P., L. Scorrano, R. Colonna, V. Petronilli and F. Di Lisa (1999). Mitochondria and cell death. Mechanistic aspects and methodological issues. Eur J Biochem 264(3): 687-701.

Bernardi, P., S. Vassanelli, P. Veronese, R. Colonna, I. Szabo and M. Zoratti (1992). Modulation of the mitochondrial permeability transition pore. Effect of protons and divalent cations. J Biol Chem 267(5): 2934-9.

Block, M. L., L. Zecca and J. S. Hong (2007). Microglia-mediated neurotoxicity: uncovering the molecular mechanisms. Nat Rev Neurosci 8(1): 57-69.

Bopassa, J. C., D. Vandroux, M. Ovize and R. Ferrera (2006). Controlled reperfusion after hypothermic heart preservation inhibits mitochondrial permeability transition-pore opening and enhances functional recovery. American journal of physiology 291(5): H2265-71.

Brini, M., P. Pinton, T. Pozzan and R. Rizzuto (1999). Targeted recombinant aequorins: tools for monitoring [Ca2+] in the various compartments of a living cell. Microsc Res Tech 46(6): 380-9.

Broekemeier, K. M., M. E. Dempsey and D. R. Pfeiffer (1989). Cyclosporin A is a potent inhibitor of the inner membrane permeability transition in liver mitochondria. J Biol Chem 264(14): 7826-30.

Brookes, P. S., Y. Yoon, J. L. Robotham, M. W. Anders and S. S. Sheu (2004). Calcium, ATP, and ROS: a mitochondrial love-hate triangle. Am J Physiol Cell Physiol 287(4): C817-33.

Brown, M. R., P. G. Sullivan, J. W. Geddes (2006). Synaptic mitochondria are more susceptible to $Ca^{2+}$ overload than nonsynaptic mitochondria. J Biol Chem 281(17):11658-68.

Buntinas, L., K. K. Gunter, G. C. Sparagna and T. E. Gunter (2001). The rapid mode of calcium uptake into heart mitochondria (RaM): comparison to RaM in liver mitochondria. Biochim Biophys Acta 1504(2-3): 248-61.

Castilho, R. F., A. J. Kowaltowski, A. R. Meinicke, E. J. Bechara and A. E. Vercesi (1995). Permeabilization of the inner mitochondrial membrane by Ca2+ ions is stimulated by t-butyl hydroperoxide and mediated by reactive oxygen species generated by mitochondria. Free Radic Biol Med 18(3): 479-86.

Castilho, R. F., A. J. Kowaltowski, A. R. Meinicke and A. E. Vercesi (1995). Oxidative damage of mitochondria induced by Fe(II)citrate or t-butyl hydroperoxide in the presence of Ca2+: effect of coenzyme Q redox state. Free Radic Biol Med 18(1): 55-9.

Chernyak, B. V. and P. Bernardi (1996). The mitochondrial permeability transition pore is modulated by oxidative agents through both pyridine nucleotides and glutathione at two separate sites. Eur J Biochem 238(3): 623-30.

Cortassa, S., M. A. Aon, et al. (2003). An integrated model of cardiac mitochondrial energy metabolism and calcium dynamics. Biophys J 84(4): 2734

Costantini, P., B. V. Chernyak, V. Petronilli and P. Bernardi (1996). Modulation of the mitochondrial permeability transition pore by pyridine nucleotides and dithiol oxidation at two separate sites. J Biol Chem 271(12): 6746-51.

Crofts, A.R. and J.B. Chappell (1965). Calcium ion accumulation and volume changes of isolated liver mitochondria: reversal of calcium ion-induced swelling. Biochem J 95: 387–92.

Csordas, G., C. Renken, P. Varnai, L. Walter, D. Weaver, K. F. Buttle, T. Balla, C. A. Mannella and G. Hajnoczky (2006). Structural and functional features and significance of the physical linkage between ER and mitochondria. J Cell Biol 174(7): 915-21.

Curie, T., K. L. Rogers, C. Colasante and P. Brulet (2007). Red-shifted aequorin-based bioluminescent reporters for in vivo imaging of Ca2 signaling. Mol Imaging 6(1): 30-42.

Das, A. M. and D. A. Harris (1990). Intracellular calcium as a regulator of the mitochondrial ATP synthase in cultured cardiomyocytes. Biochem Soc Trans 18(4): 554-5.

Das, A. M. and D. A. Harris (1990). Regulation of the mitochondrial ATP synthase in intact rat cardiomyocytes. Biochem J 266(2): 355-61.

de Brito, O. M. and L. Scorrano (2008). Mitofusin 2 tethers endoplasmic reticulum to mitochondria. Nature 456(7222): 605-10.

Defagot, M. C., M. J. Villar and M. C. Antonelli (2002). Differential localization of metabotropic glutamate receptors during postnatal development. Dev Neurosci 24(4): 272-82.

Desagher, S., J. Glowinski and J. Premont (1996). Astrocytes protect neurons from hydrogen peroxide toxicity. J Neurosci 16(8): 2553-62.

Deshpande, L. S., D. D. Limbrick, Jr., S. Sombati and R. J. DeLorenzo (2007). Activation of a novel injury-induced calcium-permeable channel that plays a key role in causing extended neuronal depolarization and initiating neuronal death in excitotoxic neuronal injury. J Pharmacol Exp Ther 322(2): 443-52.

Devin, A. and M. Rigoulet (2007). Mechanisms of mitochondrial response to variations in energy demand in eukaryotic cells. Am J Physiol Cell Physiol 292(1): C52-8.

Doan, T. N., D. L. Gentry, A. A. Taylor, and J. J. Elliott (1994). Hydrogen peroxide activates agonist-sensitive Ca2+-flux pathways in canine venous endothelial cells. Biochem J. 297, 209-215.

Drew, B. and C. Leeuwenburgh (2004). Ageing and subcellular distribution of mitochondria: role of mitochondrial DNA deletions and energy production. Acta Physiol Scand 182(4): 333-41.

Du, H., L. Guo, F. Fang, D. Chen, A. A. Sosunov, G. M. McKhann, Y. Yan, C. Wang, H. Zhang, J. D. Molkentin, F. J. Gunn-Moore, J. P. Vonsattel, O. Arancio, J. X. Chen and S. D. Yan (2008). Cyclophilin D deficiency attenuates mitochondrial and neuronal perturbation and ameliorates learning and memory in Alzheimer's disease. Nat Med 14(10): 1097-105.

Duchen, M. R. (1992). Ca(2+)-dependent changes in the mitochondrial energetics in single dissociated mouse sensory neurons. Biochem J 283 ( Pt 1): 41-50.

Dutta, R., J. McDonough, X. Yin, J. Peterson, A. Chang, T. Torres, T. Gudz, W. B. Macklin, D. A. Lewis, R. J. Fox, R. Rudick, K. Mirnics and B. D. Trapp (2006). Mitochondrial dysfunction as a cause of axonal degeneration in multiple sclerosis patients. Ann Neurol 59(3): 478-89.

Ehrenberg, B., V. Montana, M. D. Wei, J. P. Wuskell and L. M. Loew (1988). Membrane potential can be determined in individual cells from the nernstian distribution of cationic dyes. Biophys J 53(5): 785-94.

Ermak, G. and K. J. Davies (2002). Calcium and oxidative stress: from cell signaling to cell death. Mol Immunol 38(10): 713-21.

Eto, R., M. Abe, N. Hayakawa, H. Kato and T. Araki (2008). Age-related changes of calcineurin and Akt1/protein kinase Balpha (Akt1/PKBalpha) immunoreactivity in the mouse hippocampal CA1 sector: an immunohistochemical study. Metab Brain Dis 23(4): 399-409.

Faure, A. V., D. Grunwald, M. J. Moutin, M. Hilly, J. P. Mauger, I. Marty, M. De Waard, M. Villaz and M. Albrieux (2001). Developmental expression of the calcium release channels during early neurogenesis of the mouse cerebral cortex. Eur J Neurosci 14(10): 1613-22.

Filippin, L., M. C. Abad, S. Gastaldello, P. J. Magalhaes, D. Sandona and T. Pozzan (2005). Improved strategies for the delivery of GFP-based Ca2+ sensors into the mitochondrial matrix. Cell Calcium 37(2): 129-36.

Forte, M. and P. Bernardi (2005). Genetic dissection of the permeability transition pore. J Bioenerg Biomembr 37(3): 121-8.

Forte, M., B. G. Gold, G. Marracci, P. Chaudhary, E. Basso, D. Johnsen, X. Yu, J. Fowlkes, M. Rahder, K. Stem, P. Bernardi and D. Bourdette (2007). Cyclophilin D inactivation protects axons in experimental autoimmune encephalomyelitis, an animal model of multiple sclerosis. Proc Natl Acad Sci U S A 104(18): 7558-63.

Franzini-Armstrong, C. (2007). ER-mitochondria communication. How privileged? Physiology (Bethesda) 22: 261-8.

Geshi, E., N. Konno, T. Yanagishita, T. Katagiri (1988). Impairment of mitochondrial respiratory activity in the early ischemic myocardium-with special reference to electron transport system. Jpn Circ J 52: 535–542.

Gincel, D., H. Zaid and V. Shoshan-Barmatz (2001). Calcium binding and translocation by the voltage-dependent anion channel: a possible regulatory mechanism in mitochondrial function. Biochem J 358(Pt 1): 147-55.

Griesbeck, O., G. S. Baird, R. E. Campbell, D. A. Zacharias and R. Y. Tsien (2001). Reducing the environmental sensitivity of yellow fluorescent protein. Mechanism and applications. J Biol Chem 276(31): 29188-94.

Griffiths, E. J. and A. P. Halestrap (1993). Protection by Cyclosporin A of ischemia/reperfusion-induced damage in isolated rat hearts. J Mol Cell Cardiol 25(12): 1461-9.

Halestrap, A. P. (2009). Mitochondria and reperfusion injury of the heart-A holey death but not beyond salvation. J Bioenerg Biomembr.

Halestrap, A. P. and C. Brennerb (2003). The adenine nucleotide translocase: a central component of the mitochondrial permeability transition pore and key player in cell death. Curr Med Chem 10(16): 1507-25.

Halestrap, A. P., C. P. Connern, E. J. Griffiths and P. M. Kerr (1997). Cyclosporin A binding to mitochondrial cyclophilin inhibits the permeability transition pore and protects hearts from ischaemia/reperfusion injury. Mol Cell Biochem 174(1-2): 167-72.

Halestrap, A. P., E. Doran, J. P. Gillespie and A. O'Toole (2000). Mitochondria and cell death. Biochem Soc Trans 28(2): 170-7.

Halestrap, A. P., G. P. McStay and S. J. Clarke (2002). The permeability transition pore complex: another view. Biochimie 84(2-3): 153-66.

Harding, M. W. and R. E. Handschumacher (1988). Cyclophilin, a primary molecular target for cyclosporine. Structural and functional implications. Transplantation 46(2 Suppl): 29S-35S.

Harman, D. (2003). The free radical theory of aging. Antioxid Redox Signal 5(5): 557-61.

Hille, B. (2001). Ion Channels of Excitable Membrane. Third addition.

Hongpaisan, J., N. B. Pivovarova, S. L. Colegrove, R. D. Leapman, D. D. Friel and S. B. Andrews (2001). Multiple modes of calcium-induced calcium release in sympathetic neurons II: a [Ca2+](i)- and location-dependent transition from endoplasmic reticulum Ca accumulation to net Ca release. J Gen Physiol 118(1): 101-12.

Hureau, C. and P. Faller (2009). Abeta-mediated ROS production by Cu ions: Structural insights, mechanisms and relevance to Alzheimer's disease. Biochimie.

Hyun, D. H., J. O. Hernandez, M. P. Mattson and R. de Cabo (2006). The plasma membrane redox system in aging. Ageing Res Rev 5(2): 209-20.

Ichas, F., L. S. Jouaville and J. P. Mazat (1997). Mitochondria are excitable organelles capable of generating and conveying electrical and calcium signals. Cell 89(7): 1145-53.

Inoue, M., E. F. Sato, M. Nishikawa, A. M. Park, Y. Kira, I. Imada and K. Utsumi (2003). Mitochondrial generation of reactive oxygen species and its role in aerobic life. Curr Med Chem 10(23): 2495-505.

Jackson, J. G. and S. A. Thayer (2006). Mitochondrial modulation of Ca2+ -induced Ca2+ -release in rat sensory neurons. J Neurophysiol 96(3): 1093-104.

Jornot, L., P. Maechler, C.B. Wollheim and A.F. Junod (1999). Reactive oxygen metabolites increase mitochondrial calcium in endothelial cells: implication of the Ca2+/Na+ exchanger. Journal of Cell Science (112): 1013-22

Jung, D. W., K. Baysal and G. P. Brierley (1995). The sodium-calcium antiport of heart mitochondria is not electroneutral. J Biol Chem 270(2): 672-8.

Kadowaki, H., H. Nishitoh, F. Urano, C. Sadamitsu, A. Matsuzawa, K. Takeda, H. Masutani, J. Yodoi, Y. Urano, T. Nagano and H. Ichijo (2005). Amyloid beta induces neuronal cell death through ROS-mediated ASK1 activation. Cell Death Differ 12(1): 19-24.

Kandel, E., J. Schwartz, T. Jessell (2000). Principles of Neural Science. Fourth addition.

Kann, O. and R. Kovacs (2007). Mitochondria and neuronal activity. Am J Physiol Cell Physiol 292(2): C641-57.

Karbowski, M. and R. J. Youle (2003). Dynamics of mitochondrial morphology in healthy cells and during apoptosis. Cell Death Differ 10(8): 870-80.

Kawahara, M. and Y. Kuroda (2000). Molecular mechanism of neurodegeneration induced by Alzheimer's beta-amyloid protein: channel formation and disruption of calcium homeostasis. Brain Res Bull 53(4): 389-97.

Kirichok, Y., G. Krapivinsky and D. E. Clapham (2004). The mitochondrial calcium uniporter is a highly selective ion channel. Nature 427(6972): 360-4.

Kokoszka, J. E., K. G. Waymire, S. E. Levy, J. E. Sligh, J. Cai, D. P. Jones, G. R. MacGregor and D. C. Wallace (2004). The ADP/ATP translocator is not essential for the mitochondrial permeability transition pore. Nature 427(6973): 461-5.

Kornek, B., M. K. Storch, J. Bauer, A. Djamshidian, R.Weissert, E. Wallstroem, A. Stefferl, F. Zimprich, T. Olsson, C. Linington, M. Schmidbauer and H. Lassmann (2001). Distribution of a calcium channel subunit in dystrophic axons in multiple sclerosis and experimental autoimmune encephalomyelitis. Brain 124 (6): 1114-24.

Kortvely, E., A. Palfi, L. Bakota and K. Gulya (2002). Ontogeny of calmodulin gene expression in rat brain. Neuroscience 114(2): 301-16.

Kristian, T. and B. K. Siesjo (1998). Calcium in ischemic cell death. Stroke 29(3): 705-18.

Kruman, II and M. P. Mattson (1999). Pivotal role of mitochondrial calcium uptake in neural cell apoptosis and necrosis. J Neurochem 72(2): 529-40.

Lalo, U. and P. Kostyuk (1998). Developmental changes in purinergic calcium signalling in rat neocortical neurones. Brain Res Dev Brain Res 111(1): 43-50.

Lehninger, A. L. (1970). Mitochondria and calcium ion transport. Biochem J 119(2): 129-38.

Lieven, C. J., J. P. Vrabec and L. A. Levin (2003). The effects of oxidative stress on mitochondrial transmembrane potential in retinal ganglion cells. Antioxid Redox Signal 5(5): 641-6.

Litwinowicz, B., C. Labuda, P. Kowianski, J. H. Spodnik, B. Ludkiewicz, S. Wojcik and J. Morys (2003). Developmental pattern of calbindin D28k protein expression in the rat striatum and cerebral cortex. Folia Morphol (Warsz) 62(4): 327-9.

Lu, K. P., B. E. Kemp and A. R. Means (1994). Identification of substrate specificity determinants for the cell cycle-regulated NIMA protein kinase. J Biol Chem 269(9): 6603-7.

Lucas, M., G. Schmid, R. Kromas and G. Loffler (1978). Calcium metabolism and enzyme secretion in guinea pig pancreas. Uptake, storage and release of calcium in whole cells and mitochondrial and microsomal fractions. Eur J Biochem 85(2): 609-19.

Mahad, D., H. Lassmann and D. Turnbull (2008). Review: Mitochondria and disease progression in multiple sclerosis. Neuropathol Appl Neurobiol 34(6): 577-89.

Martin, L. J., B. Gertz, Y. Pan, A. C. Price, J. D. Molkentin and Q. Chang (2009). The mitochondrial permeability transition pore in motor neurons: Involvement in the pathobiology of ALS mice. Exp Neurol.

Matsuka, Y., T. Ono, H. Iwase, S. Mitrirattanakul, K. S. Omoto, T. Cho, Y. Y. Lam, B. Snyder and I. Spigelman (2008). Altered ATP release and metabolism in dorsal root ganglia of neuropathic rats. Mol Pain 4: 66.

Mattson, M. P. (2007). Calcium and neurodegeneration. Aging Cell 6(3): 337-50.

Mattson, M. P., B. Cheng, D. Davis, K. Bryant, I. Lieberburg and R. E. Rydel (1992). beta-Amyloid peptides destabilize calcium homeostasis and render human cortical neurons vulnerable to excitotoxicity. J Neurosci 12(2): 376-89.

McCormack, J. G. and R. M. Denton (1993). The role of intramitochondrial Ca2+ in the regulation of oxidative phosphorylation in mammalian tissues. Biochem Soc Trans 21 ( Pt 3)(3): 793-9.

McGivan, J. D., N. M. Bradford and J. Mendes-Mourao (1976). The regulation of carbamoyl phosphate synthase activity in rat liver mitochondria. Biochem J 154(2): 415-21.

McGuinness, O., N. Yafei, A. Costi and M. Crompton (1990). The presence of two classes of high-affinity cyclosporin A binding sites in mitochondria. Evidence that the minor component is involved in the opening of an inner-membrane Ca(2+)-dependent pore. Eur J Biochem 194(2): 671-9.

Means, A. R. (1994). Calcium, calmodulin and cell cycle regulation. FEBS Lett 347(1): 1-4.

Mildaziene, V., R. Baniene, Z. Nauciene, B. M. Bakker, G. C. Brown, H. V. Westerhoff and B. N. Kholodenko (1995). Calcium indirectly increases the control exerted by the adenine nucleotide translocator over 2-oxoglutarate oxidation in rat heart mitochondria. Arch Biochem Biophys 324(1): 130-4.

Misgeld, T., M. Kerschensteiner, F.M. Bareyre, R.W. Burgess, J.W. Lichtman (2007). Imaging axonal transport of mitochondria in vivo. Nat Methods. 4(7):559-61

Mitsumoto, H., R. M. Santella, X. Liu, M. Bogdanov, J. Zipprich, H. C. Wu, J. Mahata, M. Kilty, K. Bednarz, D. Bell, P. H. Gordon, M. Hornig, M. Mehrazin, A. Naini, M. Flint Beal and P. Factor-Litvak (2008). Oxidative stress biomarkers in sporadic ALS. Amyotroph Lateral Scler 9(3): 177-83.

Miyawaki, A., J. Llopis, R. Heim, J. M. McCaffery, J. A. Adams, M. Ikura and R. Y. Tsien (1997). Fluorescent indicators for Ca2+ based on green fluorescent proteins and calmodulin. Nature 388(6645): 882-7.

Mori, F., M. Fukaya, H. Abe, K. Wakabayashi and M. Watanabe (2000). Developmental changes in expression of the three ryanodine receptor mRNAs in the mouse brain. Neurosci Lett 285(1): 57-60.

Mutsaers, S. E. and W. M. Carroll (1998). Focal accumulation of intra-axonal mitochondria in demyelination of the cat optic nerve. Acta Neuropathol (Berl) 96(2): 139-43.

Nagai, T., A. Sawano, E. S. Park and A. Miyawaki (2001). Circularly permuted green fluorescent proteins engineered to sense Ca2+. Proc Natl Acad Sci U S A 98(6): 3197-202.

Nakagawa, T., S. Shimizu, T. Watanabe, O. Yamaguchi, K. Otsu, H. Yamagata, H. Inohara, T. Kubo and Y. Tsujimoto (2005). Cyclophilin D-dependent mitochondrial permeability transition regulates some necrotic but not apoptotic cell death. Nature 434(7033): 652-8.

Nixon, R. A. (2003). The calpains in aging and aging-related diseases. Ageing Res Rev 2(4): 407-18.

Packer, M. A. and M. P. Murphy (1994). Peroxynitrite causes calcium efflux from mitochondria which is prevented by Cyclosporin A. FEBS Lett 345(2-3): 237-40.

Palmer, A. E., M. Giacomello, T. Kortemme, S. A. Hires, V. Lev-Ram, D. Baker and R. Y. Tsien (2006). Ca2+ indicators based on computationally redesigned calmodulin-peptide pairs. Chem Biol 13(5): 521-30.

Palmieri, F. (2004). The mitochondrial transporter family (SLC25): physiological and pathological implications. Pflugers Arch 447(5): 689-709.

Paradies, G., G. Petrosillo, M. Pistolese, N. Di Venosa N, D. Serena, F.M. Ruggiero (1999). Lipid peroxidation and alterations to oxidative metabolism in mitochondria isolated from rat heart subjected to ischemia and reperfusion. Free Radic Biol Med 27: 42–50.

Paradies, G., G. Petrosillo, M. Pistolese, N. Di Venosa, A. Federici, F.M. Ruggiero (2004). Decrease in mitochondrial complex I activity in ischemic/reperfused rat heart: involvement of reactive oxygen species and cardiolipin. Circ Res 94: 53–59.

Paredes, R. M., J. C. Etzler, L. T. Watts, W. Zheng and J. D. Lechleiter (2008). Chemical calcium indicators. Methods 46(3): 143-51.

Petronilli, V., G. Miotto, M. Canton, M. Brini, R. Colonna, P. Bernardi and F. Di Lisa (1999). Transient and long-lasting openings of the mitochondrial permeability transition pore can be monitored directly in intact cells by changes in mitochondrial calcein fluorescence. Biophys J 76(2): 725-34.

Pozzan, T. and R. Rudolf (2008). Measurements of mitochondrial calcium in vivo. Biochim Biophys Acta.

Riley, W. W. Jr. and D. R. Pfeiffer (1986). Rapid and extensive release of Ca2+ from energized mitochondria induced by EGTA. J Biol Chem 261: 28-31.

Rizzuto, R., M. Brini, M. Murgia and T. Pozzan (1993). Microdomains with high Ca2+ close to IP3-sensitive channels that are sensed by neighboring mitochondria. Science 262(5134): 744-7.

Rizzuto, R., M. R. Duchen and T. Pozzan (2004). Flirting in little space: the ER/mitochondria Ca2+ liaison. Sci STKE 2004(215): re1.

Romagnoli, A., P. Aguiari, D. De Stefani, S. Leo, S. Marchi, A. Rimessi, E. Zecchini, P. Pinton and R. Rizzuto (2007). Endoplasmic reticulum/mitochondria calcium cross-talk. Novartis Found Symp 287: 122-31; discussion 131-9.

Rose, C. R. and A. Konnerth (2001). Stores not just for storage. intracellular calcium release and synaptic plasticity. Neuron 31(4): 519-22.

Rottenberg, H. and M. Marbach (1990). Regulation of Ca2+ transport in brain mitochondria. I. The mechanism of spermine enhancement of Ca2+ uptake and retention. Biochim Biophys Acta 1016(1): 77-86.

Rottenberg, H. and M. Marbach (1990). Regulation of Ca2+ transport in brain mitochondria. II. The mechanism of the adenine nucleotides enhancement of Ca2+ uptake and retention. Biochim Biophys Acta 1016(1): 87-98.

Sanvicens, N., V. Gómez-Vicente, I. Masip, A. Messeguer, T.G. Cotter (2004). Oxidative stress-induced apoptosis in retinal photoreceptor cells is mediated by calpains and caspases and blocked by the oxygen radical scavenger CR-6. J Biol Chem 79(38):39268-78.

Sathornsumetee, S., D. B. McGavern, D. R. Ure and M. Rodriguez (2000). Quantitative ultrastructural analysis of a single spinal cord demyelinated lesion predicts total lesion load, axonal loss, and neurological dysfunction in a murine model of multiple sclerosis. Am J Pathol 157(4): 1365-76.

Sattler, R. and M. Tymianski (2001). Molecular mechanisms of glutamate receptor-mediated excitotoxic neuronal cell death. Mol Neurobiol 24(1-3): 107-29.

Schinzel, A. C., O. Takeuchi, Z. Huang, J. K. Fisher, Z. Zhou, J. Rubens, C. Hetz, N. N. Danial, M. A. Moskowitz and S. J. Korsmeyer (2005). Cyclophilin D is a component of mitochondrial permeability transition and mediates neuronal cell death after focal cerebral ischemia. Proc Natl Acad Sci U S A 102(34): 12005-10.

Scorrano, L. and S. J. Korsmeyer (2003). Mechanisms of cytochrome c release by proapoptotic BCL-2 family members. Biochem Biophys Res Commun 304(3): 437-44.

Simpson, P. B., R. A. Challiss and S. R. Nahorski (1995). Neuronal Ca2+ stores: activation and function. Trends Neurosci 18(7): 299-306.

Stout, A. K., H. M. Raphael, B. I. Kanterewicz, E. Klann and I. J. Reynolds (1998). Glutamate-induced neuron death requires mitochondrial calcium uptake. Nat Neurosci 1(5): 366-73.

Szabadkai, G., K. Bianchi, P. Varnai, D. De Stefani, M. R. Wieckowski, D. Cavagna, A. I. Nagy, T. Balla and R. Rizzuto (2006). Chaperone-mediated coupling of endoplasmic reticulum and mitochondrial Ca2+ channels. J Cell Biol 175(6): 901-11.

Szabadkai, G. and M. R. Duchen (2008). Mitochondria: the hub of cellular Ca2+ signaling. Physiology (Bethesda) 23: 84-94.

Szabo, I., V. De Pinto and M. Zoratti (1993). The mitochondrial permeability transition pore may comprise VDAC molecules. II. The electrophysiological properties of VDAC are compatible with those of the mitochondrial megachannel. FEBS Lett 330(2): 206-10.

Szabo, I. and M. Zoratti (1991). The giant channel of the inner mitochondrial membrane is inhibited by cyclosporin A. J Biol Chem 266(6): 3376-9.

Talos, D. M., R. E. Fishman, H. Park, R. D. Folkerth, P. L. Follett, J. J. Volpe and F. E. Jensen (2006). Developmental regulation of alpha-amino-3-hydroxy-5-methyl-4-isoxazole-propionic acid receptor subunit expression in forebrain and relationship to regional susceptibility to hypoxic/ischemic injury. I. Rodent cerebral white matter and cortex. J Comp Neurol 497(1): 42-60.

Tang, T. S., E. Slow, V. Lupu, I. G. Stavrovskaya, M. Sugimori, R. Llinas, B. S. Kristal, M. R. Hayden and I. Bezprozvanny (2005). Disturbed Ca2+ signaling and apoptosis of medium spiny neurons in Huntington's disease. Proc Natl Acad Sci U S A 102(7): 2602-7.

Tang, Y. and R. S. Zucker (1997). Mitochondrial involvement in post-tetanic potentiation of synaptic transmission. Neuron 18(3): 483-91.

Tarnawa, I., H. Bolcskei and P. Kocsis (2007). Blockers of voltage-gated sodium channels for the treatment of central nervous system diseases. Recent Pat CNS Drug Discov 2(1): 57-78.

Trapp, B., R. Ransohoff, E. Fisher and R. Rudick (1999). Neurodegenration in multiple sclerosis: Relationship to neurological disability. Neuroscientist 5(1): 48-57.

Wang, X., Y. Carlsson, E. Basso, C. Zhu, C. I. Rousset, A. Rasola, B. R. Johansson, K. Blomgren, C. Mallard, P. Bernardi, M. A. Forte and H. Hagberg (2009). Developmental shift of cyclophilin D contribution to hypoxic-ischemic brain injury. J Neurosci 29(8): 2588-96.

Wernette, M. E., R. S. Ochs and H. A. Lardy (1981). Ca2+ stimulation of rat liver mitochondrial glycerophosphate dehydrogenase. J Biol Chem 256(24): 12767-71.

Yamada, T., P. L. McGeer, K. G. Baimbridge and E. G. McGeer (1990). Relative sparing in Parkinson's disease of substantia nigra dopamine neurons containing calbindin-D28K. Brain Res 526(2): 303-7.

Zhang, Y., O. Marcillat, C. Giulivi, L. Ernster, K.J. Davies (1990). The oxidative inactivation of mitochondrial electron transport chain components and ATPase. J Biol Chem 265: 16330–36.

Zhu, L. P., X. D. Yu, S. Ling, R. A. Brown and T. H. Kuo (2000). Mitochondrial Ca2+ homeostasis in the regulation of apoptotic and necrotic cell deaths. Cell Calcium 28(2): 107-17.

Zimprich, F., K. Torok and S. R. Bolsover (1995). Nuclear calmodulin responds rapidly to calcium influx at the plasmalemma. Cell Calcium 17(3): 233-38.

Zizi, M., M. Forte, E. Blachly-Dyson and M. Colombini (1994). NADH regulates the gating of VDAC, the mitochondrial outer membrane channel. J Biol Chem 269(3): 1614-6.

Zoratti, M. and I. Szabo (1995). The mitochondrial permeability transition. Biochim Biophys Acta 1241(2): 139-76.